A STUDY OF THE E REGION OF THE IONOSPHERE.

A Thesis presented for the degree of Master of Science of the University of South Africa

by

A. J. BARNARD

Physics Department,
Rhodes University College,
Grahamstown,

Dec., 1950.

CONTENTS.

- - - - - - - - - - -

ACKNOWLEDGEMENTS

The author wishes to express his appreciation and thanks to:

Professor R.W. Varder, M.A. for his encouragement and interest in this research;

Dr. M.E. Szendrei,Ph.D., who directed the work, for his help and advice;

Mr. F.J. Hewitt, M.Sc., for the loan of ionosphere records from the Telecommunications Research Laboratory, Johannesburg;

Mr. W.D. Mills, for the use of his typewriter.

- - - - - - - - - - - -

SUMMARY

After a brief historical introduction, the apparatus used in the investigation of the ionosphere in Grahamstown, is described with special reference to the recording equipment, which consists essentially of a camera focussed on the screen of a C.R.O. with z-axis deflection. The equations of the magneto-ionic theory are quoted. The basic formulae of the theories of layer formation in an isothermal (Chapman's), and linear temperature gradient (Gledhill and Szendrei) atmosphere are also quoted.

A study of the E layer critical frequencies is then presented. It is pointed out that there occur two types of irregularities in the E region, namely the Sporadic E layer and the Abnormal E layer, the latter being controlled to a marked extent by the sun. Reasons are given why the frequency where F reflections are first visible, should not be

used as E layer critical frequency. The graphs of log f_c against log cosχ were found to be straight lines, and from their slopes a value of the temperature gradient could be deduced. The earth's magnetic field in the ionosphere was also evaluated, the limitations of the method being pointed out.

The three main methods of determining true heights, namely the Booker and Seaton, Pierce and Pekeris methods, are briefly described. Results from these methods are quoted showing that the first two methods give too low a value for the actual height. The thickness of the Abnormal layer is found to be of the order of a few kilometers.

The errors in the Pekeris analysis are described, with special reference to the earth's magnetic field. It is shown that due to the neglect of the field, our values of scale height of the E layer are probably 10% too small. Methods are suggested of finding actual heights from the extra-ordinary curve, and of evaluating true heights, taking into account the magnetic field.

Values of temperature calculated from the scale height are in good agreement with other estimates. Methods are

outlined for the determination of the temperature gradient from the distribution curves. High values of the gradient are found for the E layer.

Finally, theories for the formation of the abnormal layer are discussed. Subjects for further study are suggested.

- - - - - - - - - - - - - -

INTRODUCTION.

The term ionosphere is reserved for the ionised region in the upper atmosphere, concentric with the surface of the earth and extending mainly from a height of 100 kilometer upwards. This region of ionised particles forms a conductig surface which is capable of reflecting electromagnetic waves of a suitable wavelength.

As early as 1878 Stewart had suggested that conducting layers in the upper atmosphere could account for certain variations in the earth's magnetic field, but his theory was not generally accepted. Hence when Marconi first transmitted radio signals across the Atlantic in 1901, physicists had difficulty in explaining how the electro-magnetic waves could be bent around the surface of the earth. Many investigators tried to account for this phenomenon by ascribing it to a diffraction effect, but this theory did not meet with any success. In 1902 Kenelly and Heaviside independently postulated that a conducting layer exists in the upper atmosphere. This layer would reflect wireless waves and hence make long-distance radio

communication possible (see fig. 1) .

In 1912 Eccles [1,2]) discussed the effect of solar radiation on the upper layers of the atmosphere. He also worked out the fundamental theory of ionic refraction. In 1924 Larmor [3]) ascribed the major part of ionic refraction to the presence of free electrons in large numbers in the upper atmosphere.

But it was not till 1925 that the presence of a conducting layer was experimentally verified. In that year Appleton and Barnett [4]) continuously varied the frequency of a transmitter through a small range and found interference fringes between the ground wave (i.e. the wave travelling directly from the transmitter to the receiver) and the wave reflected from the ionosphere.

During the same year Breit and Tuve [5,6,7]) developed a method for measuring the group-time τ of travel of the waves directly. Radio pulses of very short duration were emitted by a transmitter. Both the ground pulse and the reflected pulse were recorded by a receiver coupled to an oscillograph. The time τ could then be measured directly on the oscillograph screen. This method of measuring the group-time has proved to be by far the most generally useful.

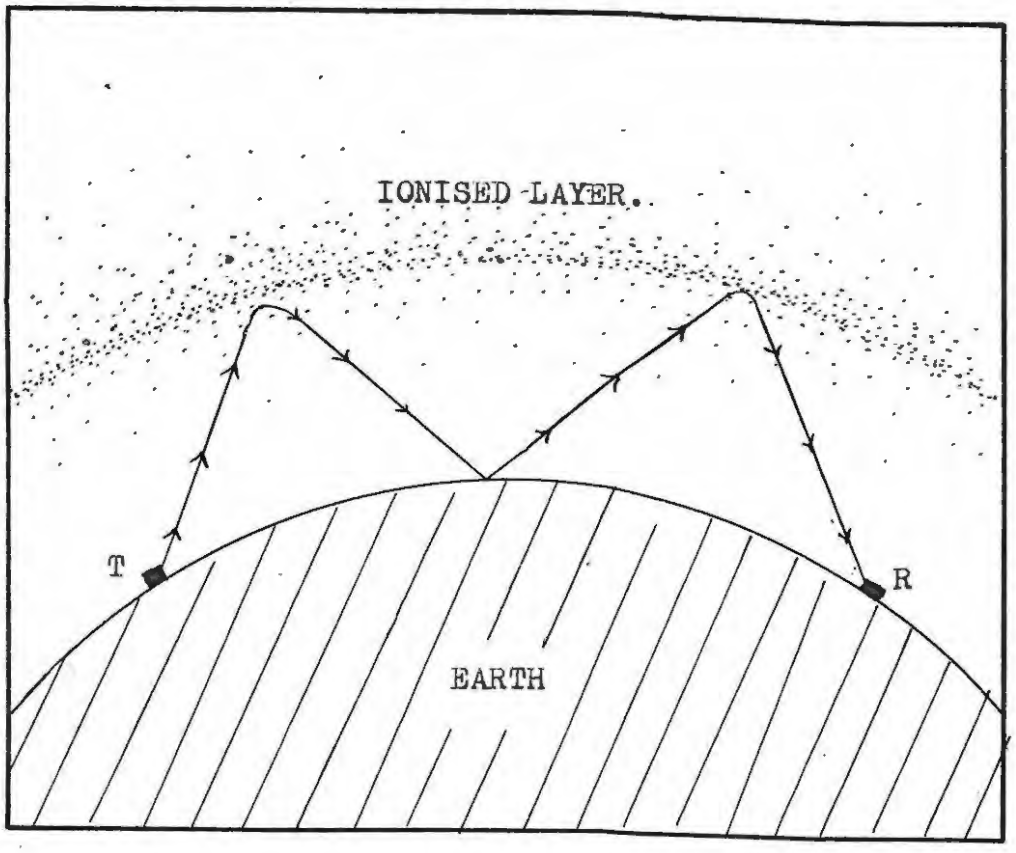

FIG. 1 - REFLECTION FROM IONISED LAYER.

T - Transmitter.

R - Receiver.

The equivalent path P′ traversed by the waves is defined as the group-time multiplied by the velocity of electromagnetic waves in vacuo. Half the equivalent path is called the virtual height, usually denoted by h′. Hence

$$h' = P'/2$$
$$= c\tau/2 ,$$

c being the velocity of electromagnetic waves in vacuo. Therefore by suitably calibrating the time base of the cathode ray oscillograph, the value of h′ may be read off directly from the screen.

Of the many ways of exploring the ionosphere by means of radio waves, the study of the variation of h′ with frequency has proved to be the most fruitful. Most ionosphere data are in the form of curves showing the variation of h′ with frequency.

A study of these curves soon revealed that the ionosphere consists of two main "layers",distinguished by the letters E and F. The E layer is found at a height of approximately 120 kilometer and is normally 10 to 15 km. thick. During the night the ionisation falls to such a low value that this layer is not normally detected on ordinary equipment. The F layer, occurring at a height of 200 to 300 km. ,is much thicker and more densely

ionised. During the day in summer it usually splits in two layers, namely the F_1 and F_2 layers. The F_1 layer is the lower one and occurs at about 200 km. above the earth's surface. The F_2 layer which is the main one, is found at a height of approximately 300 km.

Below these, at a height of 60 km. yet another layer of very low ionisation occurs. Two types of reflections from the so-called D layer have been distinguished by Pfister [8]. The first is a reflection from a normal layer with a very low ionisation. The second type may be observed on ordinary equpment and has recently been reviewed by Ellyet [9]. It is sporadic in nature, relatively high ionisation being found to occur at irregular intervals.

These ionosphere layers are not however sharply defined. They can best be described as maxima in an ionised medium of increasing density. In what follows we shall be mainly interested in the E layer, also referred to as the Kenelly-Heaviside layer.

EXPERIMENTAL METHODS.

The method employed in this laboratory for the study of the ionosphere is the standard Breit and Tuve amplitude modulation method. A pulse of very short duration is emitted by a transmitter and both the ground and reflected waves are recorded by a receiver coupled to an oscillograph. The time delay can then be measured directly on the oscillograph screen.

A brief description of the existing equipment in the laboratory will now be given. It was designed and built by M.E.Szendrei and J.A.Gledhill [11]) a few years ago. It consists of a transmitter, pulse generator, receiver, height marking oscillator and a photographic recorder. The apparatus is manually operated and is laid out on a single bench, except for the photographic recorder which is in a darkroom. The recorder is operated from controls next to the receiver.

Transmitter:

The transmitter consists of a shunt-fed push pull oscillator of the Hartley type. It is first adjusted to work as a

Class C power oscillator and then biased so as to be completely cut off except when a pulse of suitable amplitude and polarity is applied from the pulse generator.

For the investigaton of the E layer the transmitter was modified by the author to cover the frequency range 1.3 to 8.0 mc./sec. spread over four bands. The coils for the three higher frequency bands have separate dipole antennas about half as long as the mean wavelength radiated by the coil. In the case of the lower band (range 1.3 to 1.9 mc./sec.) there was not enough space for a dipole antenna. This coil was therefore coupled to a straight wire aerial 70 m. long.

Pulse Generator and Modulator:

The pulse generator and modulator has recently been rebuilt by O'Brien [12]. A sine wave from the mains (which can be varied in phase) is applied to two pentodes which acts as "clippers" producing very nearly square waves. The wave is then "pipped" by a simple differentiating circuit and the resulting pulses are amplified. In this way pulses of about 150 microseconds duration are produced which are automatically synchronised with the A.C. mains.

Receiver:

The receiver covers the range of the transmitter in three bands. It is specially designed for sensitivity and has very small time constants in the R.F. section. The audio section has very long time constants so that all the harmonics may be amplified without lengthening the duration of the pulse.

Height-marking Oscillator:

The height-marking oscillator has a frequency of 1500 cycles per sec. Therefore when it is applied to the recorder one complete oscillation corresponds to 100 km. virtual height. The oscillator therefore marks out heights very conveniently on the cathode ray screen.

By means of a foot key either the receiver or the height-marking oscillator can be connected to the recorder.

Recording Equipment:

The usual metod of recording pulses is to apply the output of the receiver to the vertical deflecting plates of a cathode ray tube. The appearance of the screen is then as shown in fig.2(a). The strong vertical deflection on the left represents the ground pulse, while the others correspond to pulses reflected from the ionosphere.

When a lead sheet with a horizontal slit is placed over the screen, a line with a series of gaps results, as shown in fig. 2(b). A camera with a film moving vertically at constant speed, is focussed on the slit. By changing the frequency of the receiver at constant rate, the displacement along the film is made proportional to the frequency. In this way photographic (h,f) curves are produced. This method has been used in this laboratory by Gledhill and Szendrei and O'Brien. A 35 mm. film is driven slowly through a specially constructed camera by a synchronous motor.

The method has however a disadvantage in that interference and atmospherics displace the whole pattern on the oscillograph screen vertically. The image may therefore be displaced off the slit thus causing parts of the record to be missing. In the case of the E layer this can be a serious disadvantage as the echoes are rather weak.

The author therefore modified the existing apparatus by applying the pulse from the receiver to the grid of the cathode ray tube. In this way the vertical displacement is replaced by a displacement perpendicular to the screen of the oscillograph (the so-called z-axis deflection) The pattern on the screen becomes a line with a number

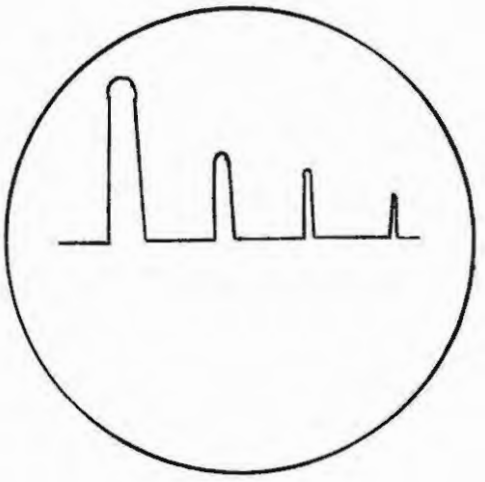

FIG. 2(a).

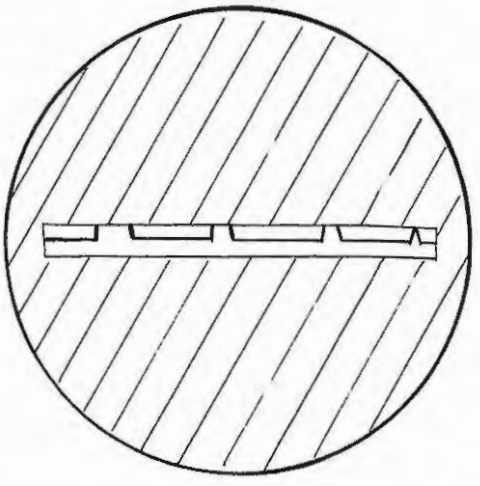

FIG. 2(b).

FIG. 2

APPEARANCE OF C.R.O. SCREEN
(a) WITHOUT AND (b) WITH LEAD SCREEN.

of breaks in it. Although no longer necessary, it was convenient to use a lead foil with a wide slit in order to eliminate stray light from the screen.

The circuit diagram is given in figs.3(a) and 3(b). The time base of the oscillograph is supplied by the gas-filled thyratron T_6, the condenser C_{10} being charged through the resistances R_{29}, R_{30}, and R_{31} in series. The sweep frequency of the trace can be adjusted by varying these resistances. Synchronisation with the A.C. mains is obtained by a square wave from tube T_7 which acts as a "clipper" , its grid bias being small compared with the injected voltage. By means of the resistance R_{39} the phase of the injected voltage can be changed by about 120°. It was also found convenient to have a key S_1 whereby the synchronisation can be switched off when the sweep frequency is adjusted.

Operation of Apparatus:

In the operation of the apparatus, the frequency of both the receiver and transmitter has to be increased simultaneously. To keep the receiver and transmitter in tune the output of the receiver was also applied to a general purpose oscillograph placed next to the transmitter and receiver. The loudspeaker of the receiver also serves as a monitoring device, a change of note being heard when the

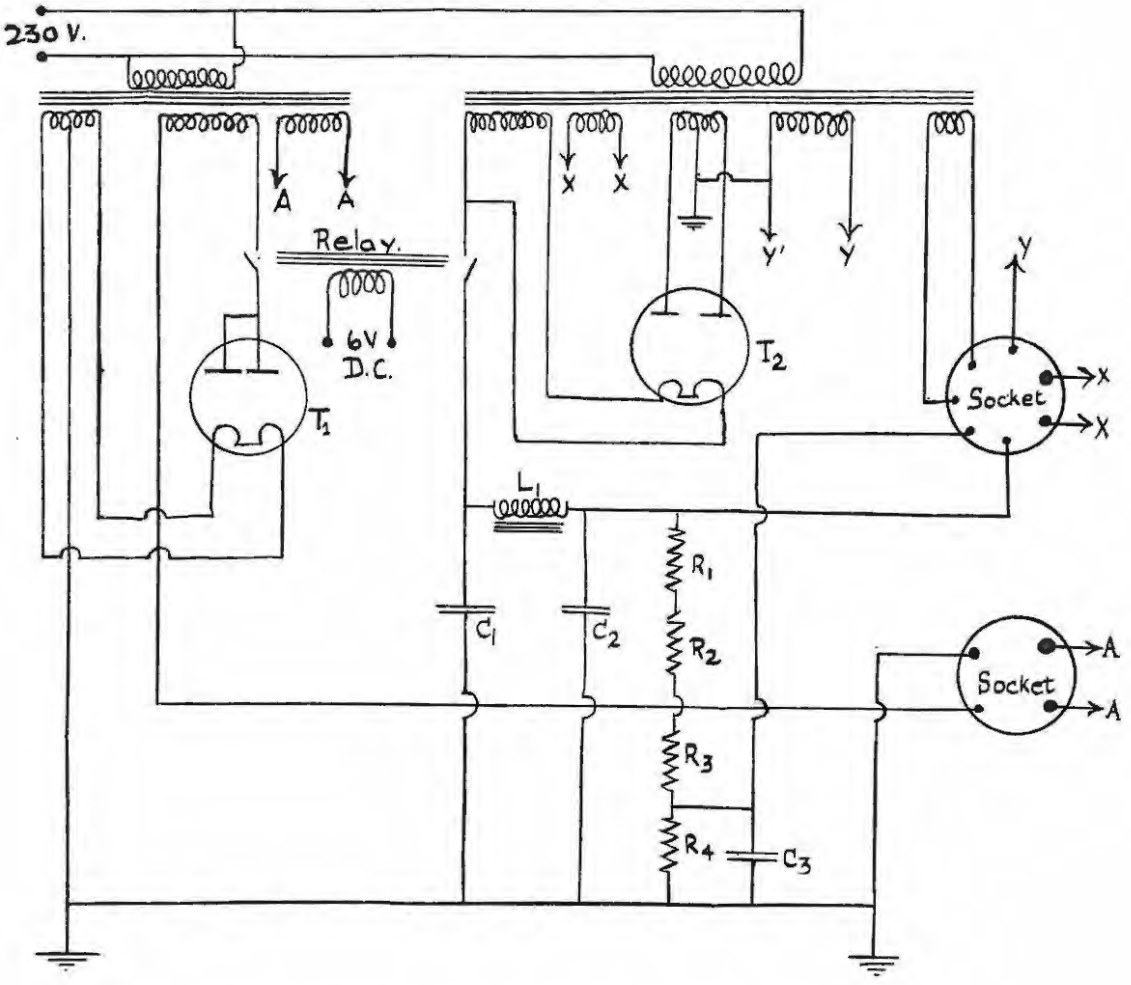

FIG. 3(a) - POWER SUPPLY FOR C.R.O.

LEGEND.

T_1 - DW 15

T_2 - 5Y3G.

C_1, C_2 - 10 Fd. 450 W.V. (Electrolytic).

C_3 - 16 Fd. 450 W.V. (Electrolytic).

R_1 - 75,000 ohms

R_2 - 75,000 ohms.

R_3 - 50,000 ohms.

R_4 - 3,000 ohms.

L_1 - 20 mH.

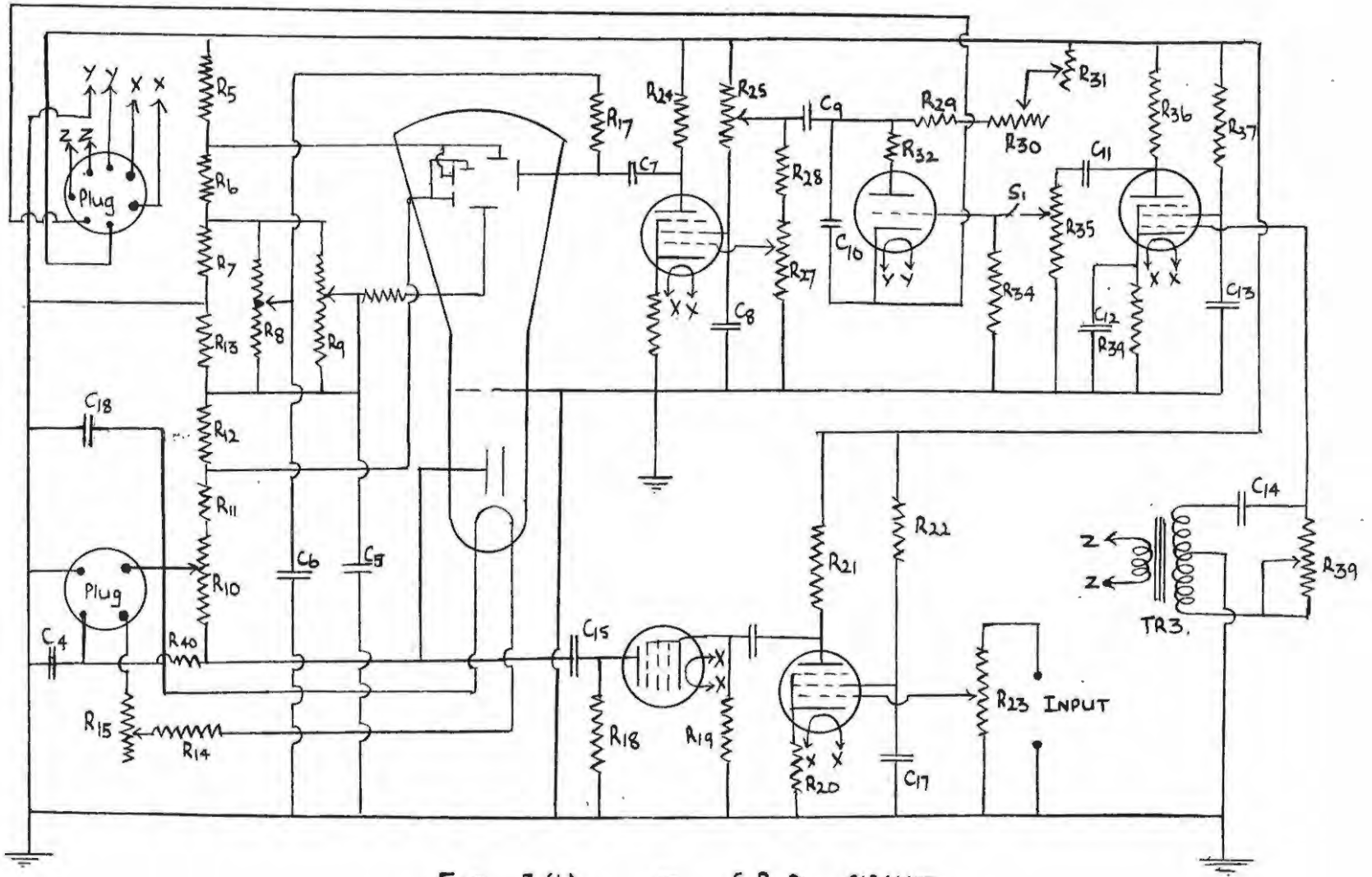

FIG 3(b) – C.R.O. CIRCUIT.

LEGEND TO FIG. 3(b).

R_5 - 1.0 Megohm
R_6 - 0.2 megohm.
R_7 - 0.8 megohm.
R_8 - 1.0 megohm (Hor.Pos)
R_9 - 1.0 megohm (Vert.Pos)
R_{10} - 0.25 megohm (Focus)
R_{11} - 2.0 megohm.
R_{12} - 0.2 megohm.
R_{13} - 1.0 megohm
R_{14} - 0.15 ohm.
R_{15} - 0.3 ohm(Intensity)
R_{16} - 5.0 megohm.
R_{17} - 5.0 megohm.
R_{18} - 0.5 megohm.
R_{19} - 1.0 megohm.
R_{20} - 500 ohms.
R_{21} - 0.12 megohm.
R_{22} - 0.5 megohm.
R_{23} - 2.0 megohm (Vert.Gain)
R_{24} - 0.2 megohm.
R_{25} - 0.04 megohm.
R_{26} - 1000 ohm.
R_{27} - 2.0 megohm(Hor.Amp.)
R_{28} - 0.5 megohm.
R_{29} - 60,000ohm
R_{30} - 0.1 megohm(Frequency)
R_{31} - 1.0 megohm(Frequency)
R_{32} - 400 ohms
R_{33} - 15,000 ohms
R_{34} - 75,000 ohms.
R_{35} - 1.0 Megohm (Synchron.)
R_{36} - 0.1 megohm.
R_{37} - 0.5 megohm.
R_{38} - 400 ohms.
R_{39} - 2.0 megohm (Synchr.Phase).
R_{40} - 2500 ohms.

.....

C_4 - 2 Fd. 800 W.V.
C_5 - 0.5 Fd. 450 W.V.
C_6 - 0.5 Fd. 450 W.V.
C_7 - 0.1 Fd 600 W.V.
C_8 - 0.5 Fd 600 W.V.
C_9 - 0.5 Fd. 600 W.V..
C_{10} - 0.1 Fd. 600 W.V.
C_{11} - 0.5 Fd. 600 W.V.
C_{12} - 0.5 Fd. 600 W.V.
C_{13} - 0.25 Fd. 600 W.V.
C_{14} - 0.005 Fd. 1600 W.V.
C_{15} - 0.045 Fd. 1600 W.V.
C_{16} - 0.25 Fd. 600 W.V.
C_{17} - 0.5 Fd. 600 W.V.

.....

T_3 - 6F6
T_4 - 6SJ7
T_5 - 6SJ7
T_6 - GTIA.
T_7 - 39.

TR_3 - Transformer.
S_1 - Synchr. switch.

receiver is in tune.

The method of operation of the apparatus is briefly as follows. Starting at the low frequency end of the scale, the frequency of the receiver is increased at a constant rate and the transmitter kept in tune by means of the two monitoring devices. At intervals of 0.2 mc./sec. the output of the height-marking oscillator is applied to the recorder for a few seconds, using the foot key. The height-marking oscillator thus also marked out the frequency.

Using this method, the author obtained a number of records taken at half hourly intervals, for the morning period of the month September 1950. The nature of these records will be discussed later.

Johannesburg Records:

The ionosphere records obtained at the Telecommunication Research Laboratory in Johannesburg for the year 1949 have been put at the disposal of the author. These records are taken every 20 mins. throughout the day using automatic equipment. The apparatus covers the whole range of frequency used in one band. The frequency marks are at intervals of 1 mc./sec. and the height marks at 50 km. intervals.

These records are on 16 mm. film and are conveniently examined in a microfilm reader. Examples of records, as they appear in the reader, is shown in figs. 7 and 8.

MAGNETO-IONIC THEORY.

Elementary Theory:

Eccles [1]) and Larmor [3]) first applied the magneto-ionic theory of Lorentz [13]) to the ionosphere. In their simple theory they neglected the effect of the earth's magnetic field, and of collisional friction. They obtained the following expression for the refractive index of an ionised medium,

$$\mu = \sqrt{1 - \frac{ne^2}{\pi mf^2}} = \sqrt{1 - \frac{4\pi ne^2}{mp^2}} \qquad \text{-----(1).}$$

In this formula μ is the refractive index, m the mass of the ions and e their charge, f the frequency and p the angular frequency of the electromagnetic wave ($p = 2\pi f$).

The formula shows at once that the refractive index is reduced due to the presence of the ions; also that electrons , because of their much smaller mass m; are farmore effective than ions of molecular mass in reducing μ.

Consider a wave of frequency f travelling through the ionosphere. As the density of ionisation increases, the

refractive index is reduced until it becomes zero, at which point the wave is reflected back. Hence the density of ionisation corresponding to a wave of frequency f will be given by the equation

$$\mu = 0$$

$$\text{i.e.} \quad n = \frac{\pi m}{e^2} f^2 \qquad \text{-----(2).}$$

If values of e and m corresponding to the electron are substituted, the equation becomes

$$n = 1.24 \times 10^4 f^2 \qquad \text{-----(3).}$$

f being the frequency in mc./sec.

Appleton-Hartree formula:

Appleton and others have pointed out that if the scattering ions are electrons, the effect of the earth's magnetic field is very important and must be taken into account. The general theory has been developed mathematically for the case of propagation at any angle to the earth's field by Appleton [14]) and Hartree [15]) . In his derivation Hartree included the Lorentz polarisation term, which is a term arising out of the polarisation of the medium. The resulting "Appleton-Hartree formula" has been used in extensive numerical calculations by numerous workers.

Since then the validity of the inclusion of this term has been questioned, mainly by Darwin [16]. He made a thorough theoretical investigation and concluded that the term is zero for the ionosphere. Experimental results of Smith [17] as discussed by Benyon [18] gave definite evidence in support of the theoretical conclusions of Darwin. In view of this the Lorentz polarisation term is usually neglected in recent theoretical work on the ionosphere.

If the Lorentz polarisation term is omitted, the Appleton-Hartree formula for the complex refractive index cq becomes [19,20]

$$c^2q^2 = (\mu - ick/p)^2$$

$$= 1 - \frac{2p_o^2}{2(p^2-ipv) - \frac{p^2p_T^2}{p^2-p_o^2-ipv} \mp \sqrt{\frac{p^4p_T^4}{(p^2-p_o^2-ipv)^2} + 4p^2p_L^2}} \qquad \text{-----(4).}$$

In this formula

c = velocity of electromagnetic waves in vacuo.

k = a constant

v = collisional frequency of electrons with the gas molecules

$$p_o^2 = 4\pi ne^2/m \qquad \text{-----(5).}$$

$$p_T = \frac{eH_T}{mc} \qquad \text{-----(6a).}$$

$$p_L = \frac{eH_L}{mc} \qquad \text{-----(6b).}$$

H_L and H_T are the components of the earth's field, along and transverse to the direction of propagation respectively.

The formula (4) is very complex, and difficult to apply to experimental results. A certain amount of simplification is introduced if the effect of collisional friction is neglected. In this case formula (4) becomes, putting $v = 0$,

$$\mu^2 = 1 - \frac{2p_o^2}{2p^2 - \frac{p^2p_T^2}{p^2-p_o^2} \mp \sqrt{\frac{p^4p_T^4}{(p^2-p_o^2)^2} + 4p^2p_L^2}} \qquad \text{-----(7).}$$

Both the formulae (4) and (7) show that in the presence of the earth's field, the wave is split in two components, each corresponding to a different value of the refractive index. The magneto-ionic theory also shows that these waves are elliptically polarised in opposite directions. The wave corresponding to the lower sign in (4) and (7) is called the ordinary wave, and the one corresponding to the upper sign is referred to as the extraordinary wave. In the radio frequencies normally used

for the investigation of the ionosphere, the ordinary ray is less absorbed than the extraordinary. The characteristics of the ordinary wave are also least affected by the presence of a magnetic field. For these reasons the ordinary wave is used almost exclusively for the investigation of the ionosphere.

Conditions for Reflection:

As in the simple theory, the conditions for reflection of the ordinary and extraordinary rays are obtained by putting $c^2q^2 = 0$ in equation (4).

The condition for reflection for the ordinary ray is found to be the same as given by the simple theory, namely

$$p^2 = p_o^2$$

For the extraordinary ray $c^2q^2 = 0$ when

$$p_o^2 = p^2 \pm pp_H$$

where $p_H = \sqrt{p_L^2+p_T^2} = \frac{e}{mc}\sqrt{H_L^2 + H_T^2} = \frac{eH'}{mc}$

-----(8).

H′ being the total imposed magnetic field. Of the two values for the extraordinary ray, it will be appreciated that only the the value of p which corresponds to the smallest value of p_o^2 (and hence of n) will be of physical importance. The reason for this is that the ray will be

reflected at the smallest value of n where the refractive index is reduced to zero.

In view of this we may therefore say that a wave of angular frequency p will be reflected when

$$p^2 = p_o^2 \quad \text{(ordinary ray)} \qquad \text{-----(9).}$$

$$p^2 - pp_H = p_o^2 \quad \text{(extraordinary ray)} \qquad \text{-----(10).}$$

In this connection the remarks of Pande' [20]) who has made a survey of recent theoretical work on the ionosphere, are very interesting. He points out that the refractive index is a complex quantity and that it can never become equal to zero. Booker [21]) has therefore tried to formulate another criterion for reflection, but his results are not of much practical use. Rai [22]) has shown that neglecting collisional friction, a better criterion for reflection is obtained by putting the group velocity instead of the refractive index , equal to zero. He obtained an additional condition for reflection of the extraordinary ray which was experimentally verified by Pant andBajpai [23]) , Harang [24]), Jouast [25]) and Toshniwal [26]). Saha and Rai [27]) applying wave mechanics to the theory of the ionosphere, derived nearly the same formulae as Appleton and Hartree. Contrary to the ray treatment theyn find that at the point where $\mu = 0$ there may be considerable penetration.

Virtual Height:

The virtual height h′ is defined as the product of c and the time taken by the wave to reach a height h. Hence h′ is given by

$$h' = c\int_o^h \frac{dh}{U} \qquad \text{-----(11).}$$

U being the group velocity of the wave at a height h. The standard formula for the group velocity is

$$U = \frac{d}{dp}(\mu p) = \frac{d}{df}(\mu f) \qquad \text{-----(12).}$$

The simple expression for the refractive index of an ionised medium is given in (1) as

$$\mu^2 = 1 - \frac{ne^2}{mf^2}$$

$$= 1 - f_o^2/f^2$$

where $f_o^2 = \frac{ne^2}{\pi m}$

Substituting this value of μ in (12)

$$\frac{c}{U} = \frac{1}{\sqrt{1 - f_o^2/f^2}} = \frac{1}{\mu}$$

Equation (6) becomes

$$h' = \int_o^h \frac{dh}{\sqrt{1 - f_o^2/f^2}} \qquad \text{-----(13).}$$

De Groot [28]) first pointed out that equation (13) is a special form of Abel's integral equation. Appleton writes its solution as follows

$$h = \frac{2}{\pi} \int_0^{f_h} \frac{h' df}{\sqrt{f_h^2 - f^2}} \qquad \text{-----(14)}$$

In this formula h is the true height to which a wave of frequency f_h penetrates. Thus if the earth's magnetic field is neglected, true heights may be deduced from the curve showing the variation of virtual height with frequency. The way of doing this will be discussed later.

THEORY OF LAYER FORMATION.

Chapman's Theory:

Chapman [30,31] was the first to work out the theory of the formation of an ionosphere layer, due to the ionising action of the solar ultra-violet radiation on the earth's atmosphere. He found it necessary to make the following simplifying assumptions:

(i) The radiation is monochromatic.

(ii) The density of the atmosphere varies exponentially with height.

(iii) The atmosphere is at rest and uniform in composition.

(iv) The temperature of the atmosphere is the same at all points and at all times.

(v) The force of gravitation is constant with height.

(vi) All the absorbed energy causes ionisation.

Making these assumptions Chapman obtained curves of the rate of ion-production vs. height for different

lattitudes, seasons and times of the day and night. In his first paper he neglected the curvature of the earth, and he has since shown that the flat earth theory is valid as long as the sun's zenith does not exceed 75°. He has also extended the theory to the case of absorption of a band of solar radiation.

The following expression for the number of ions produced per second, is given by Gledhill and Szendrei [32]. It is equivalent to Chapman's expression in the case of a flat earth.

$$q = \frac{\beta n_o' I_\infty}{w} \exp\left\{ - \frac{C}{T_o}(h-h_o) - \frac{\beta n_o' T_o}{C} \sec\chi \exp\left[-\frac{C}{T_o}(h-h_o)\right]\right\}$$

-----(15).

In this formula

q = number of ions produced per sec. per c.c. at a height h.

h_o = height of the reference level.

n_o' = number of molecules per cc. at height h_o.

β = atomic absorption coefficient.

w = energy absorbed in ionising one molecule.

T_o = temperature at height h_o (supposed constant).

χ = sun's zenith distance.

C = Mg/k

M = mean molecular mass

k = Boltzmann's constant.

If the ions are produced according to (15), then the rate of increase of ion density is given by

$$\frac{dn}{dt} = q - \alpha n^2 \qquad \text{-----(16).}$$

n being the number of ions per cc. and α the effective recombination coefficient. Hulburt has pointed out that during the middle part of the day $\frac{dn}{dt}$ is very small and may be neglected in order to obtain an approximate value of n. Thus, putting $\frac{dn}{dt} = 0$ in (16),

$$n^2 = \frac{q}{\alpha}$$

$$= B \exp\left\{ - \frac{C}{T_o}(h - h_o) - \frac{1}{F} \exp\left[- \frac{C}{T_o}(h - h_o)\right]\right\} \qquad \text{-----(17).}$$

where

$$B = \frac{\beta n_o' I_\infty}{\alpha w} \qquad \text{-----(18).}$$

$$F = \frac{C \cos x}{n_o' T_o \beta} \qquad \text{-----(19).}$$

The maximum value of n with height is found by equating $\frac{dn}{dh}$ to zero. In this case

$$\frac{1}{F} \exp\left[- \frac{C}{T_o}(h - h_o)\right] = 1$$

Hence if h_m is the height of maximum ion density,

$$F = \exp\left[- \frac{C}{T_o}(h_m - h_o)\right] \qquad \text{-----(20).}$$

$$\text{i.e. } h_m = h_o - \frac{T_o}{C} \log_e F \qquad \text{-----(21).}$$

Substituting back in (17), it is found that the maximum ionic density, N, is given by

$$N^2 = BF \exp(-1) \qquad \text{-----(22).}$$

Hence, dividing equation (17) by (22),

$$(n/N)^2 = \frac{1}{F}\exp\left\{-\frac{C}{T_o}(h - h_o) + 1 - \frac{1}{F}\exp\left[-\frac{C}{T_o}(h - h_o)\right]\right\}$$

Substituting for F from (20), the expression becomes

$$(n/N)^2 = \exp\left\{1 + \frac{C}{T_o}(h_m - h) - \exp\left[\frac{C}{T_o}(h_m - h)\right]\right\}$$

-----(23)

At this stage we introduce the quantity known as the scale height of the layer, usually denoted by H. It is defined by the equation

$$H = \frac{T}{C} = \frac{kT}{Mg} \qquad \text{-----(24).}$$

$$(n/N)^2 = \exp\left\{1 - \frac{h_m - h}{H} - \exp\frac{h_m - h}{H}\right\}$$

$$= \exp(1 - x - e^x) \qquad \text{-----(25).}$$

where $$x = \frac{h_m - h}{H} \qquad \text{-----(26).}$$

Linear Temperature Gradient:

The most obvious defect in Chaman's theory is the assumption that the temperature is constant throughout

the layer. Gledhill and Szendrei [32]) therefore worked out the theory of ionisation in an atmosphere where the temperature is a linear function of the height.

They assume that the temperature T at a height h is given by the equation

$$T = T_o + \gamma (h - h_o) \qquad \text{-----(27).}$$

T_o being the temparature at the reference height h_o, and γ the temperature gradient. They also make the assumptions

(i) The radiation is monochromatic.

(ii) The atmosphere is at rest and is uniform in composition.

(iii) The force of gravitation is constant with height.

(iv) All the absorbed energy causes ionisation.

Their expression for the rate of production of the ions is as follows

$$q = \frac{\beta n_o' I_\infty}{w} \left\{1 + \gamma \frac{h - h_o}{T_o}\right\}^{-(1+\frac{c}{\gamma})} \exp\left\{- \frac{\beta n_o' T_o}{C} \sec\chi \left(1+\gamma\frac{h-h_o}{T_o}\right)^{-\frac{c}{\gamma}}\right\}$$

-----(28).

Assuming as before, that during the middle part of the day $\frac{dn}{dt}$ may be neglected, it followsthat

$$n^2 = B \left(1 + \gamma \frac{h-h_o}{T_o}\right)^{-(1+\frac{C}{\gamma})} \exp\left\{- \frac{1}{F}\left(1 + \gamma\frac{h-h_o}{T_o}\right)^{-\frac{C}{\gamma}}\right\}$$

-----(29).

Putting $\frac{dn}{dh} = 0$, as before, we get the condition for maximum ionic density as

$$\frac{1}{F}\left(1 + \gamma\frac{h_M - h_o}{T_o}\right)^{-\frac{C}{\gamma}} = 1 + \frac{\gamma}{C} \qquad \text{-----(30)}.$$

This gives

$$h_m = h_o + \frac{T_o}{\gamma}\left[\left\{F\left(1 - \frac{\gamma}{C}\right)\right\}^{-\frac{\gamma}{C}} - 1\right] \qquad \text{-----(31)}.$$

The maximum ionic density is therefore given by

$$N^2 = BF\left(1 + \frac{\gamma}{C}\right)^{(1+\gamma/C)} \exp\left\{-\left(1 + \frac{\gamma}{C}\right)\right\} \qquad \text{-----(32)}.$$

Hence dividing (29) by (32),

$$(n/N)^2 = \left(1+\gamma\frac{h-h_o}{T_o}\right)^{-(1+\frac{C}{\gamma})} \left\{F\left(1+\frac{\gamma}{C}\right)\right\}^{-(1+\frac{\gamma}{C})} \exp\left\{1+\frac{\gamma}{C} - \frac{1}{F}\left(1+\gamma\frac{h-h_o}{T_o}\right)^{-\frac{C}{\gamma}}\right\}$$

$$\text{-----(33)}.$$

As pointed out by O'Brien [12], it is possible to introduce considerable simplification in the equation for (n/N) by choosing as reference height the height of maximum ionic density. This means that in the equations we substitute

$$h_o = h_m$$

$$T_o = T_m$$

$$B = B_m = \frac{\beta n_m' I_\infty}{\alpha w}$$

$$F = F_m = \frac{C \cos\chi}{n'_m T_m \beta}$$

n'_m being the number of molecules per cc. at height h_m.

Making these substitutions equation (30) becomes

$$\frac{1}{F_m} = 1 + \frac{\gamma}{C}$$

$$\therefore N^2 = B_m \exp\left[-\left(1 + \frac{\gamma}{C}\right)\right]$$

$$\therefore (n/N)^2 = \left(1 - \gamma \frac{h_m - h}{T_m}\right)^{-\left(1+\frac{C}{\gamma}\right)} \exp\left\{\left(1+\frac{\gamma}{C}\right)\left[1 - \left(1 - \frac{h_m - h}{T_m}\right)^{-\frac{C}{\gamma}}\right]\right\}$$

These equations may be simplified by introducing the variables

$$x = \frac{C}{T_m}(h_m - h) \qquad \text{-----(34).}$$

$$y = C/\gamma \qquad \text{-----(35).}$$

The expression for (n/N) becomes

$$(n/N)^2 = (1 - x/y)^{-(1+y)} \exp\left\{\left(1 + \frac{1}{y}\right)\left[1 - (1 - x/y)^{-y}\right]\right\}$$

-----(36).

It may be pointed out that if the temperature is not constant, the scale height H will vary with the height. As the scale height also depend on g and on M , the mean molecular mass, a variation in these will also cause the scale height to vary with h .In our theory

these quantities are supposed constants, but the theory will also apply to the general case where H is a linear function of the height. The value of γ found experimentally will not however necessarily be the temperature gradient.

A STUDY OF E LAYER CRITICAL FREQUENCIES.

It was pointed out in the introduction that the ionosphere consists of two main layers in the daytime, namely the E and F layers. Figure 4 shows an idealised virtual height-frequency curve obtained when only these two layers are present.

Considering the ordinary ray first, it will be seen that at low frequencies the radio waves are reflected from a virtual height of approximately 120 km., corresponding to the E layer. As the frequency is increased the wave penetrates deeper into the layer and at a frequency f_c , called the critical frequency , it penetrates the E layer. At higher frequencies the wave is reflected from the much higher F layer. If the frequency is sufficiently increased the wave penetrates the F layer too, and is not reflected back.

The extraordinary curve is very similar to the ordinary,

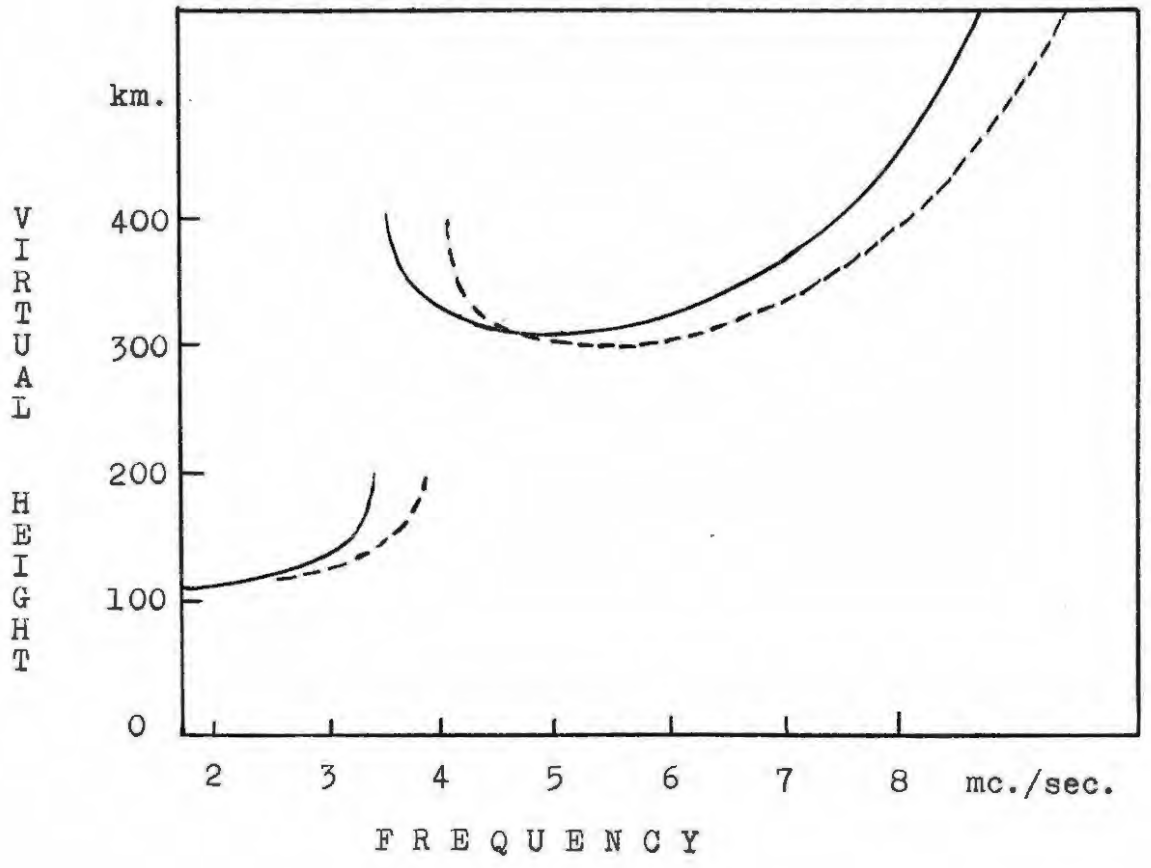

FIG. 4 - VIRTUAL HEIGHT CURVES WHEN ONLY THE E AND F LAYERS ARE PRESENT.

——— Ordinary ray

- - - - Extraordinary ray

except that it is displaced through a frequency of about 0.5 mc./sec. The splitting of the magneto-ionic components shows clearly that the scattering particles in the E and F layers are electrons. It may be remarked that due to absorption, the extraordinary reflections are much weaker than the ordinary, and that the extraordinary reflection from the E layer is not normally observed except in the early morning and late afternoon.

The E_2 layer:

During the day in summer the F layer usually splits in two separate layers. Fig. 5 shows a typical daytime record with reflections from both the F_1 and F_2 layers. For simplicity only the ordinary reflections are shown.

In 1933 Schafer and Goodall [33]) reported the occurrence of a layer intermediate between the E and F layers, at a height of approximately 150 km. They suggested that the space between the E and F layers is normally ionised to a value below the maximum of the E layer, and that the intermediate layer is observed when the ionisation rises above the E maximum. Appleton [34]) observed the layer to occur mainly in the early morning. Ratcliffe and White [35]) found that the layer consists mostly of electrons.

Hollingworth [36]) has suggested a method of measuring

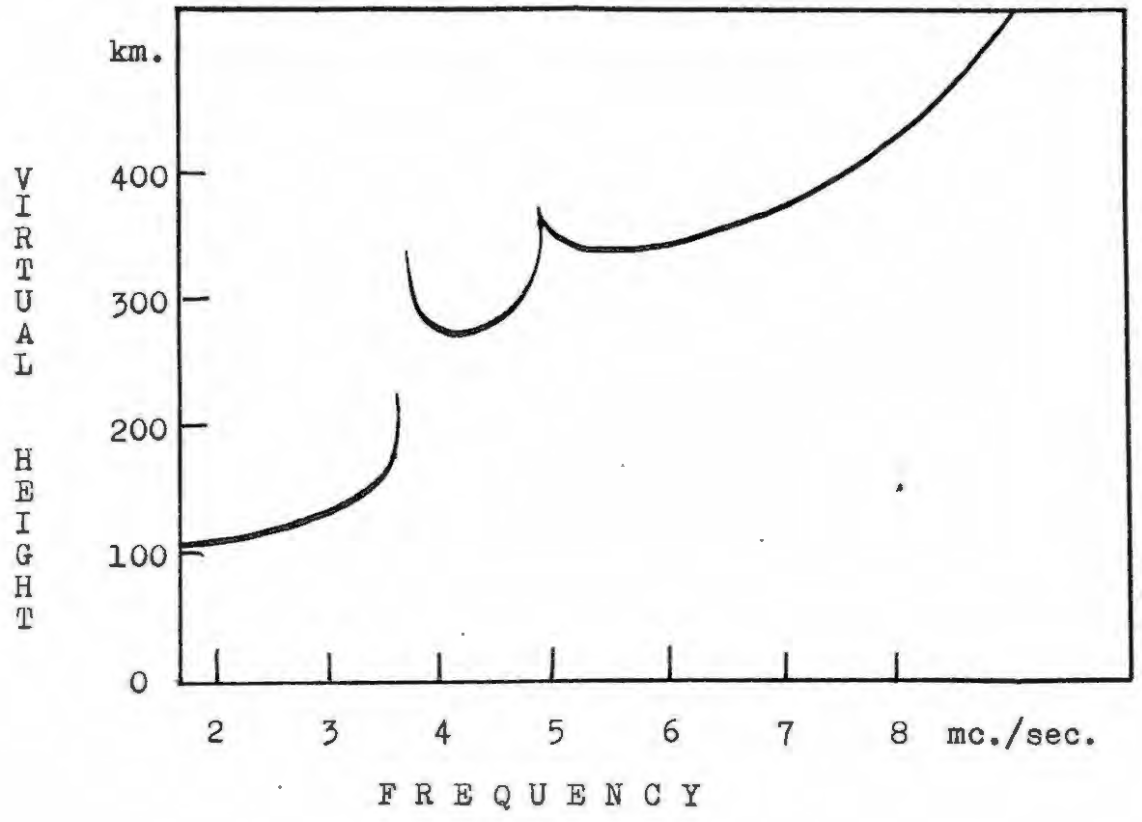

FIG. 5 - VIRTUAL HEIGHT CURVE WHEN F_1 LAYER PRESENT.

the intensity of ionisation in the space between the E and F layers by observing the relative group retardation of the two components of a pulse whose frequency is so close to the critical frequency that the one component is reflected from the E layer and the other from the F region. From his results he concluded that the space between the main layers is ionised to a value very little less than the maximum E ionisation.

Fig. 6 is a virtual height-frequency curve showing clearly the reflection from the intermediate region, usually referred to as the E_2 layer. E_2 reflections can readily be distinguished from F_1 reflections by noting that

(i) It occurs at a lower virtual height, normally below 200 km.
(ii) It occurs at lower frequencies.
(iii) It shows a marked discontinuity at the critical frequency.
(iv) The E_2 layer normally found to occur only in the early morning.

Abnormalities in the E layer:

Before the discovery of the E_2 layer, various workers had noticed another type of irregularity in the lower layers. In 1929 Eckersley [37]) found that radio signals were frequently scattered into the skip zone. He attributed

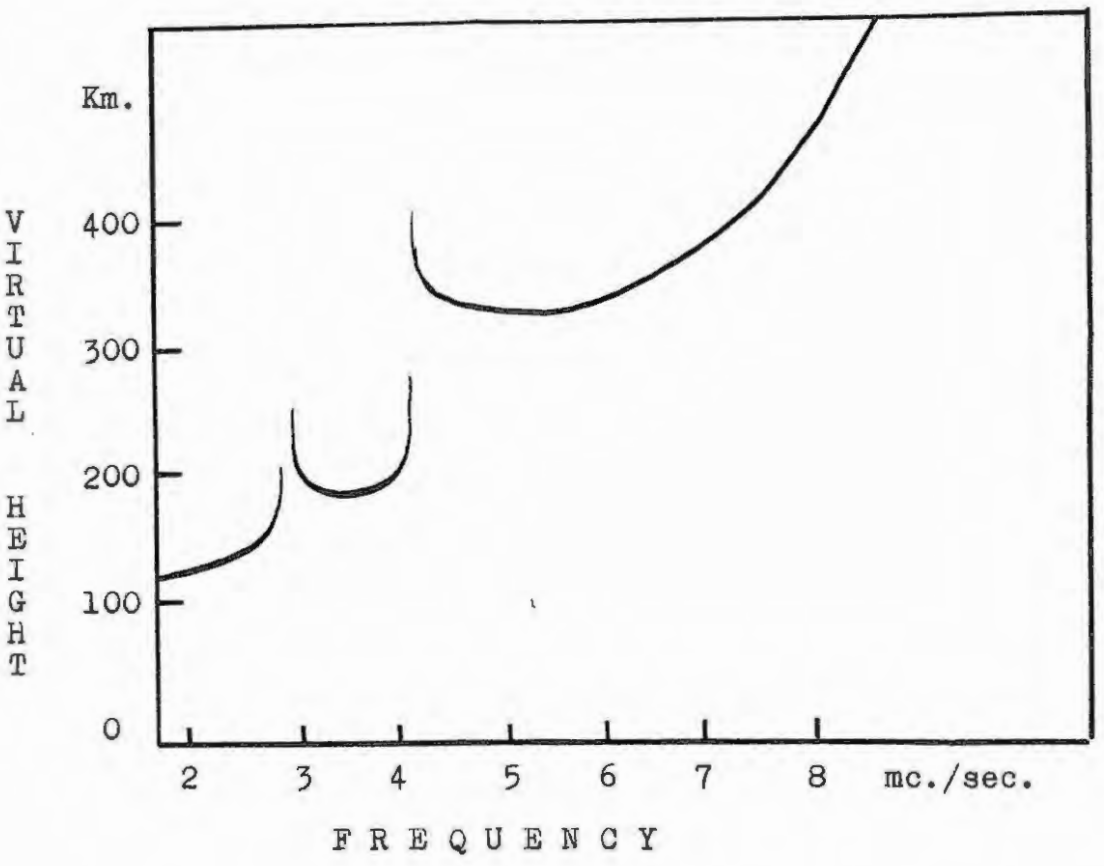

FIG. 6 - VIRTUAL HEIGHT CURVE WHEN E_2 LAYER PRESENT.

this effect to the presence of densely ionised clouds at a height of about 120 km. In 1930 Appleton [38]) noted the occurrence of echoes at nighttime from a height corresponding to the E layer, at frequencies far in excess of the normal critical frequencies. Appleton and Naismith[39]) soon found the abnormal intense ionisation to occur during the daytime as well, particularly in summer.

We shall consider abnormal effects in the E layer to be characterised by the following properties of the (h;f)-curve. The trace is very flat and shows very little rise in virtual height with increasing frequency. A sudden jump from E to F reflection occurs but there does not seem to be a definite critical frequency as there is usually some overlapping.

Figure 7 shows the usual type of record obtained during the middle part of the day in Johannesburg (only ordinary ray reflections are present in the case of the E layer) This type of record was first observed by Appleton and his collaborators [40,41,42]) .At low frequencies the wave is reflected from the normal E region which has a critical frequency f_c (see fig. 7a). At frequencies just above f_c the wave is reflected from the abnormal E region , situated just above the normal

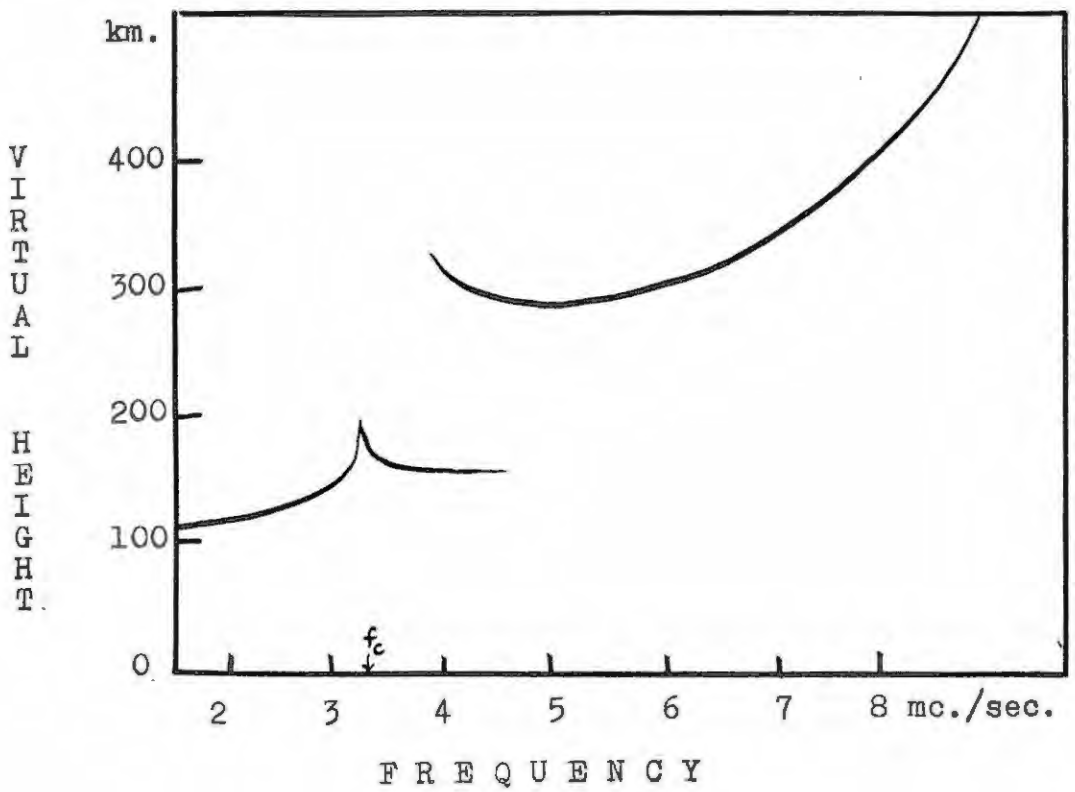

FIG. 7(a) - USUAL TYPE OF RECORD OBTAINED DURING MIDDLE PART OF DAY.

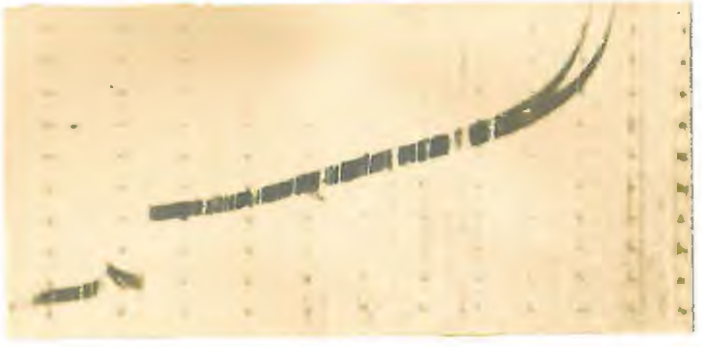

FIG. 7(b) - JOHANNESBURG RECORD
1500 HRS. 3 OCT. 1949.

(Frequency marks at intervals of 1.0 mc./sec., starting at 3.0 mc./sec.; height marks at intervals of 50 km., starting at 100 km.).

layer. The fact that the curve shows very little rise in h' with increasing frequency, indicates that the layer is very thin. The photograph shows a sudden jump from E to F reflection, but usually there is some overlapping as indicated in the diagram.

The abnormality that was first noticed by Appleton and others is however of a much more disturbed nature, and is caused by a much denser ionisation. This is well illustrated in fig. 8 which shows a "sporadic" E reflection up to a frequency of at least 16 mc./sec. This sporadic reflection may occur at any time of the day or night, and may last any length of time. In the photograph the frequency f_c is still visible at 3.9 mc./sec. , showing that the effect takes place above the normal layer. It may however, also occur below the maximum E ionisation , in which case the frequency f_c is absent.

The nomenclature at present is not uniform; following Appleton we shall refer to the above two irregularities as "abnormal E" (or E_a) and "sporadic E" (or E_s) respectively, as distinct from the E_2 layer.

Johannesburg Records:

For the purpose of studying the E layer the records from Johannesburg for the daytime period of the year 1949

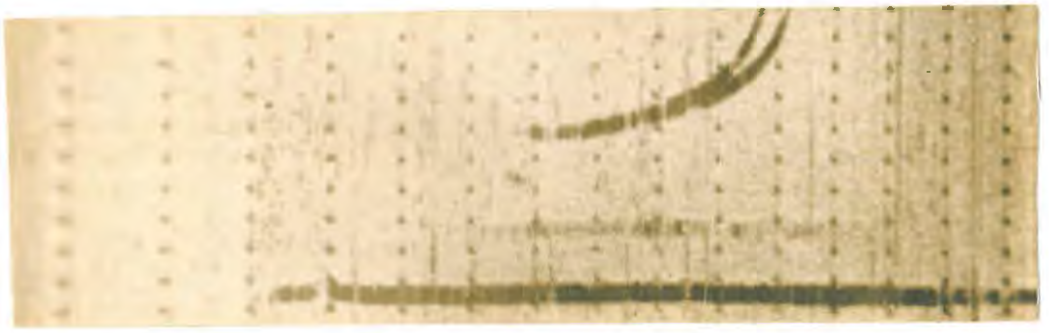

FIG. 8 - JOHANNESBURG RECORD SHOWING SPORADIC REFLECTIONS 1100 HRS. 16 NOV. 1949

(Frequency marks at intervals of 1.0 mc./sec., starting at 1.0 mc./sec.;height marks at intervals of 50 km., starting at 100 km.).

were examined in the microfilm reader. Due to lack of time it was not found possible to look at the nighttime records as well for the occurrence of the sporadic E layer.

From each record the following five quantities were read off, from the ordinary ray traces (see fig. 9):

f_1 - the frequency where E reflection shows a maximum;

f_2 - the frequency where F reflection first occurs;

f_3 - the frequency where the E reflection disappears;

h_1' - approximate height of normal E layer. This height corresponds to the virtual height at a frequency approximately 5/6 f_c (see later);

h_2' - virtual height of the flat part ofthe E_a reflection.

The frequencies could be estimated to 0.1 mc./sec. and the heights to 5 km. The records were sometimes not easy to deal with, the difficulty arising mainly from the width of the trace. This width usually corresponded to about 15 km. virtual height, so that it was sometimes difficult to distinguish between the ordinary and extraordinary reflections when both were present.

When no abnormal E reflections occurred, it was shown by the absence of the reading h_2'. Sporadic E reflections were characterised by an abnormal high value of f_3. The value of f_2 was usually affected by the presence of the sporadic layer.

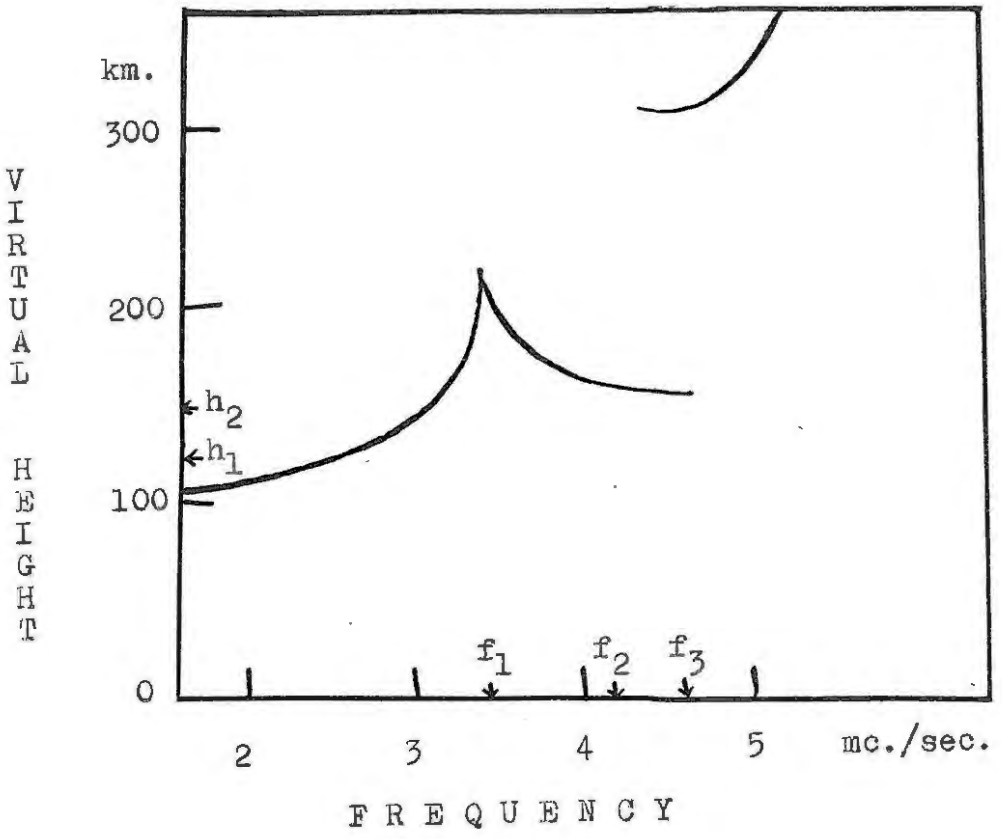

FIG. 9 - E LAYER CRITICAL FREQUENCIES AND VIRTUAL HEIGHTS.

The E_2 reflections were grouped with the normal layer; i.e. the critical frequency and approximate virtual height were entered under f_1 and h_1' respectively.

Monthly means of the quantities f_1, f_2, f_3, h_1', and h_2' at 20 mins. interval are given in table 1. In calculating these means, all values of frequency that deviated excessively from the mean values were neglected. In particular the the high values of f_2 and f_3 caused by a sporadic effect were not included in the mean values.

In table 1 the values of h_2' are only given for the times when they were found to be present for more than half the month. E_2 reflections were found to be rather infrequent, even in the early morning, so that this layer does not show in the monthly means.

It was hoped to correlate the frequencies with the magnetic activity, but this project was not found possible due to lack of time.

TABLE 1 - JANUARY 1949.

Time SAMT	f_1 mc/sec.	f_2 mc/sec	f_3 mc/sec	h'_1 km.	h'_2 km.
0600	2.02	2.36	2.62	125	136
0620	2.30	2.62	3.00	122	131
0640	2.56	2.89	3.30	121	128
0700	2.75	3.06	3.47	121	128
0720	2.89	3.33	3.72	121	129
0740	3.08	3.48	3.74	121	129
0800	3.27	3.53	3.88	121	130
0820	3.41	3.64	3.87	120	130
0840	3.51	3.85	3.81	120	128
0900	3.60	3.88	4.00	119	127
0920	3.69	4.07	4.00	119	127
0940	3.72	4.13	3.98	120	127
1000	3.79	4.23	4.10	120	127
1020	3.87	4.32	4.11	119	-
1040	3.91	4.37	4.13	120	-
1100	3.95	4.41	4.17	120	127
1120	3.92	4.47	4.21	120	129
1140	4.01	4.50	4.22	120	129
1200	4.03	4.49	4.24	120	129
1220	3.99	4.47	4.22	120	128
1240	3.93	4.51	4.35	120	128
1300	4.00	4.51	4.28	120	129
1320	3.96	4.52	4.23	120	128
1340	3.94	4.49	4.26	120	130
1400	3.87	4.54	4.32	120	130
1420	3.92	4.43	4.20	120	130
1440	3.91	4.43	4.31	120	131
1500	3.76	4.38	4.24	120	131
1520	3.71	4.33	4.30	120	130
1540	3.58	4.05	4.09	120	129
1600	3.52	4.10	4.09	120	130
1620	3.48	3.89	3.99	119	129
1640	3.32	3.93	4.14	120	131
1700	3.15	3.59	3.87	119	130
1720	2.95	3.51	3.96	120	129
1740	2.63	3.19	3.75	120	128
1800	2.47	3.11	3.64	120	128

TABLE 1 - FEBRUARY 1949.

Time SAMT	f_1 mc/sec.	f_2 mc/sec.	f_3 mc/sec.	h'_1 km.	h'_2 km.
0600	1.73	1.96	2.29	130	136
0620	2.08	2.31	2.58	127	
0640	2.39	2.57	3.00	125	134
0700	2.65	2.83	3.26	122	131
0720	2.88	3.04	3.45	120	129
0740	3.06	3.22	3.66	120	128
0800	3.24	3.39	3.80	120	128
0820	3.37	3.63	3.92	120	130
0840	3.43	3.74	4.23	121	130
0900	3.59	3.78	4.14	120	129
0920	3.73	3.96	4.19	120	128
0940	3.86	4.16	-	120	127
1000	3.94	4.20	4.16	120	128
1020	3.97	4.31	-	120	129
1040	3.97	4.33	-	120	128
1100	3.93	4.34	4.08	120	-
1120	4.03	4.43	4.06	120	-
1140	4.03	4.43	4.10	120	-
1200	4.07	4.38	4.15	120	-
1220	3.98	4.38	4.17	120	-
1240	3.96	4.34	4.12	120	-
1300	3.97	4.35	4.14	120	-
1320	3.93	4.34	4.15	120	-
1340	3.99	4.28	4.08	120	-
1400	3.87	4.21	4.22	120	-
1420	3.86	4.21	4.20	120	-
1440	3.83	4.13	4.12	120	-
1500	3.76	4.09	4.06	120	130
1520	3.79	4.09	4.10	120	128
1540	3.70	3.86	4.00	120	129
1600	3.58	3.86	3.94	120	130
1620	3.46	3.67	4.00	120	130
1640	3.33	3.50	3.84	120	129
1700	3.18	3.35	3.66	120	130
1720	2.97	3.11	3.62	120	129
1740	2.68	2.88	3.48	120	129
1800	2.35	2.60	3.35	119	129

TABLE 1 - MARCH 1949.

Time SAMT.	f_1 mc/sec.	f_2 mc/sec.	f_3 mc/sec.	h'_1 km.	h'_2 km.
0600		1.56			
0620	1.73	1.95	2.42		
0640	2.02	2.34	2.48	127	135
0700	2.43	2.67	3.00	124	140
0720	2.66	2.82	3.23	122	136
0740	2.83	3.06	3.41	121	137
0800	3.06	3.31	3.65	120	135
0820	3.19	3.68	3.79	120	133
0840	3.37	3.57	3.91	120	134
0900	3.52	3.79	4.00	120	133
0920	3.61	3.91	4.15	120	132
0940	3.64	3.97	4.14	120	131
1000	3.66	4.03	4.06	120	129
1020	3.73	4.15	4.05	120	132
1040	3.77	4.25	4.09	120	132
1100	3.85	4.24	4.17	120	131
1120	3.94	4.26	3.95	120	131
1140	3.94	4.30		120	132
1200	3.97	4.34	4.24	120	-
1220	3.89	4.31		120	-
1240	3.92	4.28	4.09	120	-
1300	3.93	4.29	4.09	120	-
1320	3.95	4.29	4.11	120	-
1340	3.93	4.22	4.03	120	-
1400	3.89	4.16	4.06	120	134
1420	3.90	4.12	4.00	121	135
1440	3.79	4.03	4.00	120	134
1500	3.71	3.90	3.90	120	134
1520	3.63	3.80	3.90	120	135
1540	3.56	3.71	3.90	120	134
1600	3.39	3.56	3.86	120	133
1620	3.23	3.44	3.84	121	133
1640	3.08	3.27	3.69	122	133
1700	2.85	3.03	3.65	123	132
1720	2.50	2.80	3.35	123	131
1740	2.23	2.56	3.08	122	131

TABLE 1 - APRIL 1949

Time SAMT.	f_1 mc/sec	f_2 mc/sec	f_3 mc/sec	h'_1 km.	h'_2 km.
0620		1.62			
0640	1.82	2.06	2.04	122	-
0700	2.12	2.37	2.80	122	-
0720	2.30	2.61	3.07	120	-
0740	2.62	2.83	3.28	120	-
0800	2.78	3.04	3.47	119	-
0820	2.99	3.22	3.47	119	--
0840	3.09	3.35	3.60	119	-
0900	3.16	3.54	3.65	119	-
0920	3.35	3.65	3.73	118	-
0940	3.46	3.73	3.87	118	--
1000	3.52	3.82	3.99	118	135
1020	3.59	3.90	4.03	118	134
1040	3.65	4.00	4.00	120	134
1100	3.71	4.00	4.06	118	132
1120	3.70	4.07	4.10	118	131
1140	3.77	4.12	4.15	118	132
1200	3.79	4.18	4.16	118	131
1220	3.82	4.19	4.23	119	133
1240	3.84	4.22	4.13	119	136
1300	3.82	4.19	4.23	119	133
1320	3.75	4.10	4.03	119	133
1340	3.75	4.10	4.03	119	131
1400	3.70	4.01	3.98	120	131
1420	3.68	3.94	4.08	120	129
1440	3.57	3.89	4.03	120	131
1500	3.50	3.86	4.02	120	127
1520	3.39	3.71	3.88	120	127
1540	3.29	3.58	3.78	120	128
1600	3.11	3.39	3.59	120	126
1620	2.89	3.15	3.36	120	131
1640	2.63	2.97	3.37	120	129
1700	2.24	2.66	3.07	120	123
1720	2.02	2.41	2.98	119	121
1740		2.19			

TABLE 1 - MAY 1949.

Time SAMT.	f_1 mc/sec.	f_2 mc/sec.	f_3 mc/sec.	h'_1 km.	h'_2 km.
0640	1.59	1.71	1.70		
0700	1.81	2.01	2.02		
0720	2.08	2.40	2.33	126	-
0740	2.34	2.59	2.66	124	-
0800	2.52	2.72	2.95	122	133
0820	2.66	2.92	3.21	121	132
0840	2.92	3.10	3.32	120	137
0900	3.08	3.26	3.38	119	137
0920	3.18	3.31	3.47	120	-
0940	3.25	3.43	3.53	120	-
1000	3.35	3.53	3.58	120	-
1020	3.34	3.61	3.71	120	147
1040	3.45	3.72	3.75	120	135
1100	3.53	3.74	3.81	120	137
1120	3.56	3.86	3.84	120	136
1140	3.61	3.87	3.86	120	137
1200	3.63	3.93	3.95	119	141
1220	3.63	3.89	3.94	119	140
1240	3.58	3.86	3.90	119	148
1300	3.55	3.82	3.80	119	148
1320	3.54	3.71	3.78	119	150
1340	3.52	3.73	3.73	119	139
1400	3.50	3.68	3.70	119	139
1420	3.36	3.60	3.69	119	138
1440	3.32	3.53	3.56	119	135
1500	3.20	3.47	3.51	120	139
1520	3.06	3.34	3.43	120	130
1540	2.90	3.16	3.37	120	132
1600	2.71	2.95	3.23	120	136
1620	2.55	2.74	3.01	120	132
1640	2.28	2.58	2.88	119	136
1700	1.95	2.39	2.75	120	-
1720		2.04			

TABLE 1 - JUNE 1949.

Time SAMT.	f_1 mc/sec	f_2 mc/sec.	f_3 mc/sec.	h'_1 km.	h'_2 km.
0700		1.89			
0720	1.94	2.27	2.39		
0740	2.28	2.48	2.61	131	-
0800	2.52	2.67	2.91	127	-
0820	2.61	2.93	3.15	124	-
0840	2.80	3.04	3.30	121	-
0900	3.01	3.20	3.40	120	-
0920	3.15	3.33	3.50	120	-
0940	3.28	3.46	3.55	120	151
1000	3.33	3.53	3.64	120	153
1020	3.43	3.62	3.77	120	151
1040	3.44	3.69	3.75	120	144
1100	3.50	3.76	3.97	120	145
1120	3.57	3.88	3.98	120	143
1140	3.56	3.85	4.02	120	153
1200	3.60	3.91	4.00	120	149
1220	3.60	3.91	4.02	120	149
1240	3.58	3.84	3.96	120	143
1300	3.54	3.84	3.96	120	139
1320	3.52	3.80	4.01	120	137
1340	3.43	3.70	3.96	120	135
1400	3.36	3.66	4.10	120	133
1420	3.29	3.59	3.91	120	136
1440	3.22	3.55	3.85	120	134
1500	3.11	3.39	3.80	120	130
1520	2.97	3.21	3.66	120	130
1540	2.80	3.03	3.66	120	137
1600	2.65	2.91	3.42	120	136
1620	2.98	2.82	3.89	122	136
1640	2.07	2.60	3.02	121	-
1700	1.98	2.32	2.89	122	--
1720		1.89			

TABLE 1 - JULY 1949.

Time SAMT.	f_1 mc/sec	f_2 mc/sec	f_3 mc/sec.	h'_1 km.	h'_2 km.
0700	1.75	1.84	1.87		
0720	2.00	2.22	2.26	132	182
0740	2.23	2.46	2.62	124	-
0800	2.52	2.70	2.91	123	-
0820	2.71	2.85	3.10	121	-
0840	2.89	2.98	3.23	120	-
0900	3.07	3.18	3.34	120	-
0920	3.19	3.31	3.51	120	-
0940	3.28	3.48	3.64	119	-
1000	3.35	3.56	3.66	119	147
1020	3.44	3.60	3.78	119	148
1040	3.48	3.66	3.80	118	157
1100	3.54	3.73	3.91	119	157
1120	3.54	3.83	3.95	120	150
1140	3.57	3.85	3.95	120	149
1200	3.56	3.96	3.99	120	146
1220	3.58	3.94	3.99	120	149
1240	3.60	3.89	3.94	120	138
1300	3.54	3.92	4.01	120	138
1320	3.52	3.81	3.95	120	139
1340	3.46	3.79	3.95	120	138
1400	3.43	3.70	3.89	120	142
1420	3.33	3.59	3.93	120	133
1440	3.28	3.50	3.96	120	145
1500	3.16	3.44	3.92	119	145
1520	3.07	3.37	3.82	119	135
1540	2.89	3.14	3.59	119	133
1600	2.78	2.98	3.62	119	139
1620	2.62	2.74	3.31	119	-
1640	2.58	2.52	3.12	119	-
1700	2.00	2.40	3.08	120	-

TABLE 1 - AUGUST 1949.

Time SAMT.	f_1 mc/sec.	f_2 mc/sec.	f_3 mc/sec.	h'_1 km.	h'_2 km.
0640		1.82			
0700	1.73	2.16	2.17		
0720	2.07	2.43	2.56	127	-
0740	2.47	2.57	2.87	122	-
0800	2.72	2.84	3.18	121	-
0820	2.91	3.00	3.22	120	-
0840	3.10	3.16	3.43	119	-
0900	3.19	3.29	3.53	118	-
0920	3.33	3.39	3.68	118	-
0940	3.45	3.49	3.70	118	-
1000	3.51	3.59	3.71	118	159
1020	3.56	3.67	3.79	118	150
1040	3.65	3.70	3.86	118	148
1100	3.62	3.82	3.92	118	147
1120	3.65	3.81	3.91	119	147
1140	3.68	3.87	3.97	119	143
1200	3.74	3.89	3.94	119	142
1220	3.73	3.91	3.96	119	142
1240	3.62	3.93	3.99	119	139
1300	3.65	3.92	3.98	119	138
1320	3.62	3.90	4.01	119	138
1340	3.56	3.80	4.00	120	138
1400	3.50	3.76	3.97	120	129
1420	3.45	3.68	3.81	120	127
1440	3.32	3.46	3.79	120	128
1500	3.32	3.46	3.66	120	129
1520	3.16	3.39	3.66	120	131
1540	3.05	3.21	3.60	120	126
1600	2.94	3.03	3.37	120	-
1620	2.79	2.88	3.19	122	-
1640	2.62	2.65	3.08	123	-
1700	2.45	2.48	2.75	123	-
1720	2.09	2.20			

TABLE 1 - SEPTEMBER 1949.

Time SAMT.	f_1 mc/sec.	f_2 mc/sec.	f_3 mc/sec.	h'_1 km.	h'_2 km.
0640	2.24	2.35	2.51	128	-
0700	2.48	2.59	2.90	126	-
0720	2.74	2.81	3.09	123	-
0740	2.92	3.02	3.30	121	-
0800	3.15	3.19	3.38	118	-
0820	3.25	3.32	3.55	117	-
0840	3.39	3.48	3.62	117	-
0900	3.51	3.59	3.75	117	-
0920	3.61	3.69	3.87	118	-
0940	3.70	3.77	3.84	118	-
1000	3.78	3.83	3.91	117	-
1020	3.78	3.89	3.95	118	-
1040	3.87	3.96	3.98	118	-
1100	3.88	4.03	3.98	118	-
1120	3.91	4.12	4.02	118	158
1140	3.90	4.08	4.05	118	154
1200	3390	4.08	4.05	119	154
1220	3.90	4.09	4.03	119	155
1240	3.88	4.14	4.04	119	146
1300	3.89	4.08	4.03	119	148
1320	3.86	4.09	4.03	119	148
1340	3.84	4.02	4.01	119	139
1400	3.77	3.98	4.00	119	133
1420	3.71	3.92	3.98	119	136
1440	3.64	3.81	3.99	120	136
1500	3.53	3.72	3.92	119	130
1520	3.43	3.60	3.97	119	127
1540	3.31	3.50	3.93	119	127
1600	3.14	3.25	3.78	119	126
1620	2.93	3.09	3.55	120	123
1640	2.68	2.84	3.32	121	-
1700	2.42	2.69	3.16	123	-
1720	2.10	2.47	2.64	121	-
1740		2.14			

TABLE 1 - OCTOBER 1949.

Time SAMT.	f_1 mc/sec.	f_2 mc/sec.	f_3 mc/sec.	h'_1 km.	h'_2 km.
0600	1.97	2.20	2.19		
0620	2.28	2.53	2.64		
0640	2.59	2.72	2.96	122	-
0700	2.80	2.95	3.20	120	-
0720	2.98	3.15	3.44	118	158
0740	3.17	3.32	3.57	117	148
0800	3.34	3.48	3.67	117	142
0820	3.44	3.64	3.75	117	143
0840	3.55	3.73	3.93	117	137
0900	3.61	3.88	3.92	117	150
0920	3.73	3.90	4.03	117	151
0940	3.79	4.08	4.00	117	149
1000	3.85	4.09	3.96	118	-
1020	3.94	4.09	4.01	118	-
1040	3.95	4.16	4.05	118	-
1100	3.99	4.19	4.09	118	-
1120	4.02	4.24	4.14	118	-
1140	4.03	4.27	4.19	118	144
1200	4.03	4.24	4.12	118	150
1220	4.01	4.30	4.10	118	142
1240	4.00	4.25	4.15	118	138
1300	3.97	4.23	4.04	118	132
1320	3.93	4.16	4.10	118	139
1340	3.86	4.18	4.14	118	139
1400	3.81	4.10	4.11	118	138
1420	3.77	4.02	4.07	118	136
1440	3.69	3.98	4.03	118	135
1500	3.64	3.90	4.01	118	135
1520	3.54	3.85	4.00	119	129
1540	3.41	3.66	4.00	119	124
1600	3.29	3.54	3.96	119	129
1620	3.08	3.34	3.85	120	128
1640	2.82	3.14	3.66	122	127
1700	2.60	2.96		124	126
1720	2.30	2.74		123	123
1740	1.97	2.51			

TABLE 1 - NOVEMBER 1949.

Time SAMT.	f_1 mc/sec.	f_2 mc/sec.	f_3 mc/sec.	h'_1 km.	h'_2 km.
0600	2.33	2.48	2.70	126	-
0620	2.59	2.74	3.03	123	-
0640	2.76	2.88	3.25	120	-
0700	2.97	3.14	3.45	119	-
0720	3.17	3.31	3.64	118	-
0740	3.32	3.45	3.72	117	-
0800	3.44	3.61	3.81	117	-
0820	3.56	3.68	3.89	117	-
0840	3.61	3.76	3.88	117	143
0900	3.72	3.99	4.00	117	140
0920	3.76	4.00	4.00	117	138
0940	3.82	4.11	4.09	117	135
1000	3.91	4.19	4.15	117	135
1020	3.95	4.23	4.18	117	-
1040	3.98	4.30	4.15	117	133
1100	4.03	4.32	4.21	117	131
1120	4.06	4.33	4.12	117	--
1140	4.00	4.36	4.13	117	-
1200	4.03	4.31	4.18	117	-
1220	4.04	4.34	4.17	117	-
1240	4.04	4.33	4.17	117	-
1300	4.02	4.33	4.07	117	-
1320	4.04	4.23	4.14	117	-
1340	3.99	4.18	4.08	118	-
1400	3.95	4.11	4.06	117	-
1420	3.83	4.09	4.01	117	-
1440	3.80	3.98	4.00	118	-
1500	3.73	3.94	4.05	118	-
1520	3.64	3.79	3.93	118	-
1540	3.55	3.67	3.88	118	-
1600	3.38	3.54	3.76	119	131
1620	3.34	3.26	3.62	118	132
1640	3.03	3.23	3.67	118	133
1700	2.83	3.28	3.42	118	130
1720	2.63	2.83	3.28	120	-
1740	2.47	2.64	3.00	122	127

TABLE 1 - DECEMBER 1949.

Time SAMT.	f_1 mc/sec.	f_2 mc/sec.	f_3 mc/sec.	h'_1 km.	h'_2 km.
0520	1.67	1.83	1.72		
0540	1.89	2.23	2.41		
0600	2.30	2.50	2.88	129	-
0620	2.55	2.70	3.12	127	153
0640	2.76	2.91	3.38	121	142
0700	2.99	3.11	3.44	119	-
0720	3.17	3.30	3.68	120	143
0740	3.29	3.45	3.97	119	139
0800	3.44	3.60	4.04	118	132
0820	3.53	3.68	4.09	119	134
0840	3.64	3.78	4.19	119	136
0900	3.69	3.83	4.25	119	135
0920	3.77	3.93	4.24	119	132
0940	3.82	4.01	4.22	118	130
1000	3.90	4.10	4.16	119	132
1020	3.98	4.25	4.32	119	132
1040	3.98	4.25	4.36	119	134
1100	3.99	4.28	4.26	119	127
1120	3.98	4.30	4.38	119	-
1140	4.01	4.30	4.38	119	-
1200	4.03	4.30	4.36	118	131
1220	4.03	4.38	4.45	119	130
1240	4.02	4.34	4.52	120	129
1300	4.01	4.33	4.53	118	127
1320	3.98	4.24	4.34	119	-
1340	3.95	4.20	4.37	119	126
1400	3.87	4.18	4.36	119	-
1420	3.82	4.08	4.37	119	129
1440	3.71	3.97	4.36	119	126
1500	3.67	3.86	4.23	118	128
1520	3.61	3.75	4.01	118	129
1540	3.54	3.69	4.06	120	-
1600	3.39	3.64	3.96	120	-
1620	3.29	3.44	3.98	120	-
1640	3.12	3.33	3.73	118	-

Observations on Records:

While reading off the critical frequencies and virtual heights, some interesting features of the records were observed.

The frequency f_1 was usually very clearly defined and could easily be read off. Even when the cusp part of the curve was missing, the frequency could still be estimated quite accurately. However sometimes during the middle part of the day the virtual height curve did not rise to a high maximum value, and then the frequency f_1 was rather difficult to estimate. The frequency was found to vary during the day in a very regular manner.

The values of f_1 on days when the abnormal E were absent and present respectively, were grouped together in calculating the means. This procedure is justified by the fact that the values of f_1 are very nearly the same on such occasions.

The frequency f_2 were sometimes ill-defined, especially during the middle part of the day. It did not vary as regularly as f_1. Besides showing huge variations due to sporadic effects, the behaviour of f_3 was very irregular. The end part of the E trace was usually diffuse, so that the frequency f_3 was rather difficult to read off.

The monthly means of maximum electron density N, corresponding to the frequencies in table 1, can be calculated from the equation

$$N = 1.24 \times 10^4 f_c^2 \qquad \text{-----(3).}$$

Strictly speaking, the values of f_c used in (3) should be the root mean square frequencies. In the case of f_1 however, the values deviate very little from the mean, so that the R.M.S. does not differ appreciably from the arithmetic mean.

Application of Chapman's Theory:

In an isothermal atmosphere (Chapman's theory) the maximum electronic density is given by (22). This equation has been deduced assuming $\frac{dn}{dt}$ to be negligible, and hence it only applies to the middle part of the day.

$$N^2 = BF\exp(-1) \qquad \text{-----(22).}$$

where
$$B = \frac{\beta n_o' I_\infty}{\alpha w} \qquad \text{-----(18).}$$

and
$$F = \frac{C \cos\chi}{n_o' T_o \beta} \qquad \text{-----(19).}$$

$$\therefore N^2 = \left(\frac{CI_\infty}{\alpha w T_o \varepsilon}\right) \cos\chi \qquad \text{-----(22a).}$$

If the quantity in brackets is constant during the middle part of the day, then this equation may be written in the form

$$N^2 \propto \cos$$

Hence from (3) it follows that

$$f_c \propto (\cos\chi)^{\frac{1}{4}}$$

or $\log_{10} f_c = K + \frac{1}{4} \log \cos\chi$ -----(37).

K being a constant. Chapman's theory therefore predicts that the graph of $\log f_c$ vs. $\log \cos\chi$ should be a straight line with slope 0.25 .

In order to plot $\log f_1$ and $\log f_2$ against $\log \cos\chi$, the values of $\cos\chi$ were calculated for each month, using the formula given by Chapman[30])

$$\cos\chi = \cos\theta \sin\delta + \sin\theta \cos\delta \cos\phi \qquad \text{------(38).}$$

In this θ is the colattitude, ϕ the local time from noon, in degrees and δ the south declination of the sun. The values of δ corresponding to the 15th of each month were obtained from the Nautical Almanac, while for Johannesburg ($26^\circ 15'S$, $28^\circ 4'E$) $\theta = 63^\circ 45'$. The value of ϕ was taken to correspond to S.A.M.T. which differs from local time by about 8 mins. No appreciable error was introduced in this way as the mean of the morning and afternoon readings were always taken.

Fig. 10 shows a typical example of the graphs of $\log f_1$ and $\log f_2$. It will be seen that in both cases the points lie very nearly on a straight line. In Table 2 are

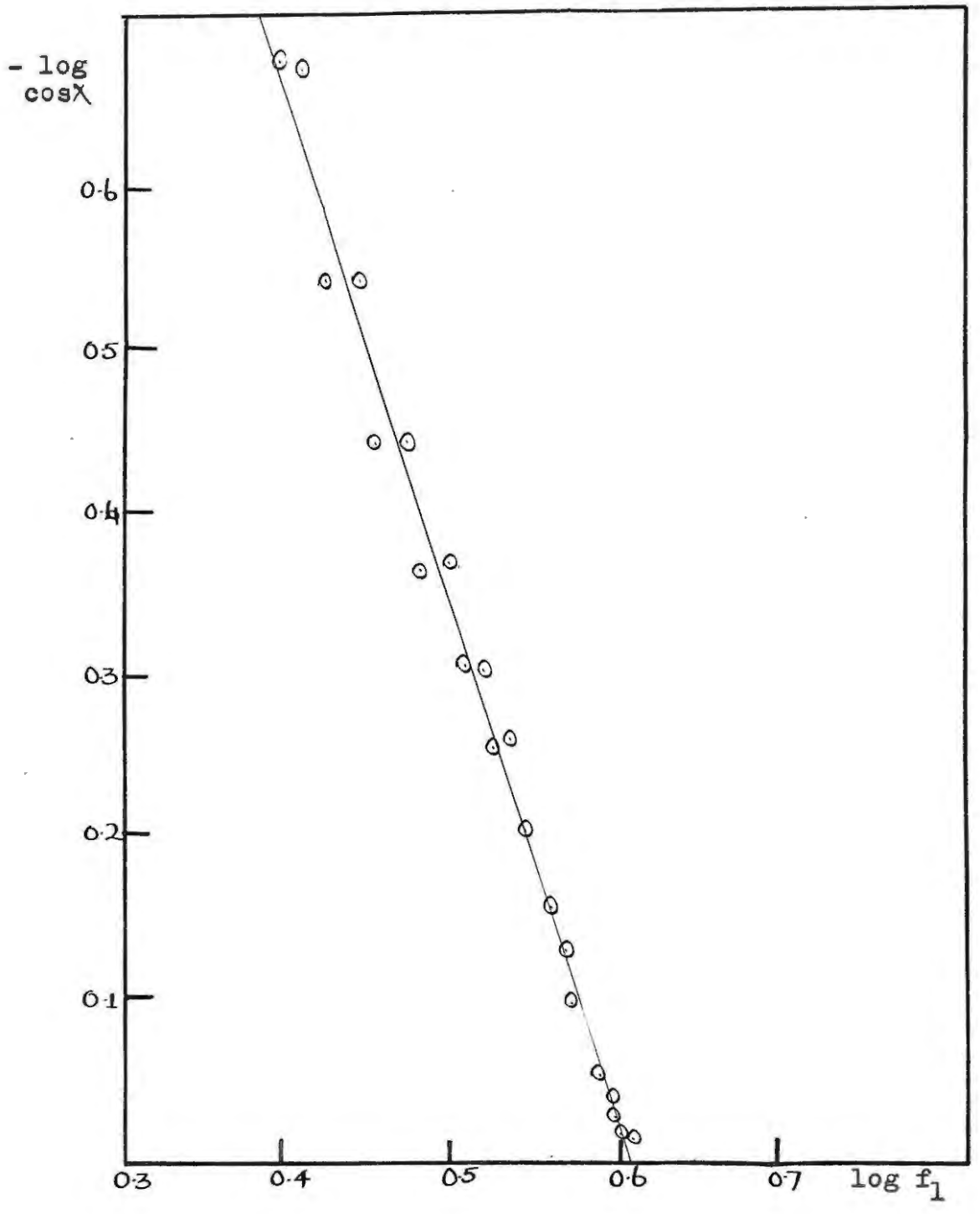

FIG. 10(a) - Variation of $\log_{10} f_1$ with $\log_{10} \cos\chi$

JOHANNESBURG , NOVEMBER 1949.

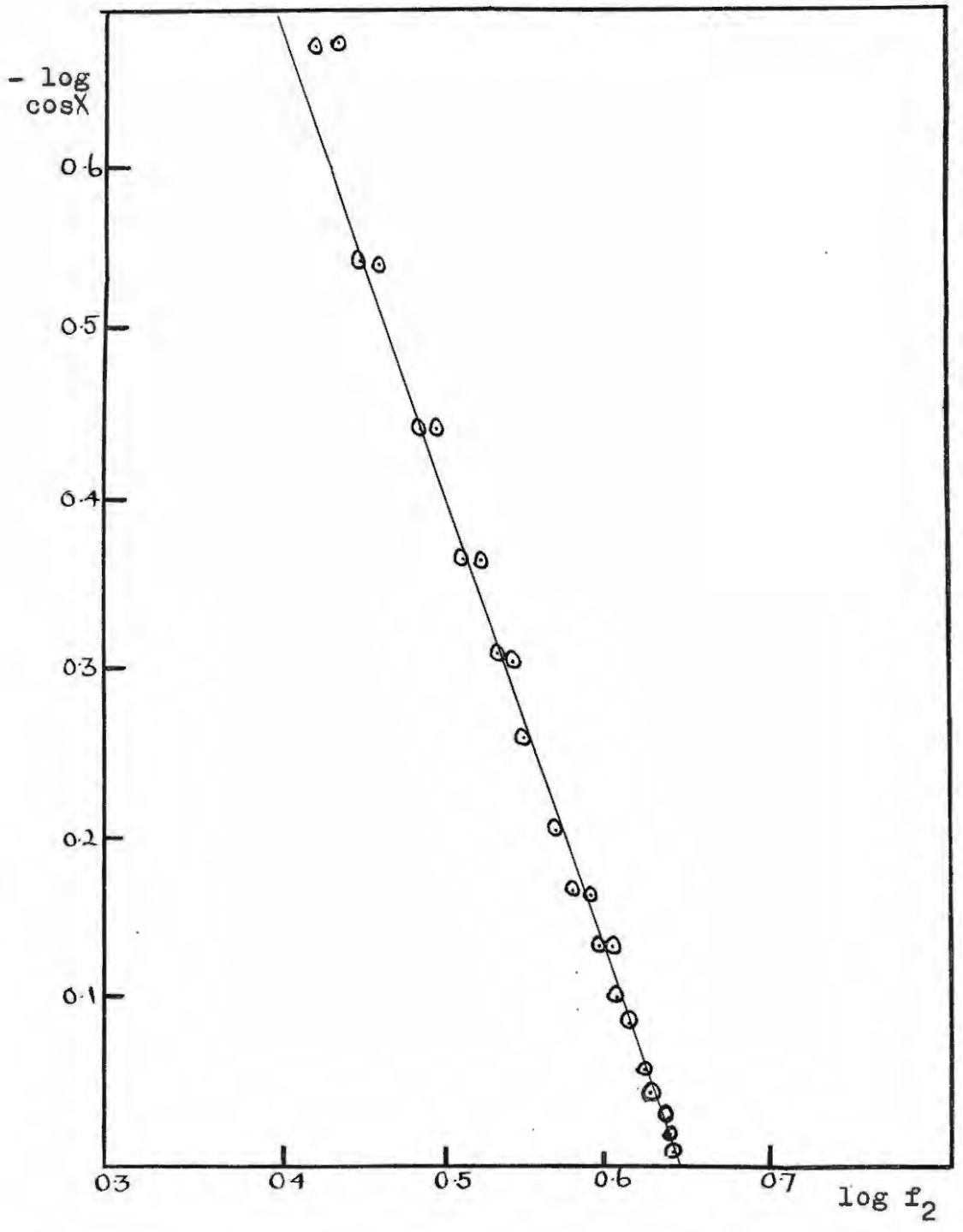

FIG. 10(b) - Variation of $\log_{10} f_2$ with $\log_{10} \cos \chi$

JOHANNESBURG , NOVEMBER 1949.

given the slopes of the lines for the different months. The mean values of 0.324 for f_1 and 0.306 for f_2 are slightly larger than the value 0.25 predicted by Chapman's theory.

TABLE 2 - JOHANNESBURG 1949.

MONTH	Slope ffor f_1	Slope for f_2
JAN.	0.322	0.286
FEB.	0.312	0.304
MAR.	0.316	0.299
APR.	0.306	0.306
MAY	0.328	0.299
JUNE	0.326	0.277
JULY	0.312	0.311
AUG.	0.329	0.301
SEP.	0.322	0.309
OCT.	0.367	0.322
NOV.	0.325	0.334
DEC.	0.341	0.328

TABLE 2 - Slopes of curves of log f_1 and log f_2 vs.logcosχ

The good agreement found with the theory is quite remarkable, considering the many simplifying assumptions made in the derivation. It therefore appears that during the middle part of the day the quantity ($CI_\infty/\alpha w T_o \epsilon$), and hence also the individual constants C, I_∞ ,α and T_o, do not show large variations.

In fig. 11 the noon values of log f_1 and log f_2 are plotted against log cosχ. For f_1 the points lie very nearly on a straight line, showing that the seasonal variation in f_1 is also very regular. In contrast to this the points for f_2 show large irregular variations, but do lie approximately on a straight line.

Application of Linear Temperature Gradient:

At this stage it is interesting to examine the effect of a linear temperature gradient on the graph of log f_c against log cos

In this case the value of N during the middle part of the day is given by equation (32),

$$N^2 = B\left\{F(1+\gamma/C)\right\}^{(1+\gamma/C)} \exp\left\{-(1+\gamma/C)\right\} \qquad \text{-----(32).}$$

As before we assume that during the middle part of the day the quantities C, I_∞, α, T_o do not vary much. In addition we shall also consider the value of the temperature

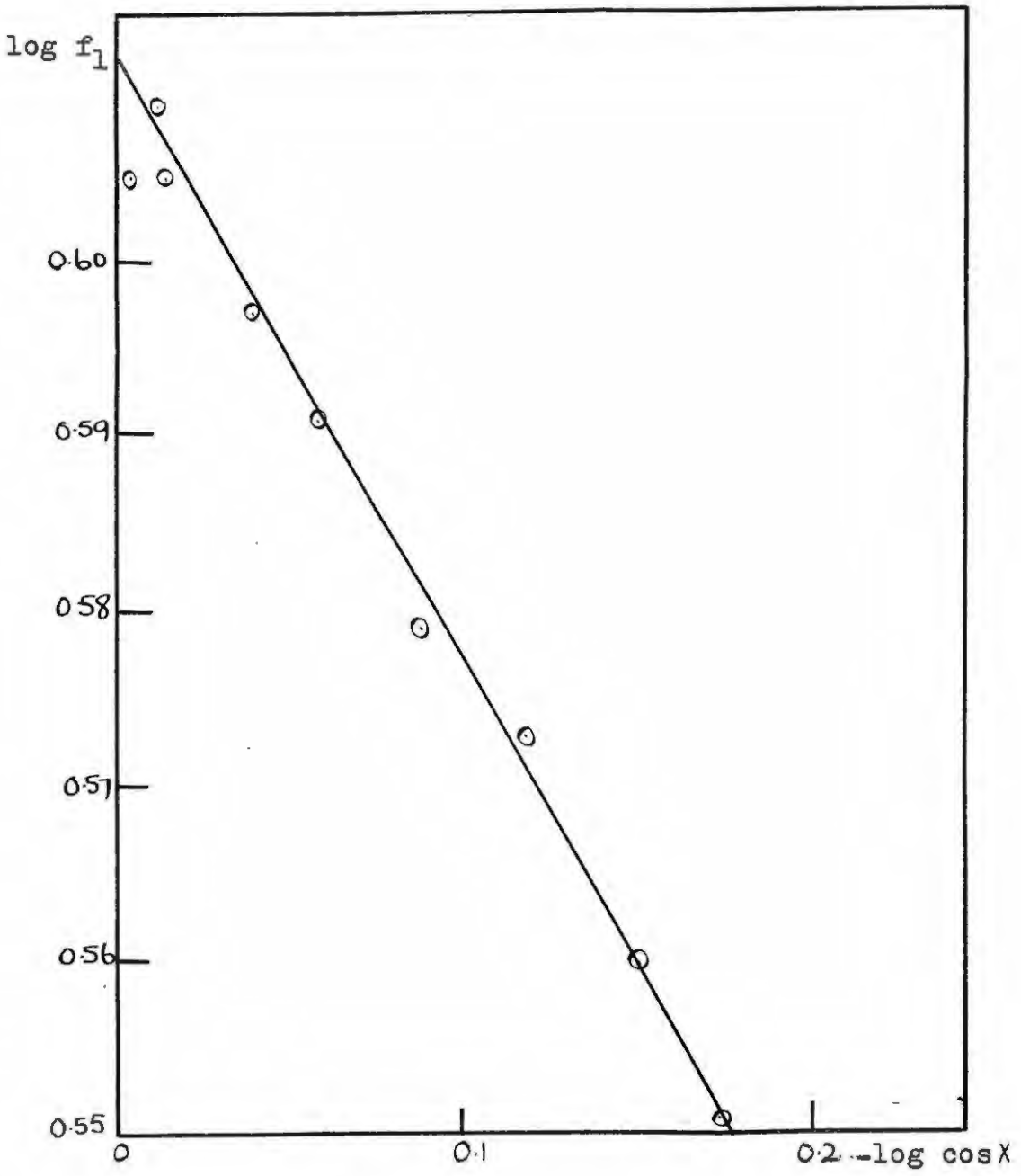

FIG. 11(a) - Noon values of $\log_{10} f_1$ plotted vs. $\log_{10} \cos \chi$. JOHANNESBORG , 1949.

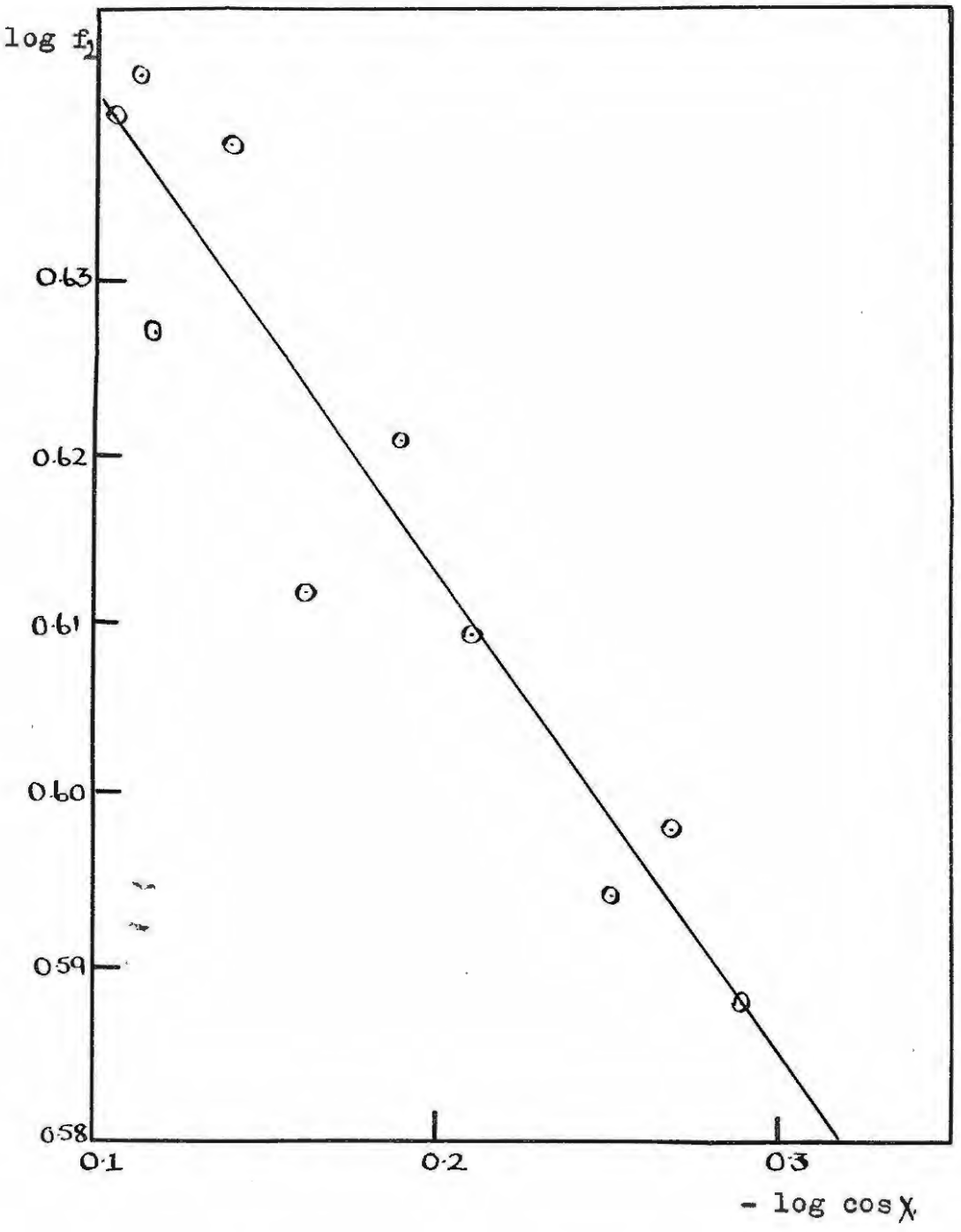

FIG. 11(b) - Noon values of log f_2 plotted vs. log cos χ

JOHANNESBURG , 1949.

gradient γ to be approximately constant during the middle part of the day. In that case equation (32) can be written in the form

$$N^2 \propto (F)^{(1 + \gamma/C)}$$

$$\text{i.e. } f_c^4 \propto (F)^{(1 + \gamma/C)}$$

$$\text{i.e. } f_c^4 \propto (\cos\chi)^{(1 + \gamma/C)}$$

$$\text{or } \log f_c = K + \tfrac{1}{4}(1 + \gamma/C) \log \cos\chi \quad \text{-----(39).}$$

Thus the theory also predicts that the graph of $\log f_c$ vs. $\log \cos\chi$ will be a straight line, but it leads to a higher value of the slope namely $\frac{1}{4}(1 + \gamma/C)$.

This is in very good agreement with our results. The fact that the variations of $\log f_1$ and $\log f_2$ with $\log \cos\chi$ are very nearly linear shows that our assumptions are approximately valid. From Table 2 it appears that there is a definite trend for the slope to be greater in summer than in winter, which is again as would be expected from the theory. Using the value for f_1 (see next section) we can calculate the mean value fof $C/$ for the E layer.

$$0.25(1 + \gamma/C) = 0.324$$

$$\text{giving} \quad C/\gamma = 3.38 \quad \text{-----(40).}$$

In spite of the many assumptions involved this value is in fair agreement with other estimates , as will be discussed later.

Critical Frequency of the E layer:

In the study of the E layer of the ionosphere, workers frequently use the threshold frequency f_2 as the critical frequency of the layer. This method, which is very convenient especially in the case of visual observation, is open to criticism. The value of f_2 depends on a large extent on the absorption conditions and on the transmitting and receiving equipment. The effect of absorption on the frequency f_2 was clearly shown by some of the midday records that were examined. In these records the first part of the F reflections were parallel to the frequency axis, while f_2 showed an abnormal high value. The threshold frequency f_2 cannot therefore be used as the E layer critical frequency.

Some writers extrapolate the F layer reflection and take the E layer critical as the frequency where the initial part of the curve tends to an infinite virtual height. This method is subject to the criticism that it is difficult to extrapolate correctly, especially during the middle part of the day.

Appleton [41]) takes the frequency f_1 to be the true E layer critical frequency. This procedure is supported by our observation that the value of f_1 is not affected by the presence of the abnormal layer. The fact that the

behaviour of f_1 is much more regular than that of f_2 also indicates that the former should always be used as the critical frequency of the E layer.

It remains to explain why the threshold frequency f_2 was found to vary with cos x in the same way as predicted by the theory for the critical frequency. This effect which was also noticed by numerous observers, can be accounted for as follows. The difference in frequency (f_2-f_1) depends to a large extent on the absorption. This means that the difference is small at sunrise and sunset, and relatively large (approximately 0.3 mc/sec. for our records) at midday. The frequency f_2 will therefore show the same characteristic variation with time as f_1.

The abnormal E layer:

In Table 1 the occurence of the abnormal E region is indicated by the presence of the value of h'_2 in the sixth column. It will be seen that the layer occurs mainly during the middle part of the day and in the afternoon. During the summer months the layer appears earlier than in winter. In summer the layer is sometimes found to be absent near noon. This effect is probably due to the strong absorption in the lower layers.

The marked solar control on the layer is well illustrated in fig. 12 . In this figure the mean values of virtual height during the middle part of the day (1000 to 1400 hrs.) are plotted against the month of the year. It will be seen that in summer the layer appears at lower virtual heights than in winter.

The mean values of h_2' for the months when the E_a layer occurs throughout the middle part of the day, are plotted in fig. 13 as a function of the time. It will be noticed that the virtual height shows a more or less steady decrease with time.

The solar control on the abnormal E layer was also noticed by Appleton[40,41]) and Berker and Dieminger [42]). Any theory for the formation of the layer must take this fact into account.

Under favourable conditions the extraordinary reflections corresponding to the E_a layer were also observed. As pointed out by Appleton [41]) this shows clearly that the scattering particles in this layer are electrons.

The Sporadic E layer:

Not much attention was given to sporadic effects as we were more interested in the regular variations of the Elayer. A very interesting effect was noticed however

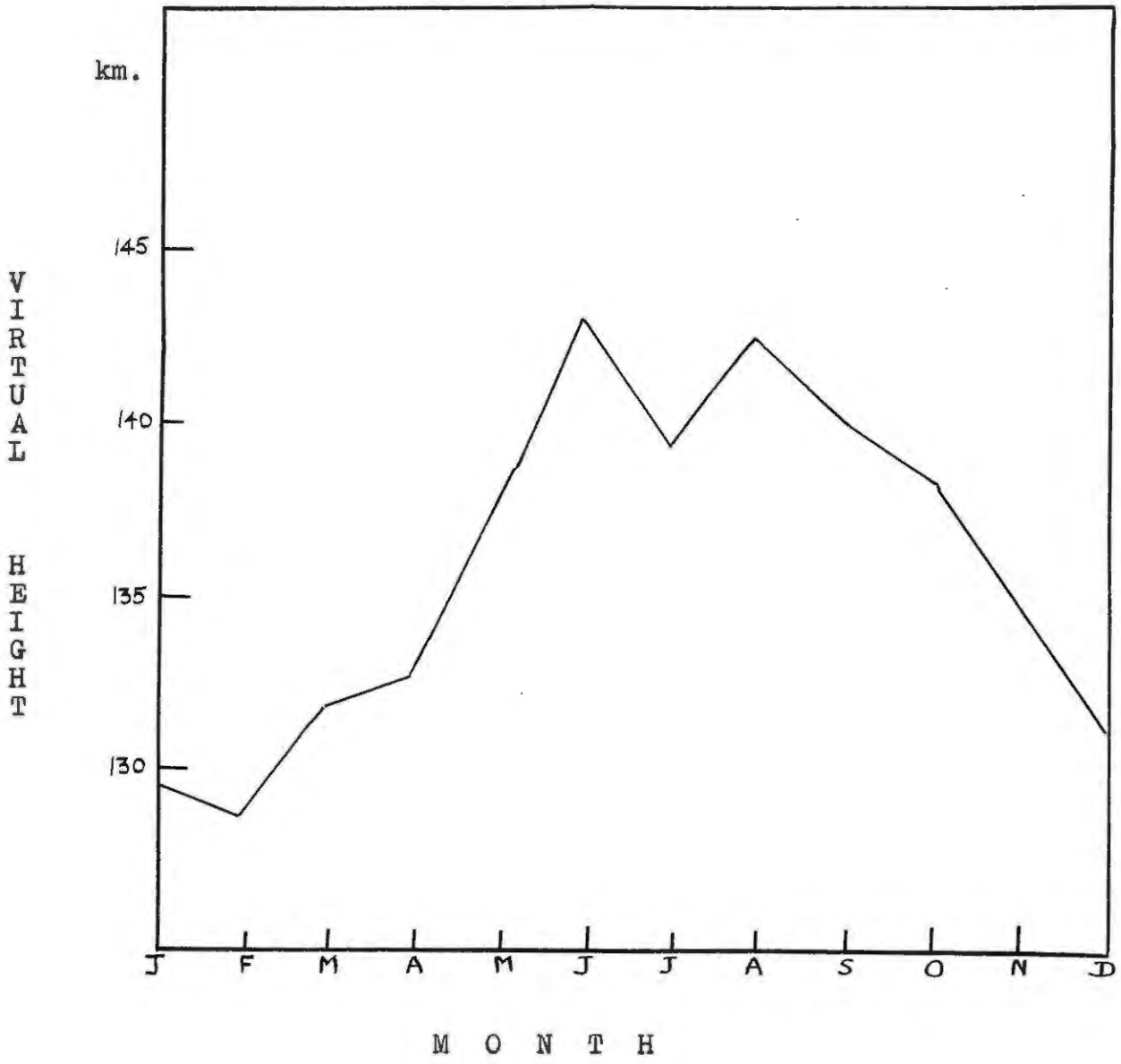

FIG. 12 - MEAN SEASONAL VARIATION OF VIRTUAL HEIGHT.

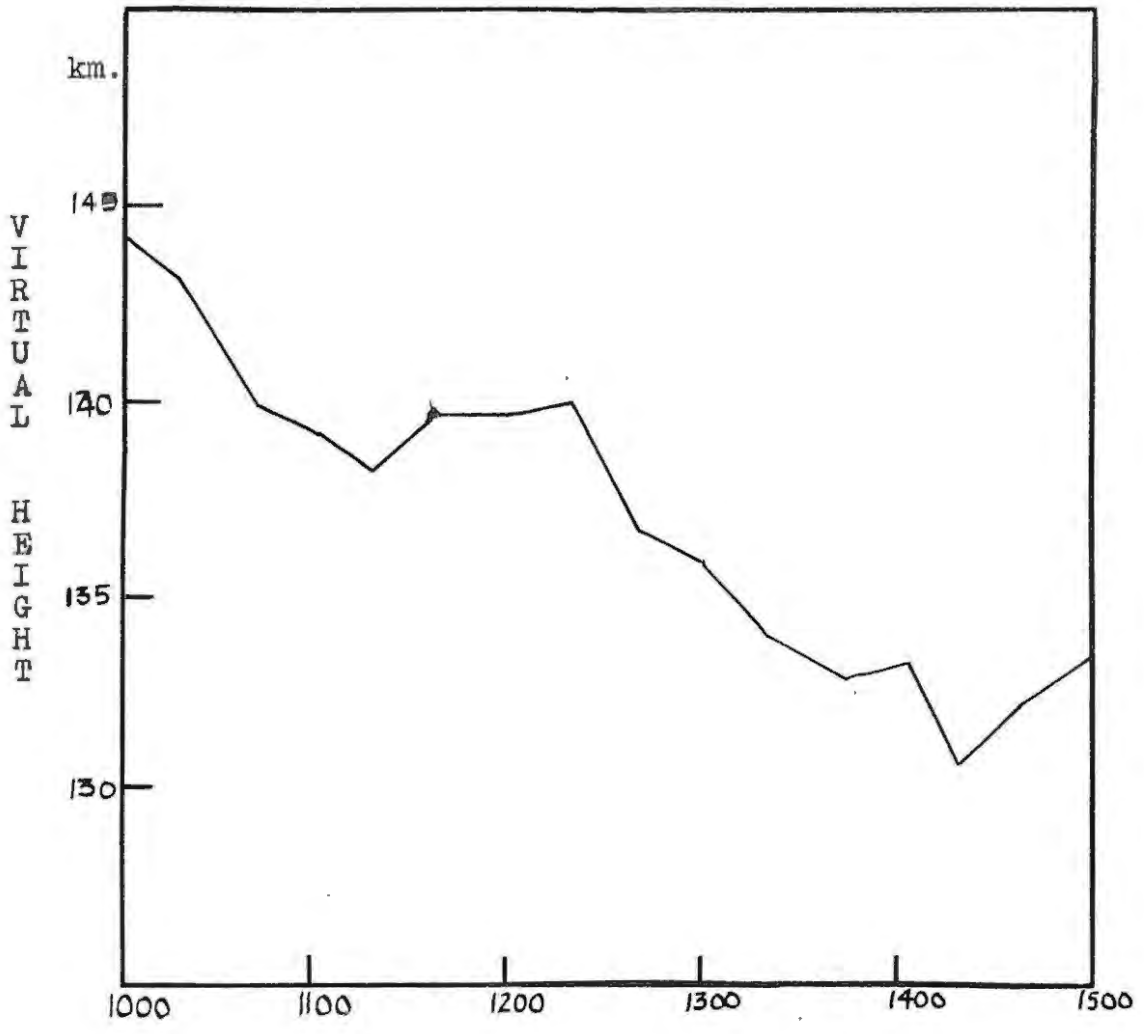

FIG. 13 - MEAN VARIATION OF VIRTUAL HEIGHT WITH TIME.

in the Johannesburg records for the daytime period of 1949. In these records the sporadic E layer rarely occurred in the morning. The frequency of occurrence increased during the afternoon and attained a maximum at sunset.

The E_2 layer:

The folowing behaviour of the E_2 layer was noticed quite frequently. In the early morning it usually appeared at a virtual height of approximately 200 km. , with well-defined critical frequencies. As time went by its virtual height decreased until, at about 1000 hrs.,it passed into an abnormal E layer with no definite critical frequency.

The Earth's Magnetic Field:

Appleton [45]) first proposed a method to measure the earth's magnetic field in the ionosphere from the values of the ordinary and extraordinary critical frequencies.

The well-known relation between the ordinary critical frequency f_c and extraordinary critical frequency f_x , is

$$f_c^2 = f_x^2 - f_x f_H \qquad \text{-----(41).}$$

which is easily deduced from equations (9) and (10).

In the above equation

$$f_H = \frac{p_H}{2\pi} = \frac{eH'}{2\pi mc} \qquad \text{-----(42).}$$

Hence, from (41) and (42),

$$H' = \frac{2\pi mc}{e}\left(\frac{f_x^2 - f_c^2}{f_x}\right) \qquad \text{-----(43).}$$

The magnetic field may therefore be determined from a knowledge of the critical frequencies only. In his early measurements Appleton found the value of H' to be about 10 % less than the ground value, which is in good agreement with the theory of terrestial magnetism. It was therefore thought that a study of the critical frequencies would give valuable information about the variation of the earth's field in the ionosphere.

But Booker has shown that even at vertical incidence the magneto-ionic components will be deviated and will therefore be reflected from different levels in the ionosphere [46]. Millington [47] and Scott [48] have also pointed out that horizontal variations in the electron densityw will cause the ordinary and extraordinary rays to be reflected from different regions. The method of Appleton may therefore lead to large errors in the study of the earth's field.

Fifty early morning and late afternoon records showing both critical frequencies clearly , were examined. It was found that the difference in frequency $f_x - f_c$, was subject to relatively large variations. The mean frequencies were

$f_x = 3.33$ mc/sec.

$f_c = 2.85$ mc/sec. ,

giving $f_H = 0.904$ mc/sec.

and $H' = 0.32$ Oersted,

which is in good agreement with the ground value.

It therefore seems that although the method cannot be used to study the variations in the earth's field, it gives the mean value of H' quite accurately.

TRUE HEIGHTS OF THE E LAYER.

The different methods of determining the true height of an ionosphere layer from the virtual height - freqency curve, have recently been reviewed extensively by O'Brien[12]). There are three main methods of scaling the (h',f) curves that are widely used, namely the (i) Booker and Seaton method; (ii) Pierce method; (iii) Pekeris method. In all three methods the earth's magnetic field and the effect of collisional friction are neglected. Only the ordinary reflection is considered in the scaling.

We shall now give a short description of the three methods as they apply in practice to the E layer.

Booker and Seaton Method:

The method of Booker and Seaton [49]) is to fit a parabolic curve of electron density to the observed virtual height-

frequency curve. For the normal E layer they assume that the curve of electron density against height is a parabola of semi-thickness τ_p and whose maximum density occurs at a height h_{mp}. They give the following useful relations between h_{mp} and τ_p and the virtual heights (Table 3):

TABLE 3

h_{mp}	τ_p
$\frac{1}{2}(h'_{648} + h'_{925})$	$(h'_{925} - h'_{648})$
$\frac{1}{2}(h'_{725} + h'_{901})$	$3/2(h'_{901} - h'_{725})$
$\frac{1}{2}(h'_{757} + h'_{887})$	$2(h'_{887} - h'_{757})$
h'_{834}	$(h'_{969} - h'_{834})$

TABLE 3 - Formulae for h_{mp} and τ_p.

In this table h'_{648} means the virtual height at a frquency 0.648 f_c. Using the above table it is therefore a simple matter to calculate the mean values of h_{mp} and τ_p from the (h';f) curve.

It will be seen from Table 3 that the height of maximum ion density is equal to the virtual height at a freqeency 0.834 of the critical. This frequency is usually referred to as the "characteristic frequency".

Pierce Method:

The method of Pierce [50] is analogous to that of Booker and Seaton, but in this case the curve of virtual height vs. frequency is fitted to a Chapman distribution of electron density. Pierce deduced the following useful formulae for the scale height H_c and the height of maximum ion density h_{mc} of the normal E layer (see Table 4).

TABLE 4.

h_{mc}	H_c
$\frac{1}{2}(h'_{762} + h'_{850})$	$2(h'_{850} - h'_{762})$
$\frac{1}{2}(h'_{558} + h'_{927})$	$\frac{1}{2}(h'_{927} - h'_{558})$
h'_{811}	$2/3(h'_{925} - h'_{811})$
$\frac{1}{2}(h'_{882} + h'_{704}$	$(h'_{882} - h'_{704})$

TABLE 4 - Formulae for h_{mc} and H_c.

It will be seen that Pierce's value of the characteristic frequency is smaller than that of Booker and Seaton, namely 0.811 of the critical. Pierce also gave the following relations whereby the Booker and Seaton parabolae may be fitted to a Chapman distribution:

$$H_c = 0.60\ \tau_p \qquad \text{-----(44).}$$

$$h_{mc} = h_{mp} - 0.14\ H_c$$

$$= h_{mp} - 0.084\ \tau_p \qquad \text{-----(45).}$$

Pekeris Method:

The method of Pekeris [51]) which is also discussed by Rydbeck [52,53]) and Manning [54]) , is the most accurate of the three. The method is based on the equation of Appleton and de Groot

$$h = \frac{2}{\pi} \int_0^{f_h} \frac{h'df}{\sqrt{f_h^2 - f^2}} \qquad \text{-----(14).}$$

in which h is the actual height to (which) wave of frequency f_h penetrates.

Following Rydbeck we introduce the new variable u given by the equation

$$u = \sin^{-1}(f/f_h) \qquad \text{-----(46).}$$

Equation (14) may then be written as

$$h = \frac{2}{\pi} \int_0^{\pi/2} h'du \qquad \text{-----(47).}$$

Thus the actual height for a given value of f_h may be deduced from the area below the curve of h' against u. The value of h' may be read off from the virtual height-frequency curve, and u may be calculated from (46), its limits being 0 and 90°.

In Table 5 are given the values of f calculated for useful values of f_h at intervals of 0.1 mc./sec. and for values of u at intervals of 9°. In this table f_1 stands for the value of f corresponding to $u = 9^\circ$, f_2 to the value corresponding to $u = 18^\circ$, etc. It is obvious that f_0 will be zero in all cases.

TABLE 5.

f_h	1.50	1.60	1.70	1.80	1.90	2.00	2.10	2.20
f_1	0.24	0.25	0.26	0.28	0.30	0.31	0.33	0.34
f_2	0.46	0.50	0.53	0.56	0.59	0.62	0.65	0.68
f_3	0.68	0.73	0.78	0.82	0.87	0.90	0.95	1.00
f_4	0.88	0.94	1.00	1.06	1.12	1.17	1.24	1.29
f_5	1.06	1.13	1.20	1.27	1.35	1.41	1.49	1.56
f_6	1.21	1.29	1.38	1.46	1.54	1.62	1.70	1.78
f_7	1.33	1.42	1.52	1.61	1.70	1.78	1.87	1.96
f_8	1.43	1.52	1.62	1.71	1.81	1.90	2.09	2.08
f_9	1.48	1.58	1.68	1.78	1.88	1.98	2.07	2.17
f_{10}	1.50	1.60	1.70	1.80	1.90	2.00	2.10	2.20

TABLE 5.

f_h	2.30	2.40	2.50	2.60	2.70	2.80	2.90	3.00	3.10
f_1	0.36	0.37	0.39	0.41	0.42	0.44	0.46	0.47	0.49
f_2	0.71	0.74	0.77	0.80	0.84	0.87	0.90	0.93	0.96
f_3	1.05	1.09	1.14	1.18	1.23	1.27	1.32	1.36	1.41
f_4	1.35	1.41	1.47	1.53	1.59	1.65	1.71	1.76	1.82
f_5	1.63	1.70	1.77	1.84	1.91	1.98	2.05	2.12	2.19
f_6	1.86	1.94	2.02	2.10	2.18	2.26	2.34	2.42	2.50
f_7	2.05	2.14	2.23	2.32	2.40	2.49	2.58	2.67	2.76
f_8	2.18	2.28	2.37	2.47	2.56	2.66	2.75	2.85	2.94
f_9	2.27	2.37	2.47	2.57	2.66	2.76	2.86	2.96	3.06
f_{10}	2.30	2.40	2.50	2.60	2.70	2.80	2.90	3.00	3.10

f_h	3.20	3.30	3.40	3.50	3.60	3.70	3.80	3.90	4.00
f_1	0.50	0.52	0.53	0.55	0.56	0.58	0.59	0.61	0.62
f_2	0.99	1.02	1.05	1.08	1.11	1.15	1.18	1.21	1.24
f_3	1.45	1.50	1.55	1.60	1.64	1.68	1.73	1.78	1.82
f_4	1.88	1.94	2.00	2.06	2.12	2.18	2.24	2.30	2.35
f_5	2.26	2.33	2.40	2.47	2.54	2.63	2.69	2.76	2.83
f_6	2.58	2.67	2.75	2.83	2.91	2.99	3.07	3.15	3.23
f_7	2.85	2.94	3.03	3.12	3.21	3.30	3.39	3.47	3.56
f_8	3.04	3.14	3.23	3.32	3.42	3.51	3.61	3.70	3.80
f_9	3.16	3.26	3.36	3.46	4.56	3.65	3.75	3.85	3.95
f_{10}	3.20	3.30	3.40	3.50	3.60	3.70	3.80	3.90	4.00

TABLE 5 - Values of f for u at intervals of 9°.

(All frequencies in mc./sec.).

The experimental procedure to find the actual height corresponding to a frequency f_h is then as follows. In the column of f_h the values of f_1, f_2, f_3, etc. are read off and the corresponding values of h'found from the (h';f) curve. These values of h' are then plotted against u, the u-axis being marked off in fractions of 90^o. The actual height is then given directly by the area underneath the graph.

Using the above method and interpolating between two columns in Table 5, the actual height corresponding to any value of f_h correct to two places of decimals can be found. In the case of the normal E layer it is unnecessary to draw curves for each value of f_h. By means of Simpson's rule,the area underneath the curves can be estimated accurately without actually drawing them. Thus if h_0, h_1, h_2,...etc. are the virtual heights corresponding to the frequencies f_0, f_1, f_2, ...etc. then it follows from Simson's rule that the area underneath the curve and therefore the true height,is given by

$$h = \frac{1}{30}\left\{(h'_0+ h'_{10}) + 4(h'_1+h'_3+h'_5+h'_7+h'_9) +2(h'_2+h'_4+h'_6+h'_8)\right\} \quad \text{-----(48).}$$

This method was found very convenient for the normal E layer. It could not be applied to the abnormal layer as the discontinuity in the (h';f) curve lead to large

errors.

Values of electron density for each f_h, calculated from (3)

$$n = 1.24 \times 10^4 f_h^2 \qquad \text{-----(3).}$$

are given in Table 6.

TABLE 6.

f_h mc/sec	n 10^5/cc.	f_h mc/sec.	n 10^5/cc.	f_h mc/sec.	n 10^5/cc.
1.5	0.279	2.4	0.714	3.3	1.350
1.6	0.318	2.5	0.775	3.4	1.434
1.7	0.359	2.6	0.838	3.5	1.519
1.8	0.402	2.7	0.904	3.6	1.607
1.9	0.448	2.8	0.972	3.7	1.697
2.0	0.496	2.9	1.042	3.8	1.791
2.1	0.547	3.0	1.116	3.9	1.887
2.2	0.600	3.1	1.192	4.0	1.985
2.3	0.656	3.2	1.270		

TABLE 6 - Values of electron density n .

Evaluation of H and h_m:

A metod of determining the scale height H of ta layer from the electron distribution curves, by fitting these to a Chapman distribution, will now be described. This method also gives a check on the value of the height of maximum ion density h_m, which cannot be determined directly with accuracy, as it involves the extrapolation of the (h,f) curve to infinite virtual height.

The Chapman distribution is given in equation (25)

$$(n/N)^2 = \exp(1 + x - e^x) \qquad \text{-----(25).}$$

where $$x = \frac{h_m - h}{H} \qquad \text{-----(26).}$$

Equation (25) may be written in the form

$$-2\log_e(n/N) = e^x - 1 - x \qquad \text{-----(49).}$$

A graph of the function

$$f(x) = e^x - 1 - x$$

is shown in fig. 14. Values of the function

$$-2\log_e(n/N)$$

are given in Table 7 for values of (n/N) ranging from 0.50 to 0.99.

TABLE 7.

n/N	0.00	0.01	0.02	0.03	0.04	0.05	0.06	0.07	0.08	0.09
0.5	1.386	1.347	1.308	1.270	1.232	1.196	1.160	1.124	1.089	1.055
0.6	1.022	0.989	0.956	0.924	0.893	0.862	0.831	0.801	0.771	0.742
0.7	0.713	0.685	0.657	0.629	0.602	0.575	0.549	0.523	0.497	0.471
0.8	0.446	0.421	0.397	0.373	0.349	0.325	0.302	0.279	0.256	0.233
0.9	0.211	0.189	0.169	0.145	0.124	0.103	0.082	0.061	0.040	0.020

TABLE 7 - The function $-2\log_e(n/N)$.

Using Table 7 and fig. 14, the value of x corresponding to any useful value of n/N can be found. Values of x for convenient values of n/N are given in Table 8. These values of n/N were chosen because thet lie on the part of the electron distribution curve for which the true heights can be most accurately determined.

Now the variation of h with x is given in equation (26) which can be written in the form

$$h = h_m - Hx \qquad \text{-----(50).}$$

Equation (50) shows that the graph of h vs. x

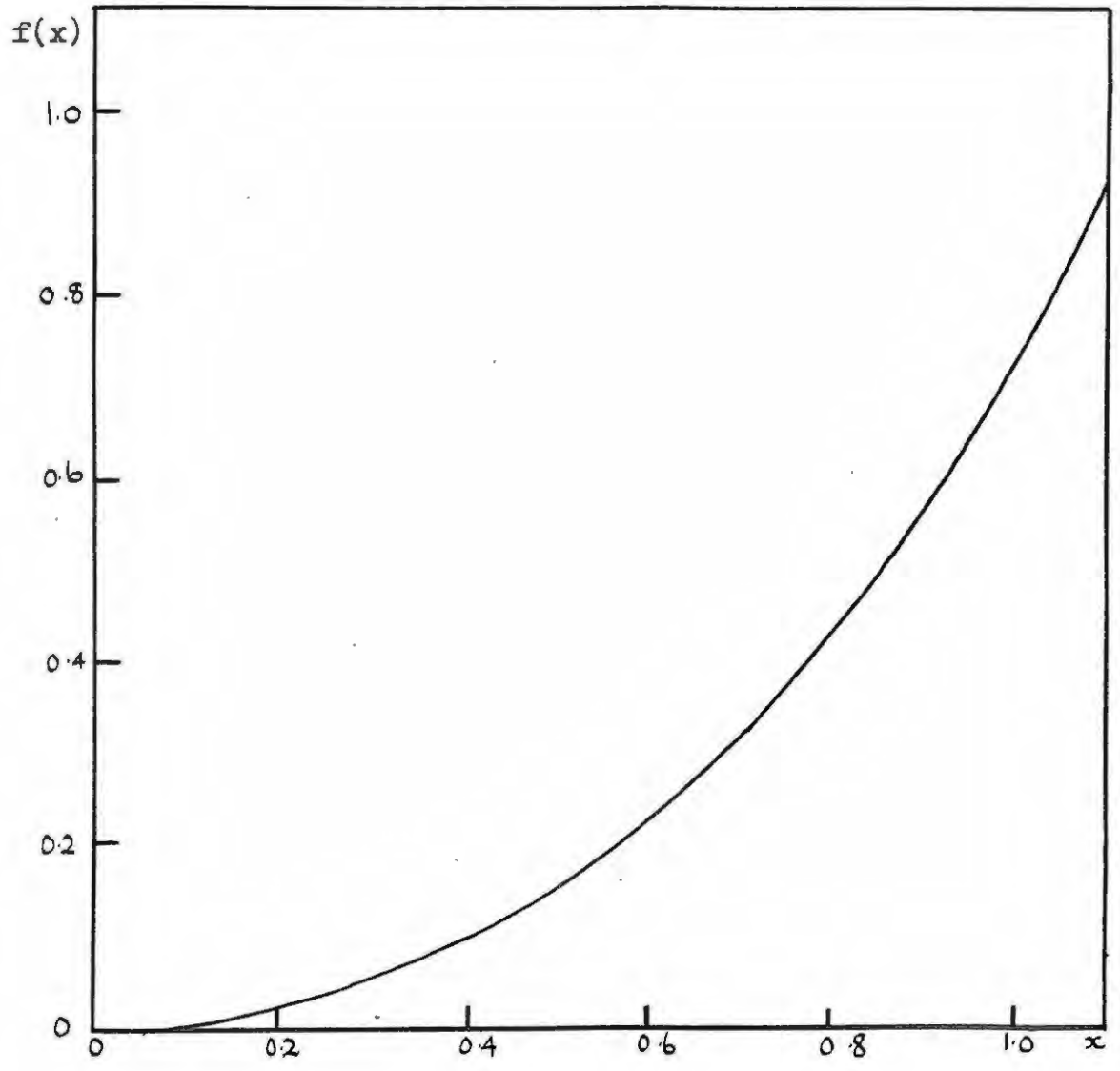

FIG. 14 - THE FUNCTION $f(x) = e^x - 1 - x$.

TABLE 8.	
n/N	x
0.95	0.417
0.92	0.526
0.90	0.589
0.85	0.710
0.80	0.816
0.75	0.910
0.70'	0.997
0.65	1.077
0.60	1.156

Table 8 - Values of x for different (n/N)

should be a straight line with slope - H , cutting the h-axis at a height h_m.

The experimental procedure is therefore to read off the values of h for the values of n/N given in Table 8, and to plot these against the corresponding values of x. A typical example of such a graph is shown in fig. 15. It will be seen that the points lie on a curve, showing that the value of H is not constant, but increases with height. The height of

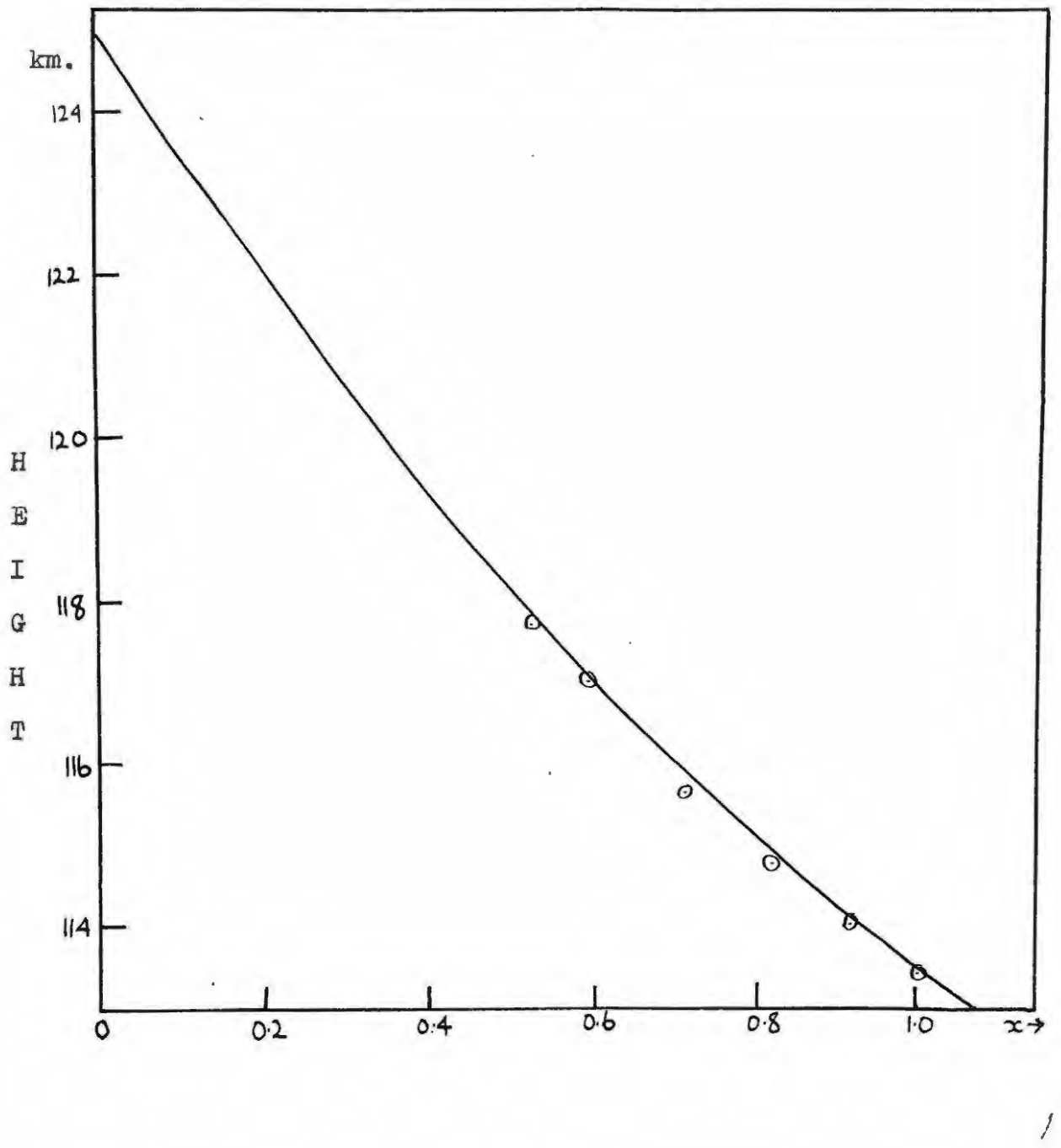

FIG. 15 - USUAL GRAPH OF h AGAINST x.

maximum density is obtained by producing the curve to the h-axis. In this way the value of h_m can be estimated with greater accuracy.

As the value of H varies along the layer, our theory does not apply strictly to the E region. In order to compare results with the linear temperature gradient theory, it seems best to determine the value H_m of H at the height of maximum electron density. H_m is given approximately by the slope of the curve of h vs. x at the point where $x = 0$.

Experimental Results:

As will be realised from the above, the process of determining the true distribution of electron density from the (h,f) curve is rather long. It was therefore decided to find the mean of the (h,f) curves before scaling them for true heights.

Mean virtual height -frequency curves for Johannesburg for the months July and December 1949 were obtained as follows. Records at hourly intervals for the daytime period were graphed by copying them from the image in the microfilm reader and superposing these on graph paper. Heights could be estimated to 2 km.

and frequencies to 0.02 mc./sec. The records were divided in two groups according to whether the E_a layer was present or not. In the case of the normal E layer the mean (h',f) curve was obtained by determining the mean values of h' at fixed fractions of the critical frequency. The virtual height-frequency curve could then be plotted knowing the mean critical frequency. The mean curve for the abnormal E layer was determined in a similar way.

In these records the E traces usually appeared at a frequency ranging approximately from 1.5 mc./sec. in the morning to 2.5 mc./sec. at noon. The curves therefore had to extrapolated to zero. Following Manning[53]) the virtual height was produced in a smooth curve, ending almost parallel to the frequency axis. The methods of extrapolation will be discussed later.

The Grahamstown records for the morning period of September 1949 were treated similarly. Thirty-six records were found suitable for scaling. In this case there were not enough records showing E_a reflections in the later part of the morning.

All the records were then scaled for true heights, using the Pekeris method, and the values of h_m and H_m determined. The results for the normal E layer

are given below in Tables 9 to 13. The results for the abnormal layer will be given later.

TABLE 9.

JOHANNESBURG , DEC. 1949 (E_a ABSENT).

Time SAMT.	h_m km.	h_o km.	$h_m - h_o$ km.	H_m km.
0600	125.7	110.8	14.9	13.9
0700	119.7	108.3	11.4	15.5
0800	123.0	109.8	13.2	13.8
0900	122.5	110.8	11.7	11.0
1000	122.6	109.0	13.6	14.0
1100	124.6	110.6	14.0	18.9
1200	122.0	110.8	11.2	13.1
1300	121.7	107.7	14.0	15.5
1400	124.0	108.8	15.2	16.6
1500	124.4	108.8	15.6	18.0
1600	124.5	111.3	13.2	16.3
1700	121.2	108.7	12.5	13.8
MEAN	122.9	109.5	13.4	14.9

TABLE 9 - True heights for the E layer.

TABLE 10.

JOHANNESBURG , DEC. 1949 (E_a PRESENT).

Time SAMT.	h_m km.	h_o km.	$h_m - h_o$ km.	H_m km.
0600	124.7	114.8	9.9	10.3
0700	122.3	110.6	11.7	9.6
0800	121.3	111.0	10.3	11.8
0900	118.9	108.7	10.2	11.1
1000	119.6	108.6	11.0	11.4
1100	119.0	112.0	7.0	9.3
1200	118.0	107.7	10.3	10.4
1300	120.5	110.5	9.5	12.4
1400	118.5	109.3	9.2	9.3
1500	119.3	110.6	8.7	8.6
1600	118.9	108.8	10.1	11.0
1700	121.3	111.0	10.3	11.0
MEAN	120.2	110.3	9.9	10.5

TABLE 10 - True heights for the E layer.

TABLE 11.

JOHANNESBURG , JULY 1949 (E_a ABSENT).

TIME SAMT.	h_m km.	h_o km.	$h_m - h_o$ km.	H_m km.
0800	124.6	114.4	10.2	11.0
0900	125.0	110.8	14.2	15.3
1000	123.3	108.2	15.1	19.3
1300	120.7	110.2	10.5	12.3
1400	120.1	108.4	11.7	11.4
1600	118.8	110.7	8.8	14.6
1700	123.7	110.6	13.1	13.9
MEAN	122.3	110.4	11.9	15.0

TABLE 12.

JOHANNESBURG , JULY 1949 (E_a ABSENT).

TIME SAMT.	h_m km.	h_o km.	$h_m - h_o$ km.	H_m km.
0900	126.3	110.8	15.5	13.9
1000	122.2	109.1	13.1	13.4
1100	122.8	108.3	13.7	13.9
1200	121.9	108.5	13.4	12.9
1300	120.7	109.4	11.3	13.4
1400	119.5	108.3	11.2	11.3
1500	120.8	107.6	13.2	11.5
1600	124.4	110.3	14.1	13.8
MEAN	122.3	109.0	13.3	13.0

TABLE 13.

GRAHAMSTOWN , SEPTEMBER 1950.

Time SAMT.		h_m km.	h_o km.	$h_m - h_o$ km.	H_m km.
0700	E_a present	139.2	122.0	17.2	15.4
0730	E_a absent	138.8	116.6	22.2	16.8
0730	E_a present	138.6	117.8	20.8	14.6
0800	E_a absent	127.0	113.2	13.8	17.7
0830	E_a absent	126.4	112.0	14.4	11.6
0900	E_a absent	128.6	114.3	14.3	13.6
1000	E_a absent	125.5	108.5	14.0	13.8
MEAN				16.7	14.8

TABLE 13 - True heights for the E layer.

Remarks on the E layer scale height:

In the case of the Johannesburg records it will be seen from Tables 9 to 12 that the mean value of the scale height is smaller when the E_a is present than when it is absent, the effect being more marked in December.

The evidence cannot be regarded as definite, however, as the mean difference is less than the experimental error. There does not seem to be a marked seasonal variation in the value of H_m for the normal E layer.

It must be remembered that the mean value of H for the layer is considerably less than H_m, and hence our results are in good agreement with other estimates for the E layer. The mean value of H_m for the few Grahamstown records scaled agrees very well with the Johannesburg means.

At this stage we may remark on a method praposed (and used) to determine the scale height of the E layer. From equation (21) in Chapman's theory,

$$h_m = h_o - \frac{T_o}{C} \log_e F \qquad \text{-----(21).}$$

it follows that the variation of $(h_m - h_o)$ with χ is given by

$$h_m - h_o = \text{Constant} - \frac{T_o}{C} \log_e \cos\chi \qquad \text{-----(51).}$$

This equation shows that the graph of $(h_m - h_o)$ vs. $\log_e \cos\chi$ is a straight line, slope T_o/C. It should therefore be possible to determine H (= T_o/C) by plotting $(h_m - h_o)$ against $\log_e \cos\chi$.

An inspection of Tables 9 to 12 shows, however, that the experimental error in $(h_m - h_o)$ is greater than the variation predicted in equation(51). There is a definite tendency for the values of $(h_m - h_o)$ to be smaller during the middle part of the day, but the method is hardly quantitative. Unless the means of a large number of records are taken, the method cannot be used in the case of the E layer.

Comparison with Booker and Seaton and Pierce Analysis:

Most of the existing data for the E layer are in the form of records analysed by the Booker and Seaton and Pierce methods. It is therefore instructive to compare the results obtained with results from these methods. O'Brien [12] compared the values of actual height from the three methods and found that both the Booker and Seaton and Pierce method gives too low a value of h_m.

For the purpose of comparing the methods, the records for December 1949 were scaled again, using the Booker and Seaton and Pierce methods. Pierce's correction to the parabolae, given in equations (44) and (45) were also applied. The results are given in Tables 14 and 15, where suffixes p refer to the Booker and Seaton

parabolae and c to the Pierce analysis. The mean Pekeris values are also given for comparison.

TABLE 14.

JOHANNESBURG, DEC. 1949 (E_a ABSENT).

	Booker & Seaton		Pierce's Correct.		Pierce	
Time SAMT	h_{mp} km.	τ_p km.	$0.6\tau_p$ km.	$h_{mp}-.084\tau_p$ km.	h_{mc} km.	H_c km.
0600	122.6	19.6	11.7	121.0	120.9	9.6
0700	114.7	12.4	7.4	113.7	113.8	5.9
0800	117.1	17.8	10.8	116.0	115.9	6.8
0900	118.5	13.8	8.3	118.3	118.0	6.9
1000	117.1	16.8	10.1	116.0	116.6	8.5
1100	117.9	15.2	9.1	116.9	117.1	6.1
1200	116.8	19.3	11.6	115.8	117.1	7.2
1300	116.4	16.1	9.7	115.4	114.9	8.2
1400	116.1	16.8	10.1	115.1	115.0	8.8
1500	116.1	18.9	11.3	115.1	115.3	8.0
1600	118.1	16.2	9.8	117.1	118.0	7.9
1700	116.1	16.5	9.9	115.1	114.4	6.8
MEAN	117.3	16.7	10.0	116.3	116.4	7.7

TABLE 14 - Comparison of methods of evaluating true heights.

Mean values given by Pekeris method (Table 9):

$h_m = 122.9$, $H_m = 14.9$.

TABLE 15.

JOHANNESBURG , DEC. 1949 (E_a PRESENT).

	Booker & Seaton		Pierce's Correct.		Pierce	
Time SAMT.	h_{mp} km.	τ_p km.	$0.6\tau_p$ km.	$h_{mp}-.084\tau_p$ km.	h_{mc} km.	H_c km.
0600	121.8	9.9	5.9	121.0	120.6	5.4
0700	120.7	13.1	7.9	119.6	119.1	6.1
0800	116.8	12.0	7.7	115.8	115.1	6.1
0900	115.0	8.4	5.0	114.3	114.0	4.1
1000	115.1	13.4	8.1	114.0	113.8	6.5
1100	114.5	7.9	4.7	113.8	114.6	4.0
1200	115.1	9.5	5.7	114.3	115.2	5.3
1300	115.5	11.0	6.6	114.6	114.3	4.7
1400	115.4	9.6	5.8	114.8	114.2	5.3
1500	116.9	10.4	6.2	116.0	115.5	5.7
1600	115.0	11.5	6.9	114.1	114.1	6.3
1700	117.6	8.7	5.2	116.9	116.9	3.7
MEAN	116.6	10.5	6.2	115.8	115.6	5.3

TABLE 15 - Comparison of methods of evaluating true heights.

Mean values given by the Pekeris method (Table 10):

h_m = 120.2

H_m = 19.5

In scaling these records it was found that the four values of τ_p, calculated from Table 3, shows rather large variations. The values of H_c (Table 4) were in better agreement.

From the fifth and sixth columns in Tables 14 and 15 it will be seen that the conversion formula (45) given by Pierce applies accurately to the E layer. On the other hand the value of H as calculated from formula (44) is bigger than the Pierce value. A better conversion formula in the case of the E layer therefore seems to be

$$H_c = 0.5\tau_p \qquad \text{-----(52).}$$

The value of H_c given in the last column of Tables 15 and 14 are much smaller than the corresponding values of H_m from Tables 9 and 10. This is to be expected since the value of H increases with height. The mean value of the scale height will therefore be smaller than ~~than~~ H_m.

The most striking difference between the results from the three methods, is in the value of the height of maximum ionisation, h_m. Inspection of Tables 14 and 15 reveals that the values of h_{mp} and h_{mc} are much lower than h_m given by the Pekeris method. This result was also noticed by O'Brien [12].

Another way of comparing results from the three methods is by means of the characteristic frequency, f_k. This frequency is defined as the frequency at which the virtual height of the layer is equal to the actual height of maximum ionisation. Booker and Seaton found the value of f_k to 0.834 f_c , while Pierce's value is 0.811 f_c. From what has been said, it follows that these values are far too low. In Table 16 (overleaf) the ratios f_k/f_c are given for the Johannesburg records.

The mean value of f_k/f_c is 0.904 , which is in very good agreement with the value 0.897 found by O'Brien [12] for the E layer. There does not seem to be a marked diurnal or seasonal variation in the ratio, but more evidence is required.

In conclusion we may therefore state that the usual methods of finding true heighs, namely the Booker and Seaton and Pierce methods, may lead to errors in the case of the E layer, especially in the case of h_m.

TABLE 16.

	DECEMBER 1949		JULY 1949	
Time SAMT.	E_a absent f_k/f_c	E_a present f_k/f_c	E_a absent f_k/f_c	E_a present f_k/f_c
0600	0.874	0.895	-	-
0700	0.924	0.887	-	-
0800	0.874	0.919	0.885	-
0900	0.846	0.916	0.922	0.926
1000	0.876	0.946	0.930	0.916
1100	0.882	0.919	-	0.924
1200	0.874	0.908	-	0.895
1300	0.896	0.919	0.896	0.919
1400	0.882	0.909	0.903	0.885
1500	0.886	0.895	-	0.881
1600	0.869	0.909	0.922	0.904
1700	0.913	0.921	0.915	-
MEAN	0.883	0.912	0.910	0.906

Table 16 - Ratio f_k/f_c for the Johannesburg records.

Results for Abnormal E Layer:

The Johannesburg records for the abnormal E layer for July and December 1949, were scaled using the Pekeris method. All the records had to be interpolated near the critical frequency of the E layer and this could not be done with great accuracy. As the results for the E_a layer are largely affected by the manner of extrapolation, our results for this layer are rather uncertain.

It was pointed out by Manning [54]) that the equation (14) of Appleton and de Groot only applies if the height is a single-valued function of the electron density. The Pekeris analysis for the E_a layer therefore tacitly assumes that the ionisation between the normal and abnormal layers is constant and equal to the maximum density of the lower layer. The work of Hollingworth [36]) has shown that the ionisation between the E and F_1 layers is very little less than the maximum E ionisation. Hence the assumption made cannot lead to large errors, as the distance between the E and E_a layers is usually very small.

The E_a layer was found to be very thin, as expected from the (h,f) curves. The ionisation density does not tend to a definite maximum, so that the method of evaluating H cannot be applied. In Tables 17 and 18 the results are thus given in terms of h_m, the height of maximum ionisation,

and h_n, the height corresponding to a frequency just above the E layer critical frequency.

TABLE 17.

JOHANNESBURG , JULY 1949.

Time SAMT.	h_m km	h_n km.	$h_m - h_n$ km.
0900	133.4	129.8	4.6
1000	132.4	129.2	3.2
1100	131.6	126.4	5.2
1200	130.8	128.2	2.6
1300	127.0	126.0	1.0
1400	127.6	126.8	0.8
1500	128.2	127.4	0.8
1600	130.0	128.0	1.0
1700	125.8	124.4	1.4
Mean	129.8	127.6	2.2

TABLE 17 - Actual heights for the E_a layer.

TABLE 18.

JOHANNESBURG , DECEMBER 1949.

Time SAMT.	h_m km.	h_n km.	$h_m - h_n$ km.
0600	133.4	129.8	4.6
0700	121.8	119.6	2.2
0800	122.6	120.0	0.6
0900	123.2	120.3	2.9
1000	123.1	122.0	1.1
1100	121.0	118.6	2.4
1200	122.1	120.2	0.9
1300	122.3	119.8	2.5
1400	122.6	117.8	4.8
1500	120.9	120.4	0.5
1600	120.8	120.4	0.4
MEAN	123.0	121.7	2.3

TABLE 18 - Actual heights for the E_a layer.

From these results it appears that the layer is very thin. The value of h_n is very doubtful, but even so the thickness of the layer must be correct to the order

of magnitude at least. It therefore seems that the scale height of the layer probably does not exceed 5 km.

The layer occurs at lower heights in summer than in winter, which shows again the marked solar control on the layer. There does not seem to be a seasonal variation in the value of the thickness of the layer, but, as the experimental error involved is very large, no significance can be attached to this result.

- - - - - - - - - - - - -

ERRORS IN THE PEKERIS ANALYSIS.

The Pekeris method, described in the previous section, is at present by far the best method of determining true heights from the (h',f) curves. It is however still subject to certain errors which will be dealt with in the following pages.

The errors in the method arise not only out of the approximations made in the theory, but also from the fact that the experimental (h',f) curves are always incomplete and have to be extrapolated. Thus the initial part of the curve corresponding to the lower frequencies is always missing so that the curve has to be produced to zero frequency. In the Johannesburg records dealt with, for instance, the lower frequency limit of the transmitter and receiver is 1 mc./sec. , but during the middle part of the day the trace only appears at a frequency ranging from 2 to 3 mc./sec. The method of extrapolation to

to zero is not at all clear and cannot be done accurately. Near the critical frequency the trace usually fades out so that again the curve has to be produced, which may also lead to errors.

The other factor that makes the Pekeris analysis not strictly accurate is due to the approximation made in the theory when the effects of the earth's magnetic field and of collisional friction are neglected.

In what follows we shall discuss these errors as they apply to the E layer with special reference to the effect of the earth's magnetic field on the experimental results. It must be remembered that the Booker and Seaton and Pierce methods imply exactly the the same errors and are definitely inferior to the PPekeris analysis, which must always be used.

Errors due to extrapolation to zero frequency:

The methods of extrapolating the curves to zero frequency were discussed by Manning[54]) and Rydbeck [53]) . Manning produced the virtual height in a smooth curve, most of which is at constant height. Rydbeck extended the virtual height curve at the uncertainty point by its tangent to zero frequency. O'Brien [12]) found that in the usual record there is very little difference between the two methods of

extrapolation. In records where the initial frequency of the trace is relatively high, the Rydbeck method may however lead to large errors if applied literally. The Manning method was therefore adopted in scaling our records.

Rydbeck also investigated what effect the manner of extrapolation has on the shape of the layer. He determined the distribution curve for two extreme ways of extrapolating. In the first case the curve was extended by its tangent at the uncertainty point. In the second case the curve was smoothly produced to zero virtual height at zero frequency. Rydbeck found that the main character of the layer is not affected very much by the manner of extrapolation. O'Brien [12]) points out however that the way in which the curve is extended affects the actual height of the layer considerably. If the presence of the D layer is taken into account, the value of h_m will be reduced. At present it is however difficult to decide by how much the values of h_m will be affected.

Errors near critical frequency:

Another source of error arises at the extrapolation of the virtual height curve at the critical frequency. In the case of the normal E layer a method was outlined whereby this part tof the curve is not used. Instead, the

distribution curve is extrapolated to maximum density, thus obtaining a more accurate value of h_m. In the case of the abnormal E layer, the height is considerably affected by the manner of extrapolation at the critical frequency of the lower layer. The true heights of this layer is therefore subject to large errors, in particular near the critical frequency.

All this shows clearly the need for more sensitive equipment with a larger frequency range in the investigation of the E layer.

Effect of the Earth's Magnetic Field:

We now turn to a discussion of the errors arising out of the neglect of the earth's magnetic field in the Pekeris method. All the methods used for the routine scaling of (h',f) records find it necessary to make this approximation as the general equation corresponding to (13) cannot be solved algebraically.

Booker and Seaton [49]) found that the error due to the magnetic field is small but systematic. They estimated it to be approximately five to ten km. in the case of the nighttime F layer. Rydbeck [52]) estimated that the error is less than the experimental error down to an angle of 75° between the direction of propagation and

and the earth's magnetic field. But even in such cases the error cannot be overlooked. In the first place it is systematic; and secondly the experimental error is relatively large, compared with the thickness of the layer, especially in the case of the E layer. The magnetic field will therefore have an appreciable effect on the scale height of the layer. In South Africa the angle between the field and the direction of propagation (vertical) is approximately 30^{o}, so that the error involved is even greater.

It thus seems worthwile to examine more fully the magnitude of the errors involved due to the neglect of the earth's field.

Group Velocity of E.M. wave in ionised medium:

The group velocity U of an electromagnetic wave is given by the standard formula [36]

$$\frac{1}{U} = \frac{1}{c}\frac{d}{dp}(\mu p) \qquad \text{-----(52).}$$

where μ is the refractive index and p the angular frequency of the wave. In the case of an ionised medium μ is given by the Appleton-Hartree formula. If the effect of collisional friction is neglected, the

formula becomes

$$\mu^2 = 1 - \frac{2p_o^2}{2p^2 - \frac{p^2 p_T^2}{p^2 - p_o^2} \mp \sqrt{\frac{p^4 p_T^4}{(p^2-p_o^2)^2} + 4p^2 p_L^2}} \qquad \text{-----(7).}$$

where

$$p_o^2 = \frac{4\pi ne^2}{m} \qquad \text{-----(5).}$$

$$p_T = eH_T/mc \qquad \text{-----(6a).}$$

$$p_L = eH_L/mc \qquad \text{-----(6b).}$$

In (7) the ordinary ray corresponds to the lower sign (+), while the extraordinary coefficient is given by the upper sign (-).

Now from equation (52),

$$\frac{c}{U} = \frac{d}{dp}(\mu p)$$

$$= \mu + p\frac{d\mu}{dp}$$

$$= \frac{1}{\mu}\left(\mu^2 + p\mu\frac{d\mu}{dp}\right) \qquad \text{-----(53).}$$

$$= \frac{1}{\mu}\left(\mu^2 + \frac{p}{2}\frac{d\mu^2}{dp}\right)$$

From (7) by differentiating, we get

$$\frac{d\mu^2}{dp} = \frac{2p_o^2\left\{4p + \frac{2pp_o^2p_T^4}{(p^2-p_o^2)^2} \mp \frac{4pp_L^2 - 2p_o^2p^3p_T^4/(p^2-p_o^2)^3}{\sqrt{p^4p_T^4/(p^2-p_o^2)^2 + 4p^2p_L^2}}\right\}}{\left\{2p^2 - \frac{p^2p_T^2}{p^2-p_o^2} \mp \sqrt{\frac{p^4p_T^4}{(p^2-p_o^2)^2} + 4p^2p_L^2}\right\}^2}$$

so that on simplifying

$$\mu^2 + \frac{p}{2}\frac{d\mu^2}{dp} = 1 + \frac{2p^2p_o^2\left\{\frac{p^2p_T^2}{(p^2-p_o^2)^2} \pm \frac{2p_L^2 + p^4p_T^4/(p^2-p_o^2)^3}{\sqrt{p^4p_T^4/(p^2-p_o^2)^2 - 4p^2p_L^2}}\right\}}{\left\{2p^2 - \frac{p^2p_T^2}{p^2-p_o^2} \mp \sqrt{\frac{p^4p_T^4}{(p^2-p_o^2)^2} + 4p^2p_L^2}\right\}^2}$$

-----(54).

In this formula the upper sign refers to the extraordinary and the lower sign to the ordinary wave. The value of c/U for both rays may therefore be evaluated from (53), μ being given by (7).

Approximate Formula for Ordinary Ray:

In the simple expression for c/U the earth's magnetic field is neglected as well. Thus, equating both p_L and p_H to zero, equations (7) and (54) become respectively,

$$\mu^2 = 1 - p_o^2/p^2$$

and

$$\mu^2 + \frac{p}{2}\frac{d\mu^2}{dp} = 1 ;$$

so that

$$\frac{c}{U} = \frac{1}{\sqrt{1 - p_o^2/p^2}} \qquad \text{-----(55).}$$

which is the usual formula used for the group velocity of the ordinary ray.

In order to compare this formula for c/U with the more accurate expression, the group velocity was computed for values of p, p_L and p_T characteristic of the E layer in South Africa. The following values of the constants were chosen:

$p = 2 \times 10^7$ rad./sec.

$H_L = 0.30$ Oersted.

$H_T = 0.12$ Oersted.

In this case

$p_L = eH_L/mc = 5.28 \times 10^6$ rad./sec.

$p_T = eH_T/mc = 2.11 \times 10^6$ rad./sec.

$p_H = \sqrt{p_L^2 + p_T^2} = 5.69 \times 10^6$ rad./sec.

The electron density is given by equation (5). The values of c/U for different p_o^2 are given in Table 19 and shown graphically in fig. 16. The critical value of

p_o, namely p_c, is given by

$$p_c = p = 2 \times 10^7 \text{ rad./sec.}$$

TABLE 19.

p_o^2/p_e^2	μ from(7)	$\mu^2 + \frac{p}{2}\frac{d\mu}{dp}^2$	c/U	c/U from (55)
0.0	1.000	1.000	1.000	1.000
0.2	0.918	0.984	1.072	1.128
0.4	0.827	0.977	1.172	1.291
0.6	0.722	0.961	1.333	1.581
0.7	0.662	0.957	1.446	1.824
0.8	0.594	0.997	1.680	2.23
0.9	0.509	1.150	2.28	3.16
1.0	0	-	∞	∞

TABLE 19 - Comparison of formulae for c/U (Ordinary ray)

It will be seen that the values of c/U given by the approximate formula, are always in excess of the more accurate values.

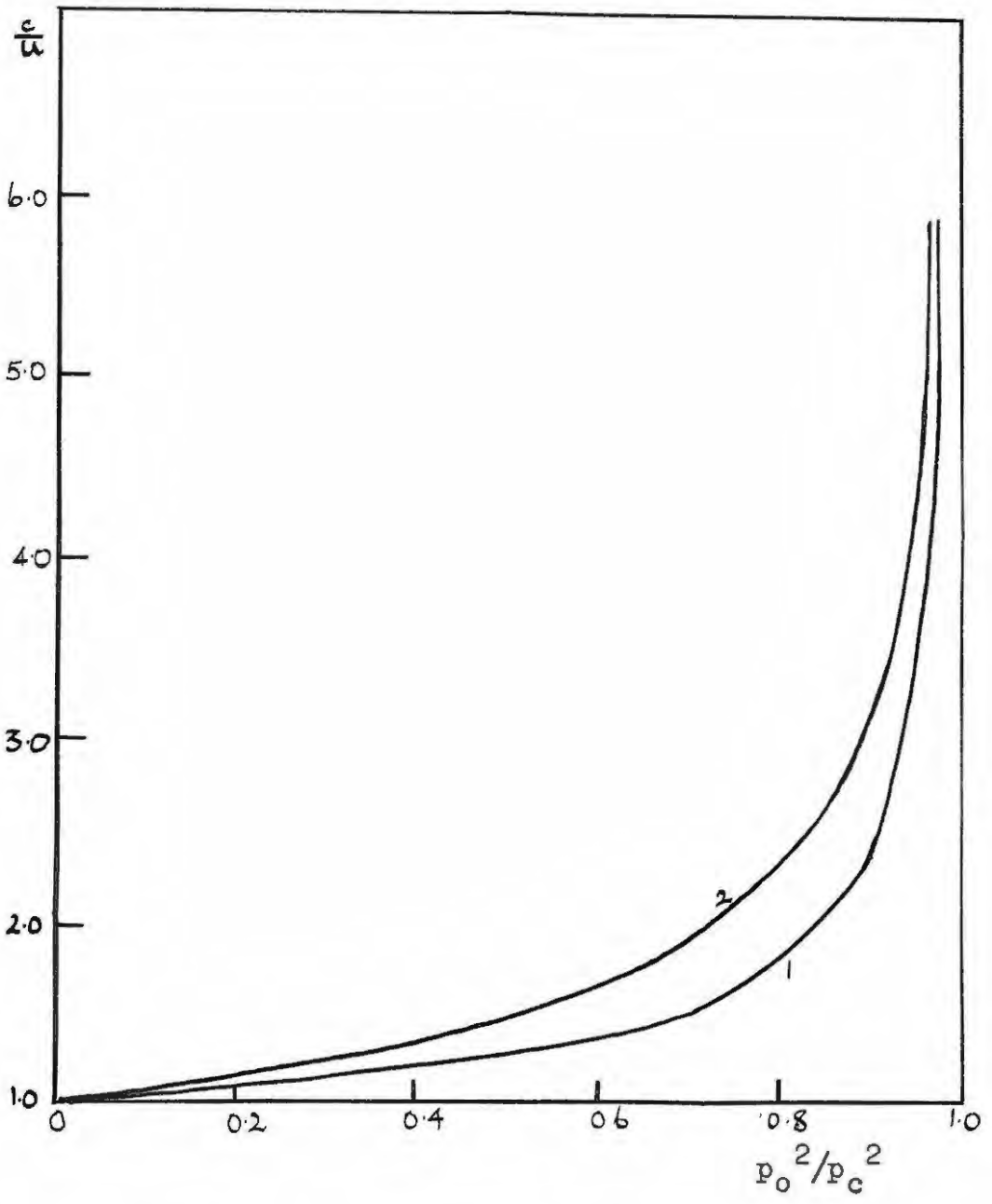

FIG. 16 - COMPARISON OF FORMULAE FOR THE GROUP VELOCITY OF ORDINARY RAY.

1. Accurate formula.
2. Approximate formula.

Virtual heights for ordinary ray:

The virtual height of an ionosphere layer is given by the equation

$$h' = \int \frac{c}{U}\, dh \qquad \text{-----(11).}$$

Since the values of c/U given by the simple expression are always greater than the true values, virtual heights calculated using equation (55) will be too large. Alternatively, if the true height is to be calculated from the virtual height, then the simple formula (55) leads to a correction which is too great. It follows that the values of true height, obtained by the Pekeris analysis, are always in excess of the true values.

In order to get an idea of the magnitude of the error involved, the virtual heights were evaluated using both formulae of c/U for a simple case which however serves to illustrate the effect. Consider the case of a layer whose critical angular frequency is $p_c = 20 \times 10^6$ rad./sec. , and whose electron density rises linearly from zero to the maximum value. It follows from (5) that p_o^2 is proportional to the height. Hence in this case, the virtual heights are simply given by the areas underneath the curves in fig. 15, multiplied by the actual height of the layer.

The areas underneath the curves are rather difficult to estimate as c/U tends to infinity in both cases. The areas were therefore plotted as a function of p_o^2/p_o^2, and the total area obtained by extrapolating to $p_o^2/p_c^2 = 1$. The virtual heights found in this way, are 1.5 (in the case of the more accurate formula) and 1.75 (for approximate formula) times the true height respectively. This means that if the Pekeris analysis is applied to this layer, the true height obtained from the virtual height curve will be about 0.85 the actual value. A conservative estimate of the error involved in the actual thickness of the layers due to the neglect of the earth's field, is therefore 10%.

The method may be extended to calculate the virtual heights for any distribution of electron density. The variation of c/U with p_o^2 may be calculated for any frequency from equations (7) and (54). Using these values the integral $\int \frac{c}{U} dh$ can be evaluated for different frequencies if the electron distribution and hence the variation of p_o^2 with height is known. The method may for instance be applied to the electron density curves obtained from the Pekeris analysis. The virtual heights thus found will give a very good indication of the error due to the neglect of the earth's field. But unfortunately the method is very long and therefore not applicable to the routine scaling of records.

Extraordinary ray group velocity:

Using the same values of the constants p, p_L, p_T, the group velocity c/U was again calculated for the extraordinary ray, for different values of p_o. In this case the critical angular frequency p_x is given by the equation

$$p_x^2 = p^2 - pp_H \qquad \text{-----(10).}$$

The values of c/U obtained are given in Table 20.

In South Africa the values of p_T^2 are small compared with p_L^2. It is therefore of interest to work out the case of longitudinal transmission. Thus, putting $p_T = 0$ and $p_L = p_H$, equations (7) and (54) become, for the extraordinary ray,

$$\mu^2 = 1 - \frac{p_o^2}{p^2 - pp_H} \qquad \text{-----(56).}$$

and

$$\mu^2 + \frac{p}{2}\frac{d\mu^2}{dp} = 1 + \frac{pp_o^2p_H^2}{2(p^2 - pp_H)^2}$$

In the last expression the last term is usually small compared with unity, so that a good approximation for the group velocity is

$$\frac{c}{U} = \frac{1}{\sqrt{1 - \dfrac{p_o^2}{p^2 - pp_H}}} \qquad \text{-----(57).}$$

This formula also leads to the correct critical condition, as will be seen from equation (10). Values calculated from this formula are given in table 20. They are always smaller than the more accurate values.

TABLE 20.

p_o^2/p_x^2	μ from (7)	$\mu^2 + \frac{p}{2}\frac{d\mu^2}{dp}$	c/U	c/U from (57)
0.0	1.000	1.000	1.000	1.000
0.2	0.897	1.065	1.188	1.149
0.4	0.774	1.068	1.380	1.291
0.6	0.640	1.071	1.673	1.582
0.7	0.309	1.117	2.006	1.824
0.8	0.209	1.178	2.58	2.25
0.9	0.049	1.257	5.67	3.16
1.0	0			

TABLE 20 - Comparison of formulae for c/U (Extraordinary).

Evaluating true heights from extraordinary curve:

If the group velocity of the extraordinary wave is given by equation (57), then it is very easy to determine the

true height of the layer from the extraordinary virtual height-frequency curve.

Thus, writing

$$f = p/2\pi ,$$

$$f_h = p_o/2\pi ,$$

$$f_H = p_H/2\pi ,$$

equation (57) becomes

$$\frac{c}{U} = \frac{1}{\sqrt{1 - \dfrac{f_H^2}{f^2 - ff_H}}}$$

The virtual height is given by the equation

$$h' = \int_o^h \frac{dh}{\sqrt{1 - f_h^2/(f^2 - ff_H)}} \qquad \text{-----(58).}$$

Introduce the new variable f′ defined by the equation

$$f'^2 = f^2 - ff_H \qquad \text{-----(59).}$$

f′ may be called the"effective frequency"

Equation (58) can now be written

$$h' = \int_o^H \frac{dh}{\sqrt{1 - f_h^2/f'^2}}$$

This is the familiar Abel integral equation, as the condition for reflection at height h is still

$$f'^2 = f^2 - ff_H = f_h^2 .$$

Hence the actual height of the layer is given by

$$h = \frac{2}{\pi}\int_0^{f_h} \frac{h'df'}{\sqrt{f_h^2 - f'^2}} \qquad \text{-----(60).}$$

The height may therefore be determined from the variation of h' with f', in exactly the same way as in the Pekeris analysis. From Table 20 it will be seen that the approximate formula (57) is at least as accurate as the one for the ordinary ray. Since the values of c/U given by this formula are smaller than the true values, the values of h deduced from (60) will be too large.

Determination of true heights:

Rydbeck [52]) has described a method of determining the true height of an ionosphere layer in the case where the transmission is along the earth's field. He estimates thaththe method leads to errors which are less than the experimental errors up to angles of 20° between the direction of propagation and the earth's magnetic field. In this

method the virtual height curve for the extraordinary ray is first corrected for the presence of the field, and is then replotted against f′, defined as in (59). The usual analysis is then applied to this curve. The method of correcting is however very long, and Rydbeck's method does not seem to have received any practical application.

A method for determining the true heights of an ionosphere layer, taking into account the effect of the earth's magnetic field, will now be described. It is rather similar to the Rydbeck method, but is far shorter. The method is based on the fact that the actual height obtained from the extraordinary ray, as described above, exceeds the true value by about the same amount as the value of h from the ordinary layer is too low.

Consider a record showing both the ordinary and extraordinary reflections. The magnetic frequency can be calculated from the formula

$$f_H = \frac{f_x^2 - f_c^2}{f_x} \qquad \text{-----(41).}$$

f_c and f_x being the ordinary and extraordinary critical frequencies respectively. Using this value of f_H the virtual height of the extraordinary reflection can be

replotted against f′. The critical value of f′ will coincide with f_c. If the mean of this curve and the ordinary curve is scaled by the usual method, more accurate values of the actual heights will be obtained. It will be seen that the procedure is quite fast. A table to convert f to f′ will be very useful.

The method has the limitation that it can only be applied to records where both the ordinary and extra-ordinary reflections are present. In this respect it is not inferior to the Rydbeck method as the ordinary reflection always occur if the extraordinary is present. In our records for the E layer the extraordinary trace was found to occur only near sunrise and sunset. Analysis of these records does however give a good indication of the errors invoved in the usual method. The method described should prove useful in the case of F layer reflections.

Typical virtual height curves for an early morning record are shown in fig. 18. The actual heights were determined for both the ordinary and extraordinary rays. It was found using the ordinary

h_m = 117.8 and H_m = 9.3 km.;

and using the extraordinary

h_m = 121.7 km. and H_m = 11.3 km.

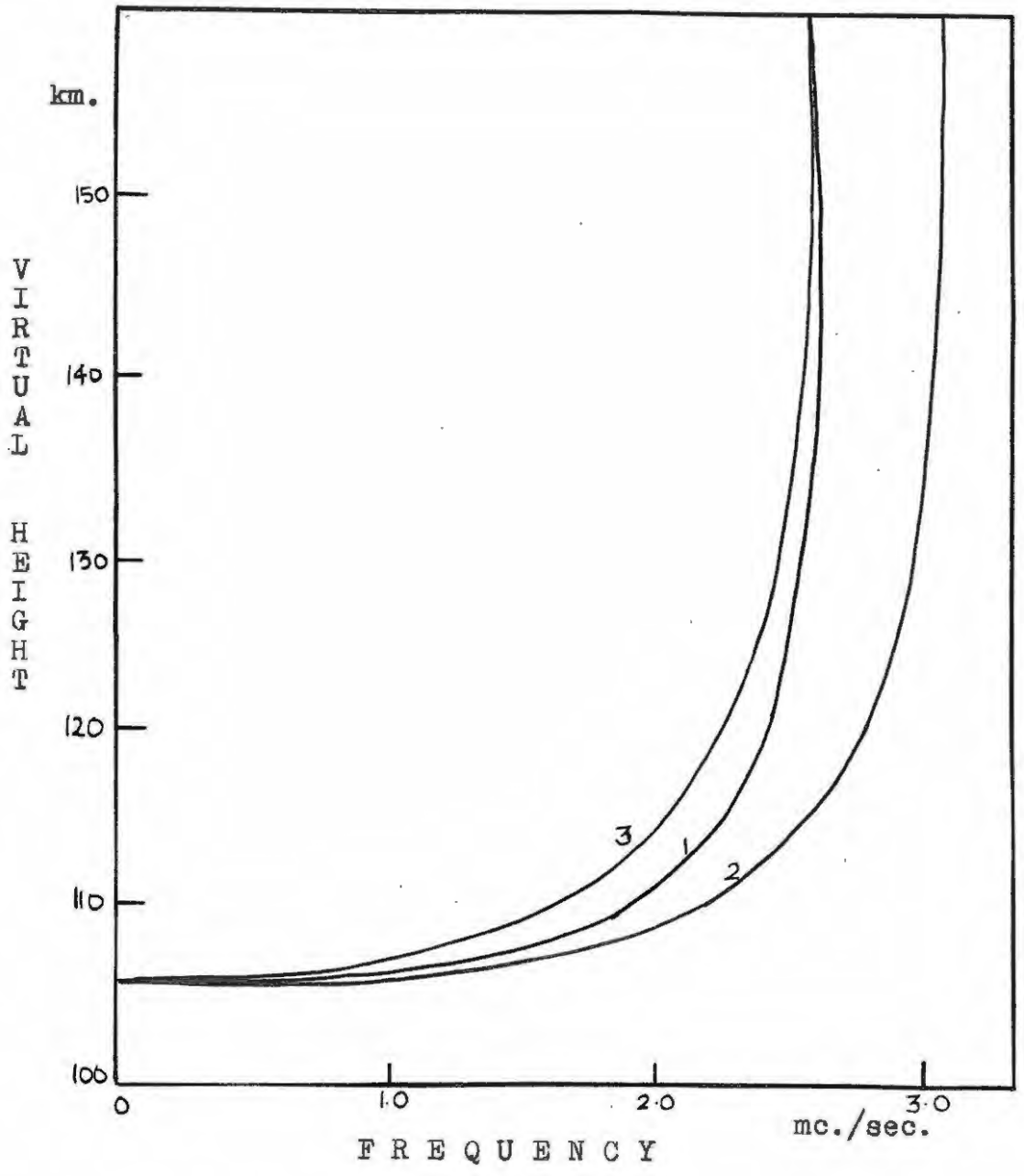

FIG. 18 - VIRTUAL HEIGHT CURVES FOR ORDINARY AND EXTRAORDINARY REFLECTIONS.

1. Ordinary curve.
2. Extraordinary curve.
3. Corrected extraordinary curve.

This again indicates that the Pekeris analysis leads to values of the scale height which is too small by about 10%.

The method outlined above can be improved by taking a weighted average of the virtual height curves before scaling for true heights. In order to decide how this is to be done, virtual heights can be calculated, as above, for both the ordinary and extraordinary rays for typical electron distributions of the layers to be scaled. In this way it can be decided which of the two rays give the best value of actual height.

It may be remarked that the method assumes that the ordinary and extraordinary rays are reflected from the same place in the ionosphere. As pointed out by Booker[46]), Millington [47]), and Scott[48]) this may not be the case, but if the means of a large number of records are taken, the error involved should be very small.

Conclusion:

We may sum up the results of this section by saying that due to the fact that the virtual height curves are always incomplete, our values of the actual height of the E layer are rather uncertain. In South Africa, also due to the earth's magnetic field, the Pekeris method leads to values

of the scale height that are about 10% too small.

The effect of the neglect of collisional friction is rather difficult to estimate. It can be done by calculating c/U using the Appleton-Hartree formula, but the arithmetic involved is very heavy, and at present it does not seem worthwile to do the numerical calculation, as the experimental errors are much larger.

- - - - - - - - - - - - - -

TEMPERATURE AND COMPOSITION OF THE E LAYER.

In this section the temperature and composition of the E layer will be dealt with. These two quantities are closely linked together in the scale height H of the layer, defined by the equation

$$H = \frac{T}{C} = \frac{kT}{Mg} \qquad \text{-----(24).}$$

In the case of the E layer $g = 950$ cm./sec.^{2}, so that

$$C = Mg/k = 1.134\ M\ {}^{\circ}K/km. \qquad \text{-----(61)}$$

M being the mean molecular mass of the constituents of the layer in a.m.u.

Composition of the E layer:

Most of the recent determinations of the temperature of

the ionosphere layers, are based on a knowledge of the scale height H. In order to calculate T from H, using equation (24), it is necessary to know the value of M, the mean molecular mass. The chief constituents of the atmosphere are oxygen and nitrogen, present approximately in the ratio 1:4. A knowledge of the state of these two constituents is therefore all that is required for the calculation of a very good approximation to M.

In 1930 Chapman [55]) deduced that above 120 km. most of the oxygen in the atmosphere exists in the atomic form. His calculation was confirmed by Wulf and Deming [56]), who by considering the times of half- recombination of the oxygen atoms, have shown that the dissociation of oxygen must be nearly complete above 100 km. Penndorf [57]) recently reviewed the distribution of atomic oxygen in the upper atmosphere. He concluded that the transition layer from molecular to atomic oxygen is about 10 km. thick, and has a mean height of between 100 and 110 km. , definitely below the E layer.

The state of nitrogen in the upper atmosphere is not as easy to deal with as that of oxygen. A considerable amount of evidence has recently accumulated indicating that nitrogen also exists in the atomic form at great altitudes. Most writers however, estimate the ~~transmission~~

transition region to occur far above the E layer.

In view of this, we shall take the E layer to be composed of oxygen atoms and nitrogen molecules in the ratio 1:2. The question cannot be regarded as definitely settled yet, especially in the case of oxygen in view of the uncertainties that prevail in the value of the actual height of the layer.

If molecular nitrogen and atomic oxygen are the principal constituents of the atmosphere, then

$$M = 24.0 \text{ a.m.u.}$$

so that $$C = 27.3 \ ^{\circ}K/km.$$

Temperature of the E region:

Various estimates of the temperature of the atmosphere in the E region have been made. Most of these were calculated from the scale height H of the layer, assuming the composition of the layer to be known.

Vassy and Vassy [58], considering the dissociation to be complete for both oxygen and nitrogen, found the temperature to be 360°K at 100 km. Hulburt [59] also adopted the value of 360°K at 100 km. Whipple [60], who has made a survey of the temperature and density of the atmosphere up to a height of 120 km., estimates the temperature to

be 350°K at 120 km. Penndorf, using the value H = 11.4 km. as given by Appleton for the E layer, calculated the temperature for various assumed compositions of the atmosphere. He found the value to be 308°K for an atmosphere consisting of 67% N_2 and 32% O. Grimminger[61]) has recently made a comprehensive analysis of the pressure, temperature and density of the atmosphere, and he adopts the value of 375°K at 120 km. O'Brien [12]) , using the results of Gledhill and Szendrei for the E layer for the four months November 1945 to February 1946, finds a temperature of 280°K for an atmosphere consisting of atomic oxygen and molecular nitrogen.

The most direct way of measuring temperatures in the upper atmosphere is by means of instruments borne by balloons or rockets. Best, Haven and others [61]) have reported on the temperature measurements made bt a V-2 rocket in New Mexico, up to heights of 120 km. They found the temperature to be 220°K at 100 km. and 330°K at 120 km.

Using our values of the scale height of the E layer for July and December 1949, the mean day temperatures were calculated for an atmosphere consisting of atomic

oxygen and molecular nitrogen. The results are given in Table 21.

TABLE 21.

	JULY 1949		DECEMBER 1949	
	E_a present	E_a absent	E_a present	E_a absent
Mean H_m(km)	13.0	14.0	10.5	14.9
Mean h_m(km.)	122.3	122.3	120.2	122.9
T_m (^oK)	355	382	287	407
T_m (^oK)	368		347	

TABLE 21 - Temperature of the E region.

The mean value of 358^oK is in good agreement with other estimates. The temperature appears to be somewhat higher in winter than in summer. This is very surprising as the heights are approximately the same. The effect is probably due to the experimental errors in the determination of the scale height of the layer.

Temperature Gradient:

It soon became evident that the simplifying assumption made by Chapman that the temperature of the layers is constant does not hold in the case of the ionosphere. In view of the uncertainties which exist, most writers adopt as a first approximation a linear temperature gradient from about 100 km. upwards. Gledhill and Szendrei [11] have worked out the theory of layer formation in an atmosphere where the temperatureat a height h is given by

$$T = T_o + \gamma(h - h_o) \qquad \text{-----(27).}$$

γ being the temperature gradient.

Various estimates of the value of γ have been made. Whipple estimates it to be 4.5 ^{o}K/km. between 100 and 120 km. The measurements of Best, Haven and others [62] using a V-2 rocket, leads to the value 5.5 ^{o}K/km. between 100 and 2120 km. Grimminger [61] assumes the temperature to rise linearly with height, and adopts the value of 4^{o}K/km. between 120 and 300 km. Gledhill and Szendrei [11], by applying their theory to experimental results in the form of Booker and Seaton parabolae, found a mean value of 8.6 ^{o}K/km. in the case of the F layer.

We have described a method of estimating the temperature

gradient of an ionosphere layer from a study of the variation of critical frequency with log cosχ, χ being the the sun's zenith distance. For the E layer it was found for the Johannesburg records for the year 1949, that

$$C/\gamma = 3.38 \qquad \text{-----(40)}.$$

Hence, inserting the value $C = 27.3$, this gives

$$\gamma = 8.1\ ^{o}K/km.$$

In view of the many simplifying assumptions made in the theory, this value is in quite good agreement with other estimates. The method seems to be as accurate as any hitherto devised for the evaluation of the temperature gradient.

Application of Linear Temperature Gradient Theory:

The next step is the application of the theory of layer formation in an atmosphere where the temperature is a linear function of the height, to our experimental results which are in the form of electron distribution curves.

The distribution of electrons with height as given by this theory is

$$(n/N)^2 = (1 - x/y)^{-(1+y)} \exp\left\{(1+ 1/y)\left[1 - (1 - x/y)^{-y}\right]\right\} \qquad \text{-----(36)}.$$

In this equation

$$x = \frac{C}{T_M}(h_m - h) = \frac{h_m - h}{H_m} \qquad \text{-----(34).}$$

and $$y = C/\gamma \qquad \text{-----(35).}$$

Equation (36) may be written in the form

$$-2\log_e(n/N) = (1+y)\log_e\left(1-\frac{x}{y}\right) - \left(1+\frac{1}{y}\right)\left[1-\left(1-\frac{x}{y}\right)^{-y}\right]$$

$$= (1+y)\left\{\log_e\left(1-\frac{x}{y}\right) - \frac{1}{y}\left[1-\left(1-\frac{x}{y}\right)^{-y}\right]\right\}$$

$$\text{-----(63).}$$

Let

$$f(x,y) = (1+y)\left\{\log_e\left(1-\frac{x}{y}\right) - \frac{1}{y}\left[1-\left(1-\frac{x}{y}\right)^{-y}\right]\right\}$$

$$\text{-----(64).}$$

The function $f(x,y)$ is plotted in fig. 17 vs. x for different values of y. When $y = \infty$, this function coincides with the Chapman function shown in fig. 14.

The problem of determining the temperature gradient thus resolves itself in determining the best value of the constant y from the distribution curves. For this purpose Table 22 was constructed from fig. 17. In this table x is given as a function of y for certain constant, convenient values of $f(x,y)$. The corresponding values of n/N are also given.

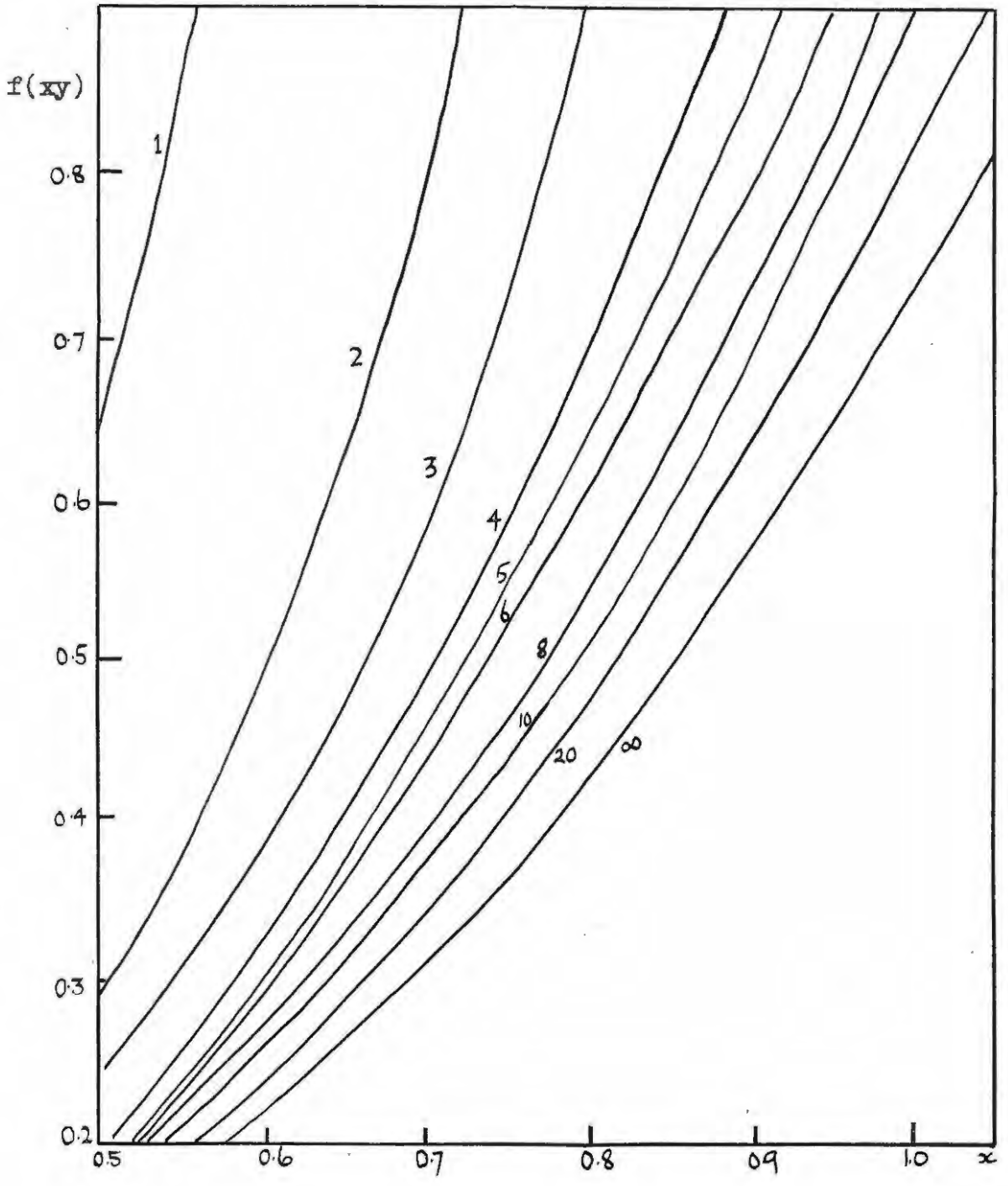

FIG. 17 - THE FUNCTION f(xy) OF EQUATION (64) FOR DIFFERENT VALUES OF y (MARKED ON THE CURVES).

		TABLE 22.						
n/N	f(xy)	y = 1	2	3	4	5	6	8
0.951	0.100	0.256	0.317	0.344	0.364	0.373	0.382	0.389
0.950	0.103	0.258	0.321	0.346	0.368	0.375	0.383	0.391
0.903	0.200	0.337	0.423	0.464	0.487	0.500	0.514	0.528
0.900	0.211	0.344	0.431	0.474	0.496		0.524	
0.861	0.300	0.394	0.496	0.544	0.568	0.589	0.607	0.621
0.850	0.325	0.404	0.514	0.561	0.589		0.628	
0.819	0.400	0.432	0.554	0.608	0.643	0.673	0.685	0.708
0.800	0.446	0.444	0.578	0.636	0.673	0.695	0.711	0.738
0.779	0.500	0.463	0.605	0.673	0.706	0.733	0.746	0.774
0.750	0.575	0.486	0.636	0.703	0.742	0.768	0.784	0.824
0.740	0.600	0.493	0.646	0.715	0.759	0.784	0.804	0.836
0.703	0.700	0.522	0.683	0.747	0.806	0.834	0.856	0.888
0.700	0.713	0.524	0.686	0.749	0.815		0.859	
0.670	0.800	0.544	0.713	0.776	0.847	0.878	0.907	0.936
0.650	0.862	0.554	0.724	0.794	0.869	0.904	0.934	0.964
0.638	0.900	0.560	0.729	0.799	0.885	0.919	0.956	0.982
0.608	1.000	0.571	0.736	0.817	0.914	0.950	0.987	1.019

TABLE 22 - Values of x for constant f(xy).

Using this table it should be possible to find the best values of y and H_m as follows. First use the usual method to find the value of h_m. Then choose a convenient value of n/N in Table 22, and read off the value of h from the distribution curve. In the row for n/N read off the x values corresponding to different values of y. For each of these calculate H_m, using

$$x = \frac{h_m - h}{H_m} \qquad \text{------(34)}$$

$$\text{i.e.} \quad H_m = \frac{h_m - h}{x}$$

and plot these values against y. Repeat the procedure for different points on the curve of electron density. The values of y and H_m will be given by the point of intersection of these curves of constant $f(x,y)$.

The method outlined above was applied to some of the distribution curves for the E layer, without much success. The curves of H_m aganst y were usually approximately parallel, so that it was very difficult to estimate the values of y correctly.

The failure of the method can be attributed to two causes. In the first plave, the shape of the layer depends

very little on the temperature gradient, so that it is very difficult to deduce an accurate value of γ from the distribution curves. Secondly, the value of h_m as determined by the method described earlier, is still rather uncertain. The experimental error is of the order of 2 km. which is quite a large fraction of the thickness of the layer.

It therefores seems that unless the electron distribution can be determined with greater accuracy, the method will fail to give the temperature gradient. It may be more fruitful in the case of the F layer. In the case of the E layer recourse was therefore taken to other methods that give an approximate value of the temperature gradient.

Temperature Gradient from Scale Height:

The first method that suggests itself is to determine γ from the variation of H with height. Let H be the scale height and T the temperature at height h.

Since $H = T/C$,

and $H_m = T_m/C$,

Therefore

$$\frac{H}{H_m} = \frac{T}{T_m} = \frac{T_m - \gamma(h_m - h)}{T_m}$$

$$\gamma = \frac{T_m(H_m - H)}{H_m(h_m - h)} = C\,\frac{H_m - H}{h_m - h}$$

Hence $$y = \frac{C}{\gamma} = \frac{h_m - h}{H_m - H} \qquad \text{-----(66).}$$

Using this relation, y can be determined from the values of H at different heights. These may be evaluated from the slopes of the curve of h against the x-values given in Table 8, as shown in fig.15. The method is therefore only approximate, as the H values are deduced on the assumption of a constant temperature throughout the layer. Since the shape of the layer is very little affected by the temperature gradient, the method will however give a good idea of the magnitude of y.

The results for the Johannesburg records are given in Table 23. The values of y are very low, giving a mean value of γ equal to 18.6 ^{o}K/km. It will be seen that the values are fairly consistent, and that γ is greater in summer than in winter, as would be expected.

TABLE 23.

Time SAMT.	DECEMBER p1949		JULY 1949	
	E_a present y	E_a absent y	E_a present y	E_a absent y
0600	1.37	1.66		
0700	1.56	0.86		
0800	1.26	1.65	2.30	
0900	1.04	1.82	1.62	1.85
1000	1.21	1.15		1.47
1100	1.31	0.72	1.31	1.30
1200	1.48	1.00		1.62
1300	1.46	0.77	1.29	1.55
1400	1.31	0.84	1.76	1.67
1500	2.22	1.12		1.79
1600	1.76	1.05	1.00	1.85
1700	1.32	1.10	2.37	
MEAN	1.47	1.15	1.66	1.64

TABLE 23 - Temperature gradient of E layer.

Evaluation of y by Iteration Process:

Another method of determining the temperature gradient of the layer is by a process of iteration, i.e. the evaluation of H_m and y in turn until the best fit is obtained. Unfortunately, the method is rather long if fully applied.

The first step in the process is the determination of H_m and h_m by the usual method. Using these values, x is found for convenient points on the distribution curve by means of equation (34). The best value of y is then read off from the appropriate row in Table 22. Better values of h_m and H_m are then obtained by replotting the heights against the x-values, read off from the appropriate ~~row~~ column in Table 22. The procedure is repeated untill the graph of h vs. x is found to be a straight line.

The method was applied to the Johannesburg records for December 1949, where the E_a layer is absent. The final results are given in Table 24. It will be seen that the mean value of y is in good agreement with the previous estimate. It also appears that the value of h_m is not affected much by the temperature gradient.

The value of H_m is found to greater than the value of 14.9 km. given by the Chapman curves.

TABLE 24.

JOHANNESBURG , DECEMBER 1949 (E_a ABSENT)

Time SAMT.	h_m km.	H_m km.	y
0700	118.3	13.2	1.8
0800	122.9	16.8	1.9
0900	122.3	12.5	2.8
1000	122.0	15.6	1.9
1100	122.5	18.0	0.9
1200	121.7	17.8	0.9
1300	121.5	22.0	1.0
1400	124.1	19.9	1.9
1500	123.9	26.4	1.0
1600	123.5	15.8	1.8
MEAN	122.7	17.8	1.59

TABLE 24 - Temperature gradient and heights of E layer.

Discussion of Results:

All our estimates of the temperature gradient of the E layer are much higher than the value usually attributed to the layer. It is difficult to see how the effect can be caused by experimental errors, as the results are fairly consistent.

Other explanations of the discrepancy must therefore be sought. It is quite possible that the high value of temperature gradient is correct, as ours is the first estimate of γ from the actual distribution curves. More evidence from other sources are required, however before the result can be accepted for the E layer. It seems at present that the high value of γ does not persist to large heights. Thus Gledhill and Szendrei [12] for instance, estimated γ to be 8.6 ^{o}K/km. for the F layer. This result will have to be verified from actual distribution curves.

It must be remembered that the high value of γ can also be explained if the E layer coincides with the transition layer from molecular to atomic oxygen. If this is the case, the mean molecular mass of the layer will decrease from 28.8 a.m.u. to 24.0 a.m.u. in about 8 km. With the present estimation of the

temperature of the E region, this is equivalent to a temperature gradient of about $6^{\circ}K/km$. In view of the calculations of Penndorf [57] on the distribution of atomic oxygen in the atmosphere, this explanation seems rather unlikely, but it cannot yet definitely be ruled out. Further measurements on the actual height of the layer, are required.

It seems fairly certain that the distribution of temperature with height is not a simple linear function. But the linear temperature gradient does serve as a very good first approximation. O'Brien [12] worked out the theory of layer formation in the case of an atmosphere where the temperature T at a height h is given by the more general relation

$$T = T_o\left\{1 + b(h - h_o)\right\}^{\delta+1} \qquad \text{-----(67).}$$

δ being a constant. He also indicated a method whereby his theory can be applied to experimental results and the value of δ found.

This generalisation will not be of much use in the case of the E layer, until the electron distribution curves can be determined with greater accuracy. For

present records the linear temperature gradient theory is good enough. A method to determine the temperature gradient with greater accuracy will be the next step in the solution of the problem of the temperature distribution in the ionosphere.

- - - - - - - - - - - - - - - - - -

CONCLUSION.

We have distinguished between three types of E layers, namely the normal, abnormal and sporadic layers. Although the abnormal layer is found to occur very regularly in contrast to the sporadic, the distinction between these two is perhaps somewhat artificial, as they are probably related phenomena. The behaviour of the normal layer is very regular, and in accordance with the predictions of the theory, showing clearly that the layer is caused by solar ultra-violet radiation. From virtual height records it is possible to deduce the scale height and temperature of the layer, but more accurate measurements are required.

The Abnormal E Layer:

As pointed out earlier, there is usually some overlapping of the E_a and F reflections. Some writers ascibe this to a partial reflection from the lower layer at points where the ionisation increases very rapidly. Best, Farmer and Ratcliffe [43]) have however pointed out that this theory does not give a reasonable explanation of disturbed conditions. They therefore proposed that the layer consists of "clouds" of greater ionisation than the surroundings. According to our measurements, these clouds are of the order of a few kilometers thick, and occurs usually just above the normal E layer maximum.

The scale height of the layer was found to be less than 5 km., so that we can only conclude that our theory does not apply at all to this layer. It seems therefore fairly certain that this layer is not caused by the same agency as the normal layer.

On the other hand, the abnormal layer must be in some way caused, at least partially, by the sun. This is shown very clearly by the marked solar control on the

layer, which was also,reported by Berker and Dieminger[44]) and Appleton and Naismith [63]). The solar control is shown conclusively by the seasonal variation of the actual and true heights of the layer. Appleton and Naismith [63]) and Berker and Dieminger [44]) both propose that the layer is caused to a great extent by solar corpuscles. This theory is very attractive and needs further investigation. Perhaps some eclipse measurements can be made to settle the question. The difficulty with this theory, as pointed out by Appleton and Naismith [63]), is to reconcile it with the fact that sporadic reflections are also observed at night. It may be possible that the layer is also produced by some other effect that occurs at random., e.g. entrance of a meteor in the earth's atmosphere.

At this stage attention may be drawn to remarks made by Rawer [64]). He states that the threshold frequency f_3 depends strictly on the output of the pulse transmitter and on the sensitivity of the receiver. As the radiated power varies considerably with frequency, it is quite possible that the statistics of this frequency reproduce essentially the properties of the equipment. He also warns against the comparison of

measurements made at different stations without taking due precautions. Thus Berkner and Wells [65]) found very little evidence of the abnormal layer at Huancayo, Peru, near the earth's magnetic equator. Appleton and Naismith [63]) find in this evidence for a marked lattitude variation in abnormal E layer ionisation, as would be expected if the ionising agents in this layer are solar particles, deflected by the earth's field. It will be realised from the above that the same effect may be caused by the fact that different measuring equipment were used. More evidence is required before the result can be accepted.

Sporadic E layer:

The sporadic layer is of a more disturbed nature than the layer described above. It occurs at random intervals, and is a much more intense ionised region, at a lower height. At present the effect is usually ascribed to meteors [66]). If meteors are the sole cause of the layer, then it is difficult to explain the effect noticed that the frequency of occurrence

of the layer increases during the afternoon, attaining a maximum at sunset. The fact that the virtual height of the abnormal layer decrease during the afternoon also shows that there must be some ionising agent which has a maximum effect just before sunset.

Suggestions for further study:

We end this discussion by making some suggestions which should prove useful in further investigation of the lower layers of the ionosphere.

In the case of the normal layer more accurate distribution curves are required. More sensitive equipment which is capable of determining virtual heights more accurately, is needed. It is advisable that the apparatus should have a lower frequency limit in order to determine the actual height of the layer with greater precision.

In the case of the abnormal layer more data on the actual heighto of the layer and its seasonal variation should be useful. It is also necessary to correlate these with the magnetic activity.

On the theoretical side a more thorough examination of the effect of the earth's magnetic field should be made. Its effect on the temperature gradient of the layer should also be investigated. At present it seems as if more accurate distribution curves are required before the temperature gradient can be estimated with accuracy.

- - - - - - - - - - - - - - - - - - - -

REFERENCES.

1) Eccles, W.H.; Proc. Roy. Soc. A 87 , 79 (1912).

2) Eccles, W.H.; Electrician 79 , 1015 (1912).

3) Larmor, J.; Phil. Mag. 48 , 1025 (1924).

4) Appleton, E.V. and Barnett, M.; Proc. Roy. Soc. A 109 ,621 (1925).

5) Breit, G. and Tuve, M.A.; Phys. Rev. 28 , 554 (1926).

6) Breit, G. and Tuve, M.A.; Terr. Mag. 30 , 15 (1925).

7) Breit, G. and Tuve, M.A.; Nature 116, 357 (1925).

8) Pfister, W.; J. Geophys. Res. 54 , 315 (1949).

9) Ellyet, C.D.; Terr. Mag. Atmos. Elect. 52, 1 (1947).

11) Gledhill, J.A. and Szendrei,M.E.; "A study of conditions in the upper atmosphere and their deductions from Radio Measurements", Ph.D. Thesis, Univ. of S.A. (1947).

12) O'Brien, P.A.; "The vertical distribution of electron density and temperature in the ionosphere " M.Sc. Thesis, Univ. of S.A. (1949).

13) Lorentz, H.A.; Theory of Electrons (1909).

14) Appleton, E.V.; Jour. Inst. Elect. Eng. 71 , 642 (1932).

15) Hartree, D.R.; Proc. Camb. Phil. Soc. 25 ,47 (1929).

16) Darwin, C.G.; Proc.Roy. Soc. A 146 ,17 (1934).

17) Smith, N.; Bur. Stan. J. Res. Wash. 26 , 105 (1941).

18) Benyon, W.J.G.; Proc. Phys. Soc. 59 ,97 (1947).

19) Mimno, H.R.; Rev. Mod. Phys. 9 , 1 (1937).

20) Pande, A.; Terr. Mag. Atmos. Electr. 52 , 375 (1947).

21) Booker, H.G.; Proc. Roy. Soc. A 150 , 267 (1935).

22) Rai; Proc. Nat. Inst. Sci. India 3 , 307 (1937).

23) Pant and Bajpai ; Science and Culture 2 , 409 (1937).

24) Harang ; Terr. Magn. 41 , 143 (1936).

25) Jouast ; l'Onde Electrique 16 , 185 (1937).

26) Toshniwal ; Nature 135 , 471 (1935).

27) Saha and Rai ; Proc. Nat. Inst. Sci. India 3, 359 (1937).

28) de Groot ; Phil. Mag. 10 , 521 (1930).

29) Appleton, E.V.; Proc. Phys. Soc. 41 , 43 (1928).

30) Chapman, S.;Proc. Phys. Soc. 43 , 26, 483 (1931).

31) Chapman, S.; Proc. Phys. Soc. 51 , 93 (1939).

32) Gledhill, J.A. and Szendrei, M.E.; Proc. Phys. Soc. B 63 , 427 (1950).

33) Schafer, J.P. and Goodall, W.M.; Nature 131 ,804 (1933).

34) Appleton, E.V.; Nature 131 , 804 (1933).

35) Ratcliffe and White ; Nature 131 , 873 (1933).

36) Hollingworth, J.; Proc. Phys. Soc. 47 , 843 (1935).

37) Eckersley, T.L.; Journ. Inst. Elect. Eng. 67, 992 (1929).

38) Appleton, E.V.; Proc. Roy. Soc. A 126 , 567(1930).

39) Appleton, E.V. and Naismith, R.; Proc. Phys. Soc. 45, 389 (1933).

40) Appleton, E.V.; Proc. Roy. Soc. A 162 , 451 (1937).

41) Appleton, E.V., Naismith, R. and Ingram, L.J.; Phil. Trans. Roy. Soc. A 236 , 191 (1935).

42) Appleton, E.V. and Naismith, R.; Proc. Roy. Soc. A 150 , 685 (1935).

43) Best, J.E., Farmer, J.T. and Ratcliffe, M.A.; Proc. Roy. Soc. A 164 , 96 (1937).

44) Berker, W. and Dieminger, W.; Naturwissenschaften 37 , 90 (1950).

45) Appleton, E.V.; Nature 133 , 793 (1934).

46) Booker, H.G.; Phil. Trans. Roy. Soc. A 237 , 425 (1938).

47) Millington ; Nature 163 , 213 (1949).

48) Scott, J.C.N.; Nature 163 , 993 (1949).

49) Booker, H.G. and Seaton, S.L.; Phys. Rev. 57 , 87 (1940).

50) Pierce, J.A.; Phys. Rev. 71 , 698 (1947).

51) Pekeris, C.L.; Terr. Mag. Atmos. Elect. 42 , 205 (1940).

52) Rydbeck, O.; Phil. Mag. 30 , 282 (1940).

53) Rydbeck, O.; Phil. Mag. 34 , 130 (1943).

54) Manning, L.A.; P.I.R.E. 35 , 1203 (1947).

55) Chapman, S.; Phil. Mag. 10 , 369 (1930).

56) Wulf, O.R. and Deming, L.S.; Terr. Mag. Atmos. Electr. 43 , 283 (1938).

57) Penndorf, R.; J. Geophys. Res. 54 , 7 (1949).

58) Vassy, A and Vassy, M.E.; J. de Phys. et Rad. Ser 8 3 , 8 (1942).

59) Hulburt,E.O.; Physics of the earth (1939).

60) Whipple, F.L. Rev. Mod. Phys. 15 , 246 (1943).

61) Best N.R. , Havens,R.J.; Phys.Rev. 70 , 985 (1946); Phys.Rev. 71 , 915 (1947).

62) Grimminger,G.; Project Rand Corp. America, No R-105, (1948).

63) Appleton, E.V. and Naismith, R.; Proc. Phys. Soc. 52 , 402 (1940).

64) Rawer, K.; Nature 163 , 528 (1949).

65) Berkner, L.V. and Wells, H.W.; Terr. Mag. Atmos. Electr. 42 , 73 (1937).

66) Lovell, A.C.B.; Rep. Prog. Phys. XI , 415 (1948).

- - - - - - - - - - - -